Exploring the role of Smad7 in antigen presenting cells

Dissertation

Zur Erlangung des Grades

Doktor der Naturwissenschaften

Am Fachbereich Biologie

der Johannes Gutenberg-Universität Mainz

Vorgelegt von

Dominika Lukas

geb. am 07.11.1981 in Beuthen, Polen

Mainz, Oktober 2015

1.Berichterstatter:

2.Berichterstatter:

Tag der mündlichen Prüfung: 08.12.2015

Die Inhalte dieser Arbeit wurden publiziert:
http://www.pnas.org/content/114/8/E1480.long
'TGF-β inhibitor Smad7 regulates dendritic cell-induced autoimmunity.
Lukas D, Yogev N, Kel JM, Regen T, Mufazalov IA, Tang Y, Wanke F, Reizis B, Müller W, Kurschus FC, Prinz M, Kleiter I, Clausen BE, Waisman A.
Proc Natl Acad Sci U S A. 2017 Feb 21; 114(8):E1480-E1489.doi:10.1073/pnas.1615065114. PMID:28167776'.

The contents of this work were published:
http://www.pnas.org/content/114/8/E1480.long
'TGF-β inhibitor Smad7 regulates dendritic cell-induced autoimmunity.
Lukas D, Yogev N, Kel JM, Regen T, Mufazalov IA, Tang Y, Wanke F, Reizis B, Müller W, Kurschus FC, Prinz M, Kleiter I, Clausen BE, Waisman A.
Proc Natl Acad Sci U S A. 2017 Feb 21; 114(8):E1480-E1489.doi:10.1073/pnas.1615065114. PMID:28167776'.

Table of contents

Abbreviations

Ab	antibody
APC	antigen presenting cell or allophycocyanin
approx.	approximately
Bio	biotinylated
β-ME	β-mercaptoethanol
bp	base pair
BSA	bovine serum albumin
°C	temperature in degrees celsius
CD	cluster of differentiation
CFA	Complete Freund's Adjuvant
cDNA	complementary DNA
CFSE	carboxyfluorescein diacetate succinimidyl ester
CNS	central nervous system
Cre	site-specific recombinase (causes recombination)
CTLA-4	cytotoxic T lymphocyte antigen-4
Cyc	cychrome
DC	dendritic cell
DMEM	Dulbecco's modified Eagle medium
DNA	desoxyribonucleic acid
dNTP	desoxynucleotide triphosphate
DPI	days post immunization
DTT	dithiothritole
e.g.	exempli gratia (for instance)
EAE	experimental autoimmune encephalomyelitis
EDTA	ethylene-diaminetetraacetic acid
ELISA	enzyme-linked immuno-sorbent assay
EtOH	ethanol
FACS	fluorescence activated cell sorting
FCS	fetal calf serum
FITC	fluorescein isothiocyanate

FoxP3	forkhead box protein 3
g	gramm
h	hour/s
HEPES	N-2-hydroxyethylpiperazine-N'-2-ethansulfonic acid
i.e.	id est (that is)
i.p.	intraperitoneally
i.v.	intravenously
IFN-γ	interferon-γ
Ig	immunoglobulin
IL	interleukin
kb	kilobase pair
l	liter
LN	lymph node/s
loxP	recognition sequence for Cre (locus of X-ing over of phage P1)
LPS	lipopolysaccharide
Ly6C	lymphocyte antigen 6 complex, locus C
M	molar
MACS	magnetic activated cell sorter
MFI	mean fluorescence intensity
MgCl2	magnesium chloride
MHC	major histocompatibility complex
min	minute
ml	milliliter
mM	millimolar
MOG	myelin oligodendrocyte glycoprotein
mRNA	messenger RNA
MS	multiple sclerosis
NaCl	sodium chloride
n	nano
NaOH	sodium hydroxide
neo	neomycin resistance gene
o/n	over night
PBS	phosphate buffered saline
PCR	polymerase chain reaction

PD-1	programmed cell death 1
PE	phycoerythrine
Ptx	Pertussis toxin
RNA	ribonucleic acid
rpm	revolutions per minute
RT	room temperature
sec	seconds
SA	streptavidine
s.c.	subcutaneously
sc	spinal cord
SDS	sodium dodecyl sulfate
Smad7	MAD homolog 7
SSC	sodium chloride/sodium citrate buffer
TAE	Tris-acetic acid-EDTA buffer
Taq	polymerase from *Thermus aquaticus*
TCR	T cell receptor
TE	Tris-EDTA buffer
TEC	thymic epithelial cell
TGF-β	transforming growth factor-β
Tregs	regulatory T cells
Tris	2-amino-2-(hydroxymethyl-)1,3-propandiole
U	units
UV	ultraviolett
V	volts
vs	versus
v/v	volume per volume
w/v	weight per volume
WT	wild type
µl	microliter
µM	micromolar
3’	three prime end of DNA sequences
5’	five prime end of DNA sequences

1 Introduction

1.1 The immune system

The vertebrate immune system provides protection against invading pathogens to the organism (Medzhitov and Janeway, 1997). One of the most crucial characteristics of the immune system is the discrimination between self and non-self that enables protection from deleterious self-recognition (autoimmunity) while providing protection against pathogens (Mogensen, 2009). The immune system can be distinguished into two parts, namely the innate and the adaptive immune system. The innate immune system plays a crucial role as the first line of defense in recognizing foreign antigens (e.g. fungi, bacteria and virus) in an unspecific manner and includes e.g. neutrophils, eosinophils, natural killer (NK) cells and macrophages. The innate immune system reacts very rapidly upon encounter of microbial components, e.g. lipopolysaccharides, zymosan or double-stranded RNA, through recognition by toll like receptors and other pattern recognition receptors (PRRs). Moreover, communication of danger signals to lymphocytes of the adaptive immune system is an important function of the innate immune system (Janeway and Medzhitov, 1998; Medzhitov and Janeway, 1998).

The adaptive immune system functions as a second line of defense and consists of T and B cells. Both cell types have highly specific methods to recognize their cognate antigen, which enables the adaptive immune system to specifically recognize and clear a huge variety of antigens. Once antigen encounter occurred, the adaptive immune system forms a memory to that specific antigen, which enables a faster, stronger and more specified reaction when recognizing the same antigen for a second time (Janeway and Medzhitov, 1998; Medzhitov and Janeway, 1998).

Dendritic cells (DCs) form a bridge between the adaptive and innate immune system. DCs take up foreign or self-antigens and present these antigens to cells of the adaptive immune system. In the context of danger signals, DCs provide co-stimuli and instruct the adaptive immune system, to eradicate the pathogen, whereas in the absence of danger signals (e.g. self-antigens), DCs induce tolerance (Steinman et al., 2003).

1.2 Dendritic cells

Dendritic cells are professional antigen presenting cells (DCs), which as sentinels of the immune system govern tolerance versus immunity decisions. DCs are characterized by their expression of the integrin CD11c (Corbi and Lopez-Rodriguez, 1997). Although CD11c expression is attributed to the DC subsets, also macrophages as well as B and T cells have been reported to express CD11c under certain conditions (Beyer et al., 2005; Huleatt and Lefrancois, 1995; Probst et al., 2005; van Rijt et al., 2005). DCs originate from haematopoetic stem cell progenitors in the bone marrow and differentiate in response to diverse environmental stimuli into different DC subsets (Ginhoux and Jung, 2014) and can be divided into four major categories, which are the conventional dendritic cells (cDCs), monocyte (m)DCs during acute inflammation, plasmacytoid (pDCs) and Langerhans cells in the skin (Geissmann et al., 2010).

1.2.1 Dendritic cell subsets and their role in immunity and tolerance

1.2.1.1 Conventional dendritic cells

The conventional DCs predominate in the steady state and can be subdivided into two main subtypes, the migratory DC's and tissue resident DC's (Belz and Nutt, 2012).

1.2.1.1.1 Migratory dendritic cells

Migratory DC's develop from early precursors in the peripheral tissues where they sense antigens and migrate to lymph nodes via afferent lymphatics. Migratory DCs are restricted to the lymph nodes and cannot be found in the spleen. (Liu and Nussenzweig, 2010). The migratory DCs can be further divided into $CD11b^+$ DCs, which are dermal or interstitial DCs and $CD11b^-$ DCs (Belz et al., 2004b), which express the αE integrin CD103 (Bedoui et al., 2009; Liu and Nussenzweig, 2010) on the cell surface.

1.2.1.1.2 Lymphoid tissue resident dendritic cells

Lymphoid tissue resident DCs are located in lymphoid organs like thymus, spleen and lymph nodes sensing pathogens or antigens respectively present in the blood (Belz et al., 2004a; Lundie et al., 2008; Sponaas et al., 2006). Lymphoid tissue resident DCs originate from precursors found in the tissue they reside in (Naik et al., 2006) and are not migrating from other tissues. In an immature stage, in absence of an

inflammation, these DCs have a high endocytic activity and express low levels of MHC-II.

According to the expression of CD4 and CD8α, lymphoid tissue resident DCs can be subdivided into three subsets ($CD8\alpha^+$ $CD4^-$; $CD4^+CD8\alpha^-$; $CD4^-$ $CD8\alpha^-$ also called double negative). The $CD4^+$ $CD8\alpha^-$ DCs as well as $CD4^-CD8\alpha^-$ DCs have been implicated in the presentation of MHC-I restricted antigens (Kim and Braciale, 2009; Lukens et al., 2009), but are primarily presenting MHC-II associated antigens to $CD4^+$ T cells (Allenspach et al., 2008; Mount et al., 2008; Pooley et al., 2001). $CD8\alpha^+CD4^-$ DCs, however are strongly involved in cross presentation of antigens to cytotoxic $CD8^+$ T cells (Allan et al., 2003; Belz et al., 2004a; Edelson et al., 2010; GeurtsvanKessel et al., 2008; Lukens et al., 2009; Smith et al., 2003; van Rijt et al., 2005).

1.2.1.2 Monocyte derived dendritic cells

Monocyte derived dendritic cells (mDCs) are mobilized under inflammatory conditions from monocytes circulating in the blood (Hohl et al., 2005; Kool et al., 2008; Leon et al., 2007; Naik et al., 2006; Serbina et al., 2003). Under steady state conditions mDCs are characterized by the expression of macrophage colony stimulating factor (M-CSFR; CD115), which is crucial for their development as well as LY6C and CX3C-chemokine receptor 1 (CX3CR1) (Belz and Nutt, 2012). Differentiation to mDCs occurs under inflammatory conditions through toll like receptor 4 (TLR4) ligands or bacteria whereas *in vitro* granulocyte-colony stimulating factor (GM-CSF) stimulation is needed (Belz and Nutt, 2012). Upon maturation mDCs loose the expression of LY6C as well as M-CSFR (Cheong et al., 2010) and express CD11c and MHC-II as well as CD24, SIRPα (CD172a) and macrophage marker MAC3 (CD107b; LAMP2). Finally maturing mDCs can be characterized by their up-regulation of DC-specific ICAM3-grabbing non-integrin (DC-SIGN; CD209a) (Naik et al., 2006; Serbina et al., 2003). Mature mDCs represent a subset of DCs that serve as a backup during acute inflammation and are strong antigen presenting cells with cross presenting capacity (Cheong et al., 2010; den Haan and Bevan, 2002; McDonnell et al., 2010).

1.2.1.3 Plasmacytoid dendritic cells

Plasmacytoid dendritic cells (pDCs) can be characterized based on the expression of sialic acid-binding immunoglobulin-like lectin H (Siglec-H) and bone marrow stromal antigen 2 (BST2) as well as CD45RA (Reizis et al., 2011a). pDCs are broadly distributed in the body and can produce high amounts of type I interferons (IFNs) which play an important role during viral infections (Perussia et al., 1985; Trinchieri et al., 1978). The antigen presenting capacity is however low (Reizis et al., 2011b).

1.2.1.4 Langerhans cells

Langerhans cells reside in the skin and arise from a local $LY6C^+$ myelomonocytic precursor cell population that originates from macrophages, which early in embryonic development are present in the skin and in the first days after birth undergo proliferative burst in the epidermis (Chorro et al., 2009). Langerhans cells are characterized by the expression of Langerin and their development is dependent on transforming growth factor beta (TGF-β) (Borkowski et al., 1996). In the skin Langerhans cells can be distinguished from dermal DCs based on the expression of EpCAM. While DCs from the dermis migrate to the draining lymph nodes and can be detected already one day post antigen encounter, Langerhans cells need 3 days to reach the draining lymph nodes.

Table 1 summarizes the different DC subsets and the expression of selected surface proteins that are commonly used for differentiating between those different subsets.

	pDC	Conventional DCs					Langerhans cells	Monocyte-derived DCs
		$CD8\alpha^+$	$CD4^+$	$CD4^-CD8^-$	$CD11b^+$	$CD103^+$		
CD8α	+/-	+	-	-	-		-	-
CD103	-	Low	-	-	+/-		-	-
CD205	-	+	-	-	+		++	-
EPCAM	-	-	-	-	-		+	-
CD11b	-	+	+	+	+		+	+
B220	+	-	-	-	-		-	-
DC-SIGN	++	-	-	-	ND		-	+
Langerin	-	+/-	-	-	-		++	-

Table 1: Classification of dendritic cell subsets based on their expression of specific surface markers. Table adapted from (Belz and Nutt, 2012).

1.3 T cell development and T cell subset differentiation

T cells derive from common lymphoid progenitors that originate in the bone marrow and migrate to the thymus where they undergo distinct developmental events including T cell receptor rearrangements (Godfrey et al., 1993). The thymus is an organ, which consists of several lobes and each lobe is composed of a cortical and an inner medullar region (Rodewald, 2008). Maturating T cells are located in distinct parts of the thymus according to the different developmental stages. The earliest developmental stages of T cells can be found in the sub- capsular region of the thymus. These T cells are termed double negative T cells (DN; $CD4^-CD8^-$) and are characterized by the lack of a T cell receptor (TCR) and CD4 as well as CD8 surface markers expression. The double negative T cells can be subdivided into four stages of differentiation (DN1-4), which are characterized by the expression of CD25 and CD44. The T cells of the DN4 stage progress to the next stage of double positive T cells (DP; $CD4^+CD8^+$). DP cells migrate further into the cortex of the thymus and interact with cortical thymic epithelial cells (cTecs), which express high levels of MHC class I (MHC-I) and MHC class II (MHC-II) molecules, which are associated with self-peptides. The interaction of the TCR with those self-peptide/MHC complexes determines the fate of the DP T cells (Robey and Fowlkes, 1994; von Boehmer et al., 1989). In the thymus the T cells undergo positive and negative selection in order to delete potential auto-reactive T cells. When the TCR signaling is not strong enough the T cells undergo delayed apoptosis, whereas acute apoptosis is induced upon too strong signaling of their TCR. The selection takes place mainly in the medulla where T cells encounter with strongly activating self-ligands on haematopoietic and DCs (Biddison et al., 1982; Freeman, 2000; Germain, 1994). The positive selection of the T cells is dependent on an intermediate level of TCR signaling which thus leads to maturation of these T cells. The fate of T cells to become $CD8^+$ cells is induced when the TCRs binds to self- peptide/–MHC-I complexes. The fate towards $CD4^+$ cells is initiated when the TCRs binds to self-peptide–MHC-II complexes. Single positive (SP; $CD4^+CD8^-$ or $CD4^-$ $CD8^+$) T cells then leave the thymus by the blood stream and migrate into the peripheral lymphoid tissues such as spleen and lymph nodes. The T cells recirculate between blood and peripheral lymphoid tissue until they encounter their specific antigen and are induced to proliferate and differentiate into effector T cells.

The activation of naïve $CD4^+$ T helper (Th) cells occurs, when the TCR recognizes a specific peptide- antigen/MHC-II complex presented on antigen-presenting cells (APCs). Subsequently the cells begin to divide giving rise to cells that are specific for the same antigen/MHC-II complex. These $CD4^+$ T cells can be divided into subtypes, with a characteristic cytokine pattern and function, referred to as Th type-1 (Th1), Th2 or Th17 cells and regulatory T cells (Kaiko et al., 2008).

Th1 cells typically secrete characteristic cytokines such as interferon (IFN)-γ, and tumor necrosis factor β (TNF-β) and are involved in the immune response against intracellular infections by viruses as well as specific bacteria and microorganisms (Kidd, 2003). A Th1 immune response is mediated by the stimulation of T cells with IFN-γ and interleukin (IL)-12, which induce JAK1/2 and STAT1/3/4 to stimulate the crucial transcription factor T-bet and further IFN-γ production (Murphy and Reiner, 2002). Th2 cells secrete the characteristic cytokines IL-4, IL-5, IL-10 and IL-13 and take part in the immune response against parasites. IL-4 triggers JAK1/3 and STAT6 to activate the transcription factor GATA3 which itself is important for Th2 differentiation. A third subset of T helper cells is represented by Th17 cells, which secrete IL17-A, IL17-F, IL-6, IL-22 and TNF-α and appear to play an essential role in both tissue inflammation and activation of neutrophils resulting in an elimination of extracellular bacteria (Dong, 2008). The development of Th17 cell is dependent on the stimulation by the cytokine TGF-β and IL-6 (McGeachy and Cua, 2008). Regulatory T cells (Tregs) are known as non-effector T cells. Tregs are essential for maintaining peripheral tolerance, preventing autoimmune diseases and limiting chronic inflammatory diseases (Vignali et al., 2008). Tregs secrete IL-10 and TGF-β, modulate helper T cell activity, suppress some of their functions and are inducing tolerance to antigens. Since TGF-β is crucial for Tregs as well as for Th17 cells it has been suggested that they share reciprocal developmental pathways during the pathogenesis or control of inflammation (Bettelli et al., 2006). Th1 cells along with Th17 cells are supposed to play a role in the pathogenesis of autoimmune diseases such as multiple sclerosis. Th1, Th2 and Th17 populations, and the cytokines they secrete, are antagonistic to each other and one or the other subsets may be dominant in response to a particular pathogen. The activation of the different Th subsets to specific pathogens, not only plays a role in immune response, but can also be crucial for the pathogenesis of autoimmunity.

1.4 Transforming growth factor- β

The TGF-β superfamily comprises over 30 members such as bone morphogenic proteins (BMPs) and transforming growth factors-β (TGF-β) and is highly conserved among species (Massague, 2012; Schmierer and Hill, 2007a). The cytokine TGF-β contributes to the maintenance of immune homeostasis and serves a predominantly tolerogenic role (Gleizes et al., 1997; Li et al., 2006b; Travis and Sheppard, 2014). In mammals three homologous TGF-β isoforms TGF-β1, TGF-β2 and TGF-β3 exist. Though they have similar functional properties, TGF-β1 is thought to be the main isoform relevant for immune cell regulation and mice devoid of TGF-β1 succumb to multi-organ inflammation early in life (Kulkarni et al., 1993b; Li et al., 2006c; Shull et al., 1992). Various cell types such as macrophages, DCs and T cells, express and respond to TGF-β (Li et al., 2006c).

TGF-β is synthesized as a precursor protein (pre-pro-TGF-β) consistent of a signaling peptide important for the direction of TGF-β to the endoplasmatic reticulum (ER), the N-terminal latency-associated polypeptide (LAP) and the C-terminal mature cytokine (Gleizes et al., 1997; Munger et al., 1997; Travis and Sheppard, 2014). In the rough ER, the pre-pro-TGF-β undergoes proteolytic processing and two monomers of TGF-β dimerize through disulphide bridges resulting in the pro-TGF-β dimer. The cleavage of pro-TGF-β by the enzyme furin is mandatory for further TGF-β activation and yields the small latent complex including the LAP sequence (Dubois et al., 1995). In the large latent complex the latent TGF-β binding protein- (LTBP) 1, 3 or 4 covalently attaches to the small latent complex (Saharinen and Keski-Oja, 2000). It can be found as a cell-surface associated form and be presented to target cells (Schmierer and Hill, 2007b). LAP impedes TGF-β1 from binding to its receptor by changing the molecular interface necessary for binding. TGF-β activation is caused by proteolytic cleavage or detachment of the inactivating component. The mechanisms of LAP cleavage and TGF-β activation includes e.g. the binding of integrin-family members such as αvβ6 expressed by epithelial cells or αvβ8 expressed by DCs and extracellular proteolysis (Travis and Sheppard, 2014). Hydrophobic interactions and disulphide bonds between the subunits stabilize the active TGF-β1 homodimer (Rubtsov and Rudensky, 2007).

DCs both secrete and respond to TGF-β and by the expression of the integrin αvβ8 contribute to the activation of latent TGF-β into its active form (Melton et al., 2010;

Travis et al., 2007; Worthington et al., 2011). TGF-β is crucial to Langerhans cell development and induces the expression of the helix-loop-helix transcription factor ID2 involved in Langerhans cell development (Borkowski et al., 1996; Hacker et al., 2003a). In addition, *in vitro* studies showed that TGF-β is important for maintaining Langerhans cells in an immature state (Geissmann et al., 1999). Furthermore, DC specific conditional ablation of the TGF-βRII or a dominant negative form of TGF-βRII renders mice prone to autoimmunity, highlighting the importance of DC specific TGF-β signaling in the maintenance of immune homeostasis (Laouar et al., 2008; Ramalingam et al., 2012).

TGF-β has various effects on T cell development and responses (Li et al., 2006a; Li et al., 2006c). TGF-β inhibits Th1 and Th2 differentiation by down-regulation of T-bet, Stat4 and GATA3/NFAT expression (Chen et al., 2003; Gorelik et al., 2002). TGF-β induces Treg cell development by enhancing FoxP3 expression (Huber et al., 2004). On the other hand TGF-β in combination with IL-6 instructs Th17 cell differentiation (Li et al., 2006a; Li et al., 2006c). Moreover, TGF-β blocks T cell proliferation through inhibition of IL-12 production in a Smad3 dependent manner and by down-regulation of cyclin D2 and E, CDK4 and c-myc expression (Kehrl et al., 1986a; Kehrl et al., 1986b). In addition to its role in regulating DC and T cell development, TGF-β has been reported to induce apoptosis in various cell types (Jang et al., 2002).

Since TGF-β controls a wide array of immune cell functions, its function must be tightly regulated.

1.4.1 The signaling pathway of TGF-β

TGF-β signaling is initiated, when active TGF-β binds to the membrane-bound TGF-β receptor type II (TGF-βRII), resulting in recruitment and phosphorylation of TGF-βRI (also known as ALK5). The TGF-βR complex is composed of a TGF-βRI dimer and a TGF-βRII dimer, whereby the intracellular threonine kinase of TGF-βRII phosphorylates the kinase domain of TGF-βRI. Subsequently, TGF-βRI phosphorylates the receptor-associated (R-) Smad-proteins Smad2 and Smad3, which form a complex with the common (Co-) Smad4, translocate into the nucleus, where they bind to the Smad binding element (SBE) (Rubtsov and Rudensky, 2007). Smads are named after the orthologues in *C. elegans* (SMA) and *Drosophila* (MAD; mothers against decapentaplegic) and are evolutionary highly conserved. In the nucleus Smads

interact with co-activators such as CBP/p300 or co-repressors like Sno/Ski and regulate target gene expression (Derynck and Zhang, 2003; Massague and Wotton, 2000; Shi and Massague, 2003). A prominent target gene of TGF-β is the inhibitory (I-) Smad7, which terminates TGF-β signaling by forming a negative feedback loop.

In addition, TGF-β signaling can also be mediated independent of Smads e.g. via phosphatidylinositol 3-kinases (PI3K), mitogen-activated protein kinase (MAPK) and Rho-GTPases (Derynck and Zhang, 2003; Mu et al., 2012).

1.4.2 The TGF-β signaling inhibitor Smad7

Smad7 is a key negative regulator of the TGF-β signaling (Figure 1) (Nakao et al., 1997). In response to TGF-β stimulation, Smad2/3 and 4 induce Smad7 expression by binding to the SBE element in the promoter region of Smad7 (Denissova et al., 2000; Stopa et al., 2000; von Gersdorff et al., 2000). Enhanced induction of Smad7 expression is mediated by additional transcription factors or co-activators such as activating transcription factor 2 (ATF2), activator protein 1 (AP-1), transcription factor E3 (TFE3), stimulating protein-1 (SP1), p300 and forkhead box H1 (FOXH1) (Brodin et al., 2000; Gohla et al., 2008; Hua et al., 2000; Jungert et al., 2006; Uchida et al., 2001). Moreover, Smad7 can be induced in response to pro-inflammatory cytokines such as interferon-γ (IFN-γ), or tumor necrosis factor (TNF-α), or in response to Stat1 or NF-κB signaling (Bitzer et al., 2000; Kume et al., 2007b; Ulloa et al., 1999; Yan and Chen, 2011).

Smad7 inhibits TGF-β signaling by binding the TGF-βRI and preventing the phosphorylation of Smad2/3 (Nakao et al., 1997). Furthermore Smad7 together with the E3 ubiquitin ligase Smad ubiquitylation regulatory factor (SMURF) targets the TGF-βR complex for proteasomal degradation, and consequently terminates TGF-β signaling (Ebisawa et al., 2001; Kavsak et al., 2000; Suzuki et al., 2002). In addition, Smad7 was suggested to affect TGF-β target gene expression by associating with the acetlytransferase p300, SIRT1 and histone deacetylases (HDCA1) (Gronroos et al., 2002a; Kume et al., 2007b; Simonsson et al., 2005).

In humans Smad7 is involved in the pathogenesis of cancer and in multiple autoimmune diseases including multiple sclerosis and inflammatory bowel disease (Kleiter et al., 2007; Kleiter et al., 2010; Massague, 2008; Monteleone et al., 2008; Monteleone et al., 2001). Moreover, Smad7 attenuates TGF-β mediated fibrosis and

was suggested to have a protective function in pulmonary, renal and pancreatic fibrosis (Chung et al., 2009; Dooley et al., 2003; He et al., 2009; Nakao et al., 1999; Wang et al., 2005).

To date several mouse models exist, enabling the study of Smad7 function *in vivo*. Firstly, one mouse model in which exon 1 of Smad7 was deleted, that encodes the Mad-homology (MH1) domain of Smad7, revealed alterations in B cell responses. Yet, in this model Smad7 largely retained its inhibitory properties (Li et al., 2006e; Mochizuki et al., 2004; Zhu et al., 2011). In a further knockout mouse model harboring a deletion of Smad7 exon 4, encoding for the MH2 domain of Smad7 protein, mice displayed severe developmental defects of the cardiovascular system accompanied by high embryonic lethality (Kamiya et al., 2010). Thirdly, conditional Smad7 knockout mice, in which promoter and exon I of Smad7 are excised, when crossed to a cell specific Cre mouse line, allow the analysis of cell specific Smad7 abrogation (Kleiter et al., 2010). T cell specific Smad7 knockout mice developed attenuated autoimmune encephalomyelitis (EAE), a murine model for the autoimmune disease multiple sclerosis (MS), while mice with a T cell specific overexpression of Smad7 (CD2-Smad7) developed exacerbated EAE (Dominitzki et al., 2007; Kleiter et al., 2010). Thus, these studies underline the importance of Smad7 in regulating immunity.

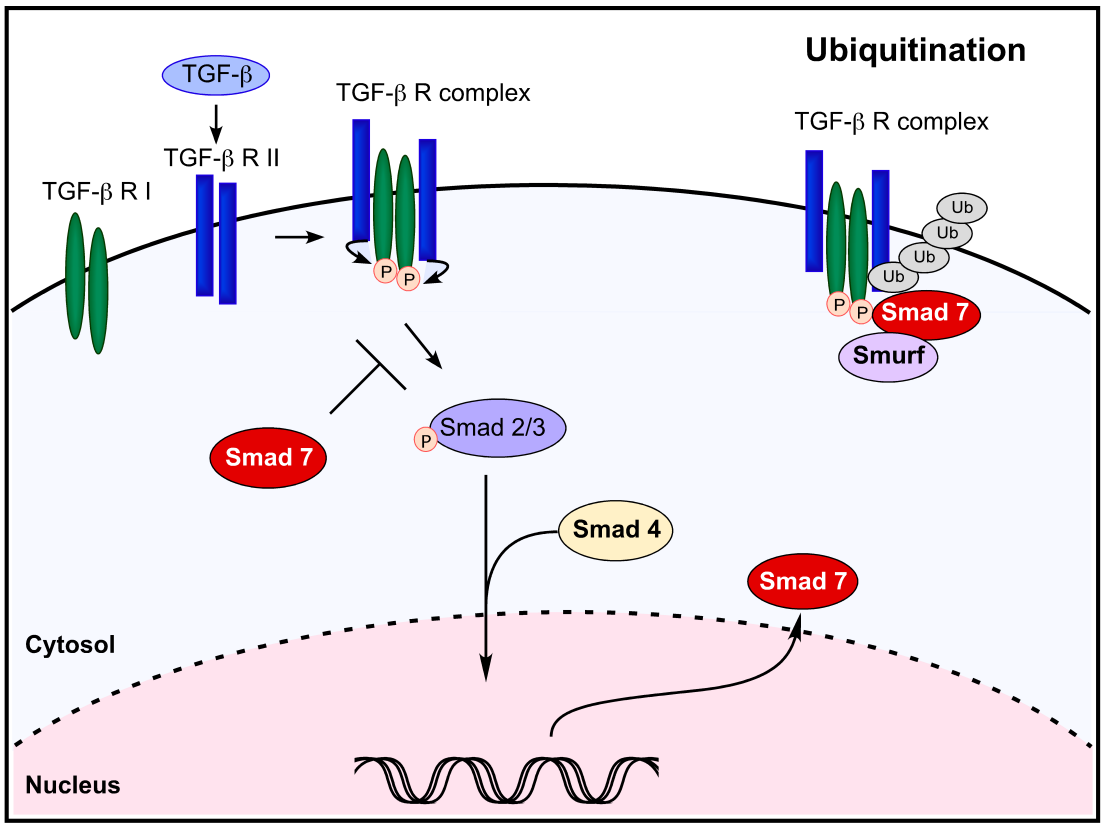

Figure 1 The TGF-β signaling pathway and its regulation by Smad7

TGF-β binds to the TGF-βRII, which leads to recruitment and phosphorylation of the TGF-βRI, forming the TGF-βR complex. Smad2/3 are subsequently phosphorylated and in combination with Smad4 transclocate into the nucleus where they activate target gene expression. A prominent target gene of TGF-β signaling is Smad7, which terminates the TGF-β signaling on one hand by competing with Smad2/3 for binding to the TGF-βR and on the other hand together with SMURF targets the TGF-βR complex for proteasomal degradation.

1.5 Experimental autoimmune encephalomyelitis

The experimental autoimmune encephalomyelitis (EAE) serves as a mouse model for multiple sclerosis (MS) an inflammatory demyelinating autoimmune disease of the central nervous system (CNS), which affects predominantly young women and manifests in motoric dysfunction ranging to severe paralysis and death (Gold et al., 2006; Steinman and Zamvil, 2006). EAE shares many features with MS, which includes perivascular inflammatory lesions, demyelination and axonal damage ultimately resulting in severe paralysis (Lassmann, 1983).

Induction of EAE in susceptible rodent strains is achieved by immunization with a CNS-specific antigen such as myelin oligodendrocyte glycoprotein (MOG), myelin basic protein (MBP) or myelin proteolipid protein (PLP) in combination with Complete Freund's Adjuvant (CFA) supplemented with heat-killed mycobacteria tuberculosis and additional immunization with pertussis toxin (PTX), which augments

blood brain barrier disruption (Billiau and Matthys, 2001; Mendel et al., 1995). Chronic-progressive disease can be studied using C57BL/6 mice immunized with MOG, which results in a monophasic disease progression while relapsing remitting disease can be studied by immunization of SJL mice with PLP (Gold et al., 2006). EAE disease can be actively induced or passively transferred by injection of activated myelin- specific T cells derived from immunized donors to recipient mice.

In response to the immunization with CNS derived antigens, myelin specific T cells are primed, proliferate and differentiate into Th1 and Th17 effector subsets. These cells subsequently migrate from the peripheral lymphoid organs into their target tissue- the CNS, where upon recognition of their cognate antigen, they induce an inflammatory cascade resulting in tissue damage (Kurschus, 2015).

Many of the original observations suggested that IFN-γ producing Th1 cells are the pathogenic cells driving the disease, as IFN-γ is present at the site of inflammation during the peak of disease and transfer of Th1 cells is sufficient to induce EAE.

Yet, EAE can be induced in mice lacking the Th1 hallmark cytokine IFN-γ or the IFN-γ receptor (Ferber et al., 1996; Willenborg et al., 1999), suggesting that Th1 cells might not be the only subset driving disease pathology. More recently, a new subset of IL-17 producing T helper cells (Th17) was identified. These Th17 cells are present in many autoimmune disorders including EAE and MS and are highly autoreactive, hinting for their role in disease pathology.

Th1 cells preferentially infiltrate the spinal cord through an α4 (VLA-4) integrin-dependent mechanism, while Th17 cells preferentially infiltrate the brain parenchyma in a manner dependent on αLβ2 (LFA-1) and independent of the α4 integrin (Rothhammer et al., 2011a). In addition, several studies have demonstrated Th17 cells to display high plasticity (Hirota et al., 2011; Kurschus et al., 2010). Thus it is likely that the different subsets of myelin-specific Th1 and Th17 cells infiltrating the CNS, have originated from a subset of IL-17 producing Th17 cells which further convert into IL17-A/IFN-γ double producing cells and IFN-γ single producing (exTh17) cells, as was previously shown by a fate-mapping study by Kurschus et al. (Kurschus et al., 2010).

In line with the above mentioned, the IL-12 superfamily member IL-23 was reported to be mandatory for disease induction as IL-23 knockout mice are resistant to EAE (Cua et al., 2003). The development of Th17 cells that confer a pathogenic phenotype

strongly depends on IL-23 (Langrish et al., 2005). Yet, Th17 hallmark cytokines IL-17A and IL-17F were shown to have little contribution to disease pathology (Haak et al., 2009), suggesting that other T cell mediated factors are crucial for their pathogenic effector function.

In addition to the generation of effector T cells, immunization with MOG induces expansion of nTregs and during the recovery phase increased Treg frequencies can be found in the CNS (Korn et al., 2007b; McGeachy et al., 2005; O'Connor et al., 2007). The protective role of Tregs during EAE was demonstrated using anti $CD25^+$ Treg depletion models (Gartner et al., 2006; Montero et al., 2004; Stephens et al., 2009; Zhang et al., 2004) or transfer of $CD25^+$ Tregs (Kohm et al., 2002; McGeachy et al., 2005; Stephens et al., 2009), which resulted in exacerbated or ameliorated EAE, respectively. Moreover, in spontaneous EAE models Tregs can delay (Lowther et al., 2013) or prevent (Hori et al., 2002; Olivares-Villagomez et al., 1998) EAE onset. In addition, Tregs in the CNS mediate T effector cell suppression by inhibiting T cell proliferation and cell motility in the brain (Koutrolos et al., 2014). The analysis of Tregs in FoxP3 reporter mice revealed, that CNS-derived MOG specific Tregs extracted on the peak of disease were however not suppressing CNS derived effector T cells efficiently *in vitro* when T effector cells were likewise extracted from the CNS on the peak of disease (Korn et al., 2007b). In another study, Tregs were reported to dampen the migration of T effector cells into the CNS (Lowther et al., 2013). The limited Treg suppressive capacity was mainly resulting from high IL-6 expression by CNS derived T effector cells. In contrast CNS derived Tregs at the peak of disease were able to suppress peripheral T effector cells efficiently. Moreover another study could show, that during the recovery phase Tregs suppress T effector cells (O'Connor et al., 2007). These studies underline the importance of Tregs in the control of EAE.

1.5.1 Role of DCs in EAE

DCs as professional APCs play an important role in EAE (Greter et al., 2005; McMahon et al., 2005; Yogev et al., 2012). During steady state DCs remain in an immature phenotype with high endocytosis and low MHC-II and co-stimuli expression. Upon inflammation in response to e.g. microbial or viral stimuli sensed by Toll-like receptors (TLR; (Kaisho and Akira, 2001)), CD40 ligand (CD40L) stimulation during T cell encounter (Bennett et al., 1998; Schoenberger et al., 1998) or in response to pro-inflammatory cytokines DCs down-modulate endocytosis, up-

regulate expression of MHC-II as well as co-stimuli and migrate to draining lymph nodes, where they activate antigen specific T cells (Guermonprez et al., 2002). In addition, secretion of cytokines as well as other stimuli mediated by DCs affects T cell subset differentiation towards either T effector or Treg cells, ultimately leading to immune response or tolerance, respectively.

DCs are potent inducers of EAE, as transfer of MBP- pulsed BMDCs results in the induction of EAE (Dittel et al., 1999). In addition, elevated DC numbers in the blood and meninges can be detected in MS patients. Albeit DCs are sparse in healthy CNS, during EAE DCs migrate from the periphery to the CNS where they are crucial for the reactivation and licensing of CNS-antigen specific T cells in the target tissue (Clarkson et al., 2015; Greter et al., 2005).

Previously believed to initiate disease by their capability to activate myelin specific auto-reactive T cells in the CNS, recent studies using DC depletion models highlighted an equally important tolerogenic function of DCs during EAE (Yogev et al., 2012). DC depletion models depicted that EAE disease severity was aggravated in the absence of DCs and that DCs during EAE induced Tregs via PD-1 / PD-L1 interaction. When DCs were absent, the major source of PD-L was likewise absent resulting in reduced numbers of protective Tregs. Though EAE induction was not prevented by the depletion of DCs (neither from birth nor later in adulthood), suggesting that in their absence other cells may take over as APCs, DCs were crucial for the upregulation of PD-1 on antigen-specific T cells and subsequently induce the *de novo* conversion of Treg cells from naive T cells during EAE, with the latter being responsible for controlling disease severity and recovery.

1.5.2 TGF-β in EAE

TGF-β is an anti-inflammatory cytokine, which predominantly plays a protective role during EAE, yet under some conditions, TGF-β may also exhibit a more inflammatory role. On one hand TGF-β induces the generation of Tregs (Fantini et al., 2004; Fu et al., 2004; Yamagiwa et al., 2001) and tolerance induction, while in combination with IL-6 TGF-β instructs Th17 differentiation (Bettelli et al., 2006; Mangan et al., 2006; Veldhoen et al., 2006). It was suggested that Th17 cells differentiated in the presence of TGF-β1 in combination with IL-6 are not pathogenic during EAE and that TGF-β3 in turn induces pathogenic Th17 cells (Lee et al., 2012). Yet, in light with the way myelin-specific T helper cells are being generated (chapter

1.3), this concept is still not fully clear, as TGF-β3 is only being produced by the activated T cells after their differentiation, while TGF-β1 is produced by many cells including APCs at the time of instructing the autoreactive T cell subsets differentiation. In another study systemic treatment of EAE-diseased mice with exogenous TGF-β or in vitro treatment of myelin basic protein (MBP)-specific T cells with TGF-β1 has been shown to inhibit and prevent EAE (Li et al., 2006c). Moreover increased expression of TGF-β1 mRNA or protein was found in inflammatory lesions during recovery. Furthermore, endogenous TGF-β1 is involved in the protection from EAE (Li et al., 2006c). Another study in which Smad7, the TGF-β negative regulator, was neutralized by antisense oligonucleotide treatment reported resistance to EAE of treated mice (Kleiter et al., 2007). Likewise, mice with a T cell-specific Smad7 deletion were resistant to EAE and displayed increased amounts of protective Tregs depicting a crucial role for TGF-β signaling in T cells for the induction of tolerance (Kleiter et al., 2010). In addition another study reported that mice with a DC-specific abrogation of TGF-βR signaling developed aggravated EAE suggesting that also TGF-β signaling on DCs mediates resistance to EAE (Laouar et al., 2008).

1.6 Objectives

TGF-β plays a prominent role in immune homeostasis and tolerance. Smad7, once expressed in response to e.g. TGF-β or IFN-γ, terminates TGF-β signaling. Abrogated TGF-β signaling in DCs, which are professional antigen presenting cells, leads to breakdown of tolerance and manifestation of an autoimmune phenotype. Yet, the role of Smad7 on DC development and function remains elusive.

The aim of this thesis was to explore the role of Smad7 during DC development *in vivo* and its influence on DC function in the context of the CNS autoimmune disease experimental autoimmune encephalomyelitis (EAE), a murine model for multiple sclerosis (MS). Therefore a conditional Smad7 knockout mouse model was used, in which the Smad7 promoter and a fragment of Exon 1 were flanked by *loxP* sites ($Smad7^{fl/fl}$; (Kleiter et al., 2010)). The cross of these mice to a DC-specific Cre line (CD11c-Cre; (Caton et al., 2007)) resulted in DC-specific Smad7 knockout mice ($S7^{\Delta DC}$ mice), which enabled the analysis of Smad7 deficient DCs *in vivo*.

2 Material and Methods

2.1 Chemicals and Biological Material

Chemicals were purchased from Sigma-Aldrich (Steinheim), Fluka Chemie (Deisenhofen), Merck (Darmstadt), or AppliChem (Darmstadt) unless stated otherwise. Solutions were prepared with double distilled water (ddH_2O). Sterility of solutions and chemicals used in cell culture was maintained by working under a sterile hood (Heraeus, Germany).

Name of chemical	Supplier
β-Mercaptoethanol (β-ME)	Fluka Chemie GmbH, Switzerland
Bovine serum albumin (BSA)	Sigma-Aldrich, Steinheim
Calcium chloride	Sigma-Aldrich, Steinheim
Citric acid	Fluka Chemie GmbH, Switzerland
2'-Deoxyguanosine Monohydrate	AppliChem, Darmstadt
Dextran sulfate	AppliChem, Darmstadt
Dextrose	Merck, Darmstadt
Dimethylsulfoxide (DMSO)	Merck, Darmstadt
dNTPs	Pharmacia Biotech, USA
Ethylendiamine tetraacetate (EDTA)	Fluka Chemie GmbH, Switzerland
Ethanol, abs.	AppliChem, Darmstadt
Ethidium bromide	Sigma-Aldrich, Steinheim
Fetal calf serum (FCS)	Boehringer Mannheim GmbH, Mannheim
Ficoll 400	Amersham Pharmacia, Freiburg
Hydrochloric acid (37 %)	Merck, Darmstadt
Isopropanol	AppliChem, Darmstadt
Magnesium chloride	Sigma-Aldrich, Steinheim
Magnesium chloride (for PCR)	Gibco Life Technologies GmbH, Karlsruhe
Potassium acetate	Fluka Chemie GmbH, Switzerland
Potassium chloride	Merck, Darmstadt
Proteinase K	Roche, Switzerland
Sodium azide	Fluka Chemie GmbH, Switzerland
Sodium chloride	AppliChem, Darmstadt
Sodium citrate	Fluka Chemie GmbH, Switzerland
Sodium dodecyl sulfate	AppliChem, Darmstadt
Sodium hydrogencarbonate	Fluka Chemie GmbH, Switzerland

Sodium hydroxide	Fluka Chemie GmbH, Switzerland
Tris base	Fluka Chemie GmbH, Switzerland
Tris/ HCl	AppliChem, Darmstadt

Table 2: Chemicals used for experiments.

Cell culture material	Supplier
15 cm plates	TPP, Switzerland
10 cm plates	Greiner Bio-One, Germany
6 well plates	Becton-Dickinson, USA
12 well plates	Becton-Dickinson, USA
24 well plates	Corning Incorporated, USA
48 well plates	Corning Incorporated, USA
96 well plates (round and flat bottom)	Costar, USA
250 ml tissue culture flask	Greiner Bio-One, Germany
Plastic pipettes (1, 5, 10 and 25 ml)	Corning Incorporated, USA
Pipette tips Tip-One	Starlab, Finnland
15 ml polystyrene tubes	Corning Incorporated, USA
50 ml polystyrene tubes	Greiner Bio-One, Germany
Medium reservoir 50 ml	Greiner Bio-One, Germany
Filter unit 250 ml	Nalgene, USA
0,22 µm filter	Millipore, Ireland

Table 3: List of cell culture material.

Devices	Supplier
BD FACSCanto II	BD Biosciences
BD FACScan	BD Biosciences
BD FACSAria II	BD Biosciences
Heraeus HA 2448 sterile hood	Heraeus, Germany
Heraeus incubator	Heraeus, Germany
Centrifuge	Heraeus, Germany
Counting chamber	Neubauer, Germany
Gel documentation	BioRad
Thermomixer	B. Braun Biotech
PCR machines	Peqlab, Corbett, Apollo
Water bath	B.Braun Biotech

Table 4: List of devices used for experiments.

Software

Canvas^{TM}X	ACD Systems Inc.
CellQuest	Becton Dickinson, Mountain View, USA
FlowJo	FlowJo Enterprise
Prism	Graph Pad
Quantity One	Bio-Rad Laboratories

2.2 Molecular biology

Standard methods of molecular biology were performed – if not otherwise stated - according to protocols described in Sambrook et al. (1989).

2.2.1 Preparation of genomic DNA from mouse tail biopsies

Genomic DNA was prepared from tail biopsies of mice (approximately 0,5 cm tail tip). Digestion of proteins was performed over night at 56°C in tail lysis buffer **(**100mM Tris/HCl pH 7.5, 5mM EDTA, 0.2% SDS, 200mM NaCl, 100mg/ml) supplemented with proteinaseK before use. The Undigested material was removed by centrifugation (13 000rpm, 10min) and the supernatant containing the genomic DNA was precipitated by addition of an equal volume of isopropanol. DNA was pelleted by centrifugation for 10min at 13 000rpm and washed in 70% EtOH, centrifuged 10min at 13 000rpm, dried at RT and subsequently dissolved in 150µl dH_2O.

2.2.2 Polymerase chain reaction (PCR)

Polymerase chain reaction (PCR) (Mullis et al., 1986; Mullis, 1990; Saiki et al., 1988) was used to screen experimental mice for presence of targeted alleles or transgenes. Genotyping of mice was in general performed in several thermal cyclers (MyCycler (Bio-Rad Laboratories Inc.), Primus 96 advanced (Peqlab)). Primers used for PCRs are listed in Table 5 according to distinct PCRs performed. In general a reaction volume of 25-30µl was selected containing 10pmol of each primer, 0.25U of *Thermus aquaticus* (*Taq*) DNA polymerase (1U/µl, Segenetics, Bonn, Germany), 25mM dNTPs, 10mM Tris-HCl pH 8.3, 50mM KCl, 2.5 (to 5) mM $MgCl_2$ and approximately 100ng template DNA were used. Alternatively a PCR Mix REDTaqReadyMix (Sigma-Aldrich, Germany) was used according to manufacturer's

protocol. Amplification started with denaturation for 4 min at 96 °C followed by 30-35cycles of 96 °C for 30-45 sec, 58-63°C for 45-60sec, 72°C for 1-2min and a final extension step at 72°C for 5 to 10min. When screening for the loxP flanked Smad7 gene, additional 1µl dimethylsulfoxid (DMSO) was supplemented to the PCR reaction followed by a touchdown PCR starting with denaturation for 4 min at 94 °C followed by 11cycles of 94 °C for 30sec, 62°C for 45sec, 72°C for 1min followed by additional 19cycles of 94 °C for 30sec, 59°C for 45sec, 72°C for 1min and a final extension step at 72°C for 10min.

Name of primer	Sequence (5´-3´)	$T_{Ann.}$ °C	Direction
S7 FLOX5	GTC AGG TTG GAT CAC CAT GCC	62/59	sense
S7 FLOX3	GAC TGC CTG GAG AAG TGT GTC	62/59	anti-sense
S7 Δ sense	TGC AGA CCC GGA AAT TAG AC	60	sense
S7 Δ anti-sense	TTG GAT CAC CAT GCC AAC TA	60	anti-sense
Cre fwd	GGA CAT GTT CAG GGA TCG CCA GGC G	58	sense
Cre rev	GCA TAA CCA GTG AAA CAG CAT TGC TG	58	anti-sense
Actin forw	TGT TAC CAA CTG GGA CGA CA	58	sense
Actin rev	GAC ATG CAA GGA GTG CAA GA	58	anti-sense
IFNgR2 delta 1	TGA GTT CCA AGC AAG ACA GAG CC	56.5	sense
IFNgR2 delta 2	GTA GAA TGC GGC CGC GTT TA	56.5	anti-sense
IFNgR2 WT 1	CCC ATC TGT CCC TCT GCT TGT	56.5	sense
IFNgR2 WT 2	AGA GCC CAT GTG GTC GGA TT	56.5	anti-sense
IFNγR2 LoxP1	TGA GTT CCA AGC AAG ACA GA	56.5	sense
IFNγR2 LoxP2	CAG GGT AGA AAA GAT GTG CA	56.5	anti-sense
IFNγR2 LoxPsite	AAG TTA TGG TCT GAG CTC GC	56.5	anti-sense
CD11c-cre_Boris_s	ACT TGG CAG CTG TCT CCA AG	63	sense
CD11c-cre_Boris_as	GCG AAC ATC TTC AGG TTC TG	63	anti-sense

Table 5: List of primers routinely used for genotyping.

Sequences of oligonucleotides are shown in 5'-3' direction. Direction is designated "sense", if the primer orientation coincides with transcriptional direction, and "anti-sense" if otherwise.

2.2.3 Agarose gel electrophoresis

Gel electrophoresis on agarose gels (1-2% (w/v); 1xTAE (Sambrook, et al. 1989); 0.5mg/ml ethidium bromide) was used to separate DNA fragments by size and visualized on UV-Documentation-system QuantityOne (Bio-Rad Laboratories Inc.).

2.2.4 RNA Extraction from Cells

Total RNA from cells was prepared using the Rneasy Mini Kit (QIAGEN, Hilden, Germany) according to the manufacturer's protocol. The cell suspension was shradded using DNA shredder columns (Quiagen, Hilden, Germany) according to manufacturer's protocol. RNA concentration and purity was assessed on a NanoDrop (Thermo Scientific) according to manufacturer's protocol.

2.2.5 Quantitative real time PCR

Total mRNA was isolated using the RNEasy®-kit (Quiagen) from MACS-purified $CD11c^+$ cells or Dynabeads® DC-enriched splenic cells. cDNA preparation was performed using SuperScript® reverse transcriptase (Invitrogen) according to manufacturer's protocol. Quantitative real-time polymerase chain reaction (qRT–PCR) of mRNA coding for IL-6, TNF-α, IL-10, TGF-β, Smad7, IRF8, Batf3, IDO1 and IDO2 was performed using primers from QIAGEN and the QuantiTect SYBR Green RT–PCR kit and the light cycler StepOnePlus (Applied Biosystems) according to manufacturer's protocol. The relative mRNA amounts were determined by normalization to the housekeeping genes glyceraldehyde 3-phosphate dehydrogenase (GAPDH) or hypoxanthine guanine phosphoribosyl transferase (HPRT). The expression levels of mRNA were calculated using the ΔCT method and normalized to the wild-type control.

Primers for Quantitative Real-Time PCR were obtained from Qiagen as described on the their homepage https://www1.qiagen.com/GeneGlobe/Default.aspx.

2.3 Cell Biology

2.3.1 Preparation of single cell suspensions from lymphoid tissues

Thymi, spleens and LN were harvested from $S7^{\Delta DC}$ and control mice and homogenized in ice cold phosphate buffered saline (PBS, -Ca^{2+}/-Mg^{2+}, Gibco) containing 2% FCS using 40µm cell strainers (BD Biosciences). For preparation of DC, lymphoid tissues were pre-incubated with 2mg/ml collagenase type II (Gibco) and 20 units DNAse (Sigma Aldrich) at 37°C. Erythrocytes were lysed from spleen and thymus preparations in 140 mM NH_4Cl, 17 mM Tris-HCl pH 7.65 for 2 min at RT.

2.3.2 CNS isolation

Mice were anesthetized using Isofluoran (Abbott) and perfused with ice cold PBS. Brain and spinal cords were removed and homogenized using a razor blade. Tissue was incubated for 30min with PBS (+Ca^{2+}/+Mg^{2+}) containing 2mg/ml collagenase type II (Gibco, Germany) and 20 units DNAse at 37°C. The tissue was then homogenized with a syringe and CNS infiltrating cells were isolated on a percoll gradient (containing 30%, 37% and 70% of percoll) (Greter et al., 2005).

2.3.3 Isolation of skin cells

Back skin and ears of naïve mice were removed, incubated with RPMI media (supplemented with 5% Penstrep, 0,4mg/ml Liberase (Roche)) in 6 well plates for 2h 5% CO_2. Enzymatic reaction was stopped by addition of RPMI media (supplemented with 10%FCS; 1% Glutamin, 1% Penstrep, 0,01% ß-Mercaptoethanol). Back skin and ears were transferred into Medicons (Becton Dickinson) and homogenized using Medimachine (Becton Dickinson; program E; tube C). Homogenates were passed through 70µM cell strainers (BD Biosciences) and used for further analysis by flow cytometry.

2.3.4 Cell counting

Cell counts were determined by staining of cells with trypan blue solution (Gibco, Long Island, NY, USA) and counting unstained life cells using a Neubauer chamber (Assistent, Sondheim, Germany). The counted cell number in 16 single quadrants (N)

was multiplied by the dilution factor (V) and the 'chamber factor' (10^4), resulting in the number of viable cells per ml ($NxVx10^4$ = cell number). Alternatively cells were counted using CASYton (Roche Applied Science) according to manufacturer's protocol.

2.3.5 Magnetic cell sorting and FACS sorting

Specific cell populations were sorted for negative and positive fraction respectively by magnetic cell sorting (MACs; Miltenyi Biotec, Bergisch Gladbach, Germany) according to manufacturers protocol (Miltenyi et al., 1990). Briefly, cell populations were labeled with antibody-coupled microbeads (10µl beads, 90µl MACs Buffer (dPBS containing 2mM EDTA 0.5% BSA) per 10^7 cells) and cells were separated on LS, MS or LD MACs columns (Milteny Biotec, Germany) in a magnetic field. Alternatively DCs were enriched using the Dynabeads Mouse DC enrichment kit (Invitrogen) according to manufacture's protocol. Cell sorting was performed after pre-enrichment of desired cells using MACS and subsequent surface staining for desired markers with fluorescently labeled antibodies and cell sorting was performed on a BD FACSAria II (Becton Dickinson) with the help of Michaela Blanfeld. Cell purity of MACS purified, Dynabeads enriched or FACs sorted cells was assessed by flow cytometry and was >70% for DCs and >90% for T cell populations.

2.3.6 Flow cytometry

After red blood cell removal and prior to surface staining αFC block (BioXcell) was perfomed. Single cell suspensions were stained with fluorescent-labeled antibodies. When biotin-conjugated antibodies were used, than cells were subsequently stained with Streptavidin-conjugated fluorescent antibodies. The following antibodies were purchased from BD Biosciences unless otherwise specified: anti-mouse CD4 (L3T4), CD8α (53-6.7), CD11b (M1/70), CD19 (1D3), CD25 (7D4), CD44 (IM7), CD45.2 (104), CD62L (MEL-14), CD69 (H1.2F3), CD90.2 (53-2.1), CD90.1 (OX7), CD11c (HL3), SiglecH (eBio440c; eBiosciences), MHC-II (M5/114; eBiosciences), CD40 (3/23), CD80 (16-10A1), CD86 (GL1; eBiosciences), B220 (RA3-6B2; Biolegend), CD103 (M290; Biolegend), CD154 (MR-1, Biolegend, eBiosciences), PDL1 (MIH5; eBiosciences), EpCAM (G8.8; eBioscience), CD24 (M1/69; Biolegend), CD64 (X54-

5/7.1; Biolegend), GR-1 (RB-8C5), Ly6c (AL-21), CTLA-4 (UC10-451011), Sirpα (P84; eBioscience), Helios (22F6; Biolegend), CD45RA (14.8), PDCA1 (eBio927; eBioscience), TCRγδ (eBioGL3; eBioscience), F4/80 (BM8; eBioscience). Intracellular staining for CD207, IL-17A, IFN-γ and IDO1 was performed after cell re-stimulation for 4h with 50ng/ml Phorbol 12-Myristate 13-Acetate, 500ng/ml Ionomycin and 5mg/ml Brefeldin A. Antibodies specific for mouse CD207 (eBioL31; eBioscience), IL-17A (clone TC11-18H10.1), IFN-γ (clone XMG1.2), FoxP3 (clone FJK-16s; eBioscience) and IDO1 (clone 2E2.6; Novus Biologicals) were used for intracellular cytokine staining. For discrimination of MOG_{35-55}-specific effector T cells, cells were stimulated with 20µg/ml MOG_{35-55} for 3h and thereafter 5mg/ml Brefeldin A was added and cells were cultured for additional 3h. Intracellular stainings were performed according to the protocol of BD Cytofix/Cytoperm^{TM} kit (BD Biosciences) or Foxp3/ Transcription Factor Staining Buffer set (eBiosciences). Dead cells were excluded using a fixable viability dye (eBioscience). Cells were analysed using a FACS-Canto (BD Biosciences) with FACSDiva software (BD Biosciences) or FACScan (BD Biosciences) with CellQuest (BD Biosciences) software. Post acquisition analysis was performed using FlowJo or CellQuest software.

2.3.7 Culture of *ex vivo* lymphocytes

2.3.7.1 BMDC culture

For preparation of BMDCs, mice were sacrificed and BM cells were flushed out of the femurs. $2x10^6$ cells/ml were incubated for at least 8 days in IMDM medium containing 5% GM-CSF, 10% FCS, 0,1% β-Mercaptoethanol, 1% Glutamin and 1% PenStrep. Maturation of BMDCs was achieved by stimulation of the cells with 1µg/ml LPS for 24 hours. Harvesting of DCs was performed by incubation of the cells with Trypsin (Gibco) for 5 min.

2.3.8 Stimulation of cells for quantitative real time PCR or CBA analysis

For real time analysis triplicates of 300 000 DCs or BMDCs were stimulated under indicated conditions with 1µg/ml LPS, 100µg/ml Poly(I:C), 10ng/ml IFN-γ, or 10ng/ml TGF-β in RPMI medium (supplemented with 10%FCS; 1% Glutamin, 1%

Penstrep, 1% Nonessential amino acids; 1% Sodiumpyruvat, 1% Hepes, 0.01% β-Mercaptoethanol) for indicated time points or were left untreated.

For further CBA analysis of cytokines in supernatants, $0.5x10^6$ cells DCs were stimulated with or without 1µg/ml LPS (*Escherichia coli* 026.B6, Sigma) in absence or presence of 10ng/ml TGF-β1 (R&D Systems) in RPMI (supplemented with 10% FCS, 1% Glutamin, 1% Penstrep, 100U/ml penicillin, and 0.01% β-mercaptoethanol) overnight. Supernatants were harvested and cells were washed with PBS and stimulated with soluble CD40L (sCD40L; PeproTech, Rocky Hill, NJ) for additional 24h when supernatants were collected.

2.3.9 CFSE labelling

10^7 sorted or MACS enriched naïve 2D2 T cells were labeled with the fluorescent dye 0.5mM CFSE (carboxyfluorescein diacetate succinimidyl ester; Molecular probes, Eugene, Oregon, USA) (Lyons and Parish, 1994). Labeling was stopped after 8 min incubation at RT with RPMI medium (supplemented with 10%FCS; 1% Glutamin, 1% Penstrep, 1% Nonessential amino acids; 1% Sodiumpyruvat, 1% Hepes, 0.01% β–Mercaptoethanol). Proliferation of the cells was determined based on the loss of fluorescent intensity with every cell cycle.

2.3.9.1 *in vitro* DC mediated T cell proliferation

$0.5x10^6$ CFSE-labeled MACS-purified $CD4^+$ 2D2 T cells were co-cultured with MACS-purified DCs, isolated from collagenase treated spleens, or GM-CSF derived BMDCs. DC/T cells were cultured in a ratio of 1:10 or 1:20 in RPMI medium (supplemented with 1% Glutamin, 1% PenStrep, 0,1% β-Mercaptoethanol and 1µg/ml or 5µg/ml MOG_{35-55}). Cells were cultured in round bottom 96-well plates, in the absence or presence of 10ng/ml TGF-β for 4-5 days at 37°C and 5% CO_2.

2.3.9.2 *in vitro* DC mediated Th1 and Th17 cell differentiation

40 000 DCs derived from spleen and LN, enriched using Dynabeads Mouse DC enrichment kit (Invitrogen), were co-cultured with 400 000 $CD4^+CD62L^+$ MACS purified naïve 2D2 T cells for 6 days in RPMI media (supplemented with 10%FCS, 1% Glutamin, 1% PenStrep, 0,1% β-Mercaptoethanol) containing either medium

alone, or medium supplemented with 20µg/ml MOG_{35-55} with or without 1µg/ml LPS and in presence or absence of 10ng/ml TGF-β.

20 000 GM-CSF derived BMDCs were co-cultured with 400 000 $CD4^+CD62L^+$ MACS purified naïve 2D2 T cells for 6 days in RPMI media (supplemented with 10%FCS, 1% Glutamin, 1% PenStrep, 0,1% β-Mercaptoethanol) containing either medium alone, or medium supplemented with 20µg/ml MOG_{35-55} with or without 1µg/ml LPS and in presence or absence of 10ng/ml TGF-β.

2.3.9.3 *in vitro* DC mediated iTreg differentiation

Duplicates of 50 000 splenic MACS-purified DCs pulsed with 20µg/ml MOG_{35-55} were further left untreated or stimulated with 4ng/ml TGF-β1 in presence or absence of 4µM 1-MT or with 4µM 1MT alone for 12h in RPMI medium (supplemented with 10%FCS; 1% Glutamin, 1% Penstrep, 1% Nonessential amino acids; 1% Sodiumpyruvat, 1% Hepes, 0,01% ß-Mercaptoethanol) in round bottom 96-well plates, 37°C and 5% CO_2. After 12h DCs were washed extensively using PBS supplemented with 2% FCS, and co-cultured with 100 000 naïve ($CD4^+CD44^-$ $CD62L^+GFP^-$) FACS sorted T cells derived from naïve 2D2 FoxP3-GFP mice for additional 4 days. The amount of iTregs was assessed based on *de novo* expression of GFP (FoxP3).

2.3.10 Immunohistochemistry

Histology was performed as described (Prinz et al., 2008). Mice were perfused during deep anaesthesia with ice-cold saline. Spinal cords were removed and fixed in 4 % buffered formalin. Then, spinal cords were dissected and embedded in paraffin before staining with haematoxylin and eosin, luxol fast blue to assess the degree of demyelination, macrophage-3 antigen (BD Pharmingen, clone M3/84, dilution 1:200) for macrophages/ microglia, CD3 for T cells (Serotec, clone CD3-12, dilution 1:100), B220 for B cells (BD Pharmingen clone RA3-6B2, dilution 1:200) and deposition of amyloid precursor protein (APP, Millipore, clone 22C11,dilution 1:3000), which reflects axonal damage. Secondary antibodies were polyclonal rabbit anti mouse biotinylated (DAKO, order number E0464, Lot 00073409) and used in a dilution 1:200, in combination with avidin-peroxidase (Sigma, order number A7419, 1:1000).

Tissue sections were evaluated on Olympus BX-61 microscope using the cell-P software (Olympus).

2.3.11 Cytokine ELISA

The supernatants collected from *in vitro* assays were used for cytokine ELISA. Levels for IL-6 were examined by BD OptEIA- Mouse IL-6 ELISA kit (BD Bioscience) according to the manufacturer's protocol.

2.3.12 Cytokine bead array

The levels of TNF-α, IL-10, IL-6, and TGF-β in supernatants of stimulated cells were determined by cytometric bead assay (Bender MedSystems, Vienna, Austria), according to the manufacturer's instructions. Analysis was performed on FACS Canto-II (BD Biosciences), and the concentration of measured cytokines was calculated using FCAP Array software (BD Biosciences).

2.4 Mouse experiments

Tail bleeding as well as the general handling of mice was performed according to Hogan (Hogan et al., 1987) and Silver (Silver, 1995).

2.4.1 Mice

CD11c-Cre$^{+/-}$ (Caton et al., 2007) were bred to Smad7$^{fl/fl}$ mice (Kleiter et al., 2010) to generate animals with a DC-specific Smad7 deletion (S7$^{\Delta DC}$). Cre-negative littermates or C57BL/6 wild type mice were used as controls. In addition S7$^{\Delta DC}$ mice were bred to IFN-γRII$^{fl/fl}$ mice (unpublished; generated in the laboratory of Prof. Werner Müller) generating a mouse line with DC specific loss of Smad7 and IFN-γRII (IFN-γR2$^{\Delta DC}$S7$^{\Delta DC}$). 2D2 TCR transgenic mice (Bettelli et al., 2003) were bred to FoxP3-GFP KI (Bettelli et al., 2006) mice resulting in a FoxP3 reporter strain with a MOG-specific TCR (2D2 FoxP3-GFP). All animals were on a C57BL/6 background and kept under specific pathogen free conditions at the central animal facility in Mainz. Experiments were performed in accordance with guidelines of the Institutional Animal Care and Use Committee of the University of Mainz.

2.4.2 Induction and clinical evaluation of EAE

In order to induce EAE, 8-10 week old mice were injected with 50µg myelin oligodendrocyte glycoprotein (MOGp$_{35-55}$; (amino acid sequence MEVGWYRSPFSRVVHLYRNGK) obtained from Research Genetics; Huntsville, Alabama, USA) in complete Freund's adjuvans (CFA; Difco Laboratories, Detroit Michigan, USA) supplemented with 8mg/ml of heat-inactivated *Mycobacerium tuberculosis* H37RA (Difco Laboratories, Detroit Muchigan, USA) in a total volume of 100 µl was administered as a subcutaneous (s.c.) injection into the tail base. On days 0 and 2, mice were injected intra-peritoneally (i.p.) with 200ng pertussis toxin in a volume of 200µl (Sigma Aldrich). Daily scoring was performed using the following criteria: 0 = healthy; 1 = limp tail; 2 = partial hindlimb weakness/ataxia; 3 = paralysis of at least one hindlimb; 4 = complete hindlimb paralysis; 5 = partial forelimb paralysis; 6 = moribund/dead.

2.4.3 Measurement of reactive oxygen species

Measurement of reactive oxygen species in the blood was performed in the laboratory of molecular cardiology, University Medical Center Mainz by Maria Isabel Schmidgen as described in (Daiber et al., 2004; Oelze et al., 2006). Mice were subjected to EAE and 14 days after MOG_{35-55} immunization venous blood was collected into 3.8% sodium citrate and further diluted 1:50 in PBS (-Mg^{2+}, -Ca^{2+}, and bicarbonate). The chemiluminescence (ECL) signal enhanced by 100µm of 8-amino-5-chloro-7-phenylpyridol [3,4-*d*] pyridazine-1,4-(2H,3H) dione sodium salt (L-012) was counted in absence or presence of 10µm phorbol 12,13-dibutyrate (PDBU). After incubation for 20min, the ECL was measured and given as counts/min/ml.

2.4.4 Ear swelling measurement

Mice were subjected to EAE immunization as described above. Five days post immunization, 3 µg MOG_{35-55} was injected into the dorsal side of the right ear. As a control, PBS was injected into the left ear. Using a caliper micrometer (Mitutoyo), ear thickness was measured prior to immunization, as well as 24h, 48h and 72h post MOG_{35-55} re-challenge. MOG_{35-55} specific ear swelling (of each individual at each time point) was assessed by subtracting ear thickness of the saline (PBS) treated from the thickness of the MOG treated ear at each measurement time point.

2.4.5 *In vivo* inhibition of IDO activity using 1-Methyl-D-Tryptophan

Mice were treated with 10mg 1-Methyl-D-Tryptophan (1-MT; Sigma Adrich) reconstituted in 2M HCl and adjusted to pH 7 using 2M NaOH or were injected with the respective vehicle control on the day of $MOG_{35/55}$/CFA immunization.

2.4.6 *In vivo* depletion of $CD25^+$ cells

Mice were treated with 0.5mg PC61 (αCD25 antibody; BioXcell) or 0.5mg IgG1 isotype control (BioXcell), five and three days prior to MOG_{35-55}/CFA immunization. To test for efficient cell depletion mice were bled one day prior to MOG_{35-55}/CFA immunization and circulating leukocytes were stained for surface CD25 expression.

2.4.7 Assessment of antigen uptake

Mice were injected subcutaneously with 50µl/mouse Fluoresbrite® YG Microspheres 1.0µm (Polysciences, Inc.) emulsified in $MOG_{35/55}$/CFA. Antigen uptake and DCs migration was assessed 24h, 48h and 72h later by analysis of fluorescently-labeled cells found in the dLN.

2.4.8 Statistical analysis

Values are presented as mean ± SEM. Statistical significance of two groups was assessed using 2-tailed Student's t test, when comparing two groups with two additional treatments two-way ANOVA and Bonferroni posttests were used. When comparing two EAE groups statistical significance was determined by measurements of EAE area under curve (AUC) followed by Student's t test. EAE significance of two groups with two different treatments was assessed by measurement of EAE area under the curve (AUC) followed by two-way ANOVA and Bonferroni posttests. *$p \leq 0.05$, **$p \leq 0.005$, ***$p \leq 0.0005$; $p > 0.05$ was considered not significant.

2.4.9 Study approval

Animal experiments were performed in accordance with guidelines of the Institutional Animal Care and Use Committee of the University of Mainz.

3 Results

3.1 Mouse model of DC specific Smad7 deletion

To study the role of Smad7 specifically in DCs, a conditional Smad7 knockout mouse model was used, in which the promoter and exon1 of Smad7 were flanked by loxP sites (Smad7$^{fl/fl}$) (Kleiter et al., 2010). Upon cross of these mice to a DC-specific Cre-mouse line (CD11c-Cre) (Caton et al., 2007), subsequent Cre mediated recombination occurred, resulting in a mouse strain specifically devoid of Smad7 in DCs, which for simplicity is from here on termed S7$^{\Delta DC}$. Figure 1 depicts the targeting strategy of conditional Smad7 knockout mice (Kleiter et al., 2010).

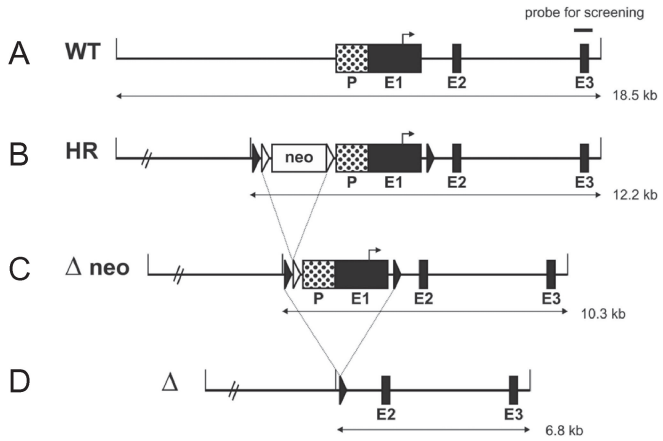

Figure 1: Targeting strategy of conditional Smad7 knockout mice

(A) Schematic overview of the wild-type smad7 locus. **(B)** Upon homologous recombination (HR) in the murine smad7 genomic locus, promoter (P) and exon1 (E1) of smad7 were flanked by loxP-sites (black triangles) and in addition an frt-flanked (white triangles) neomycin resistance cassette (neo) was inserted between the first loxP site and the smad7 promoter. The translational start site in exon I is indicated by a black arrow. **(C)** The neo cassette was excised upon Flp-mediated recombination (Δ neo). **(D)** Conditional deletion of the promoter and exon I of smad7 occurred upon Cre-mediated recombination (Δ). Adapted from Kleiter et al., 2010.

At first the efficiency of Smad7 deletion in DCs derived from S7$^{\Delta DC}$ mice was assessed. Therefore real time analysis for Smad7 transcripts in CD11c MACS purified splenic DCs from S7$^{\Delta DC}$ and control mice, stimulated with either TGF-β1 or IFN-γ for the indicated time points, was performed (Figure 1A). Indeed, DCs derived from S7$^{\Delta DC}$ mice showed significantly reduced Smad7 expression levels by 80-90% as compared to controls, irrespective of the stimuli used.

The yield of *ex vivo* isolated DCs is relatively low and often limits consecutive experimental setup. Yet, DCs can be generated *in vitro* by stimulating bone -marrow derived cells with granulocyte-macrophage-colony stimulating factor (GM-CSF), resulting in elevated amounts of DCs. These cells are termed bone marrow derived DCs (BMDCs) and show many similarities to monocyte derived DCs, which are predominantly present upon inflammation. To test for Smad7 deletion efficiency in BMDCs generated from $S7^{\Delta DC}$ mice, real time analysis for Smad7 transcripts was performed. The efficiency of Smad7 deletion in BMDCs generated from $S7^{\Delta DC}$ mice (Figure 1B) reached 80%, when no additional stimulus was added and was comparable to untreated splenic DCs (Figure1A). LPS and Poly-IC treatment of $S7^{\Delta DC}$ BMDCs likewise resulted in 80-90% Smad7 deletion efficiency. However when an additional Smad7 expression inducing stimulus like TGF-β was used, only 40-60% Smad7 deletion efficiency could be observed in BMDCs of $S7^{\Delta DC}$ mice as compared to corresponding controls. Therefore, when comparing Smad7 expression levels of TGF-β treated $S7^{\Delta DC}$ BMDCs (Figure 1A) to the respective splenic DCs expression levels in knockout mice (Figure 1A) a discrepancy of 40-50% could be detected. This reduced Smad7 deletion efficiency is taken into account when performing and interpreting experiments performed with BMDCs.

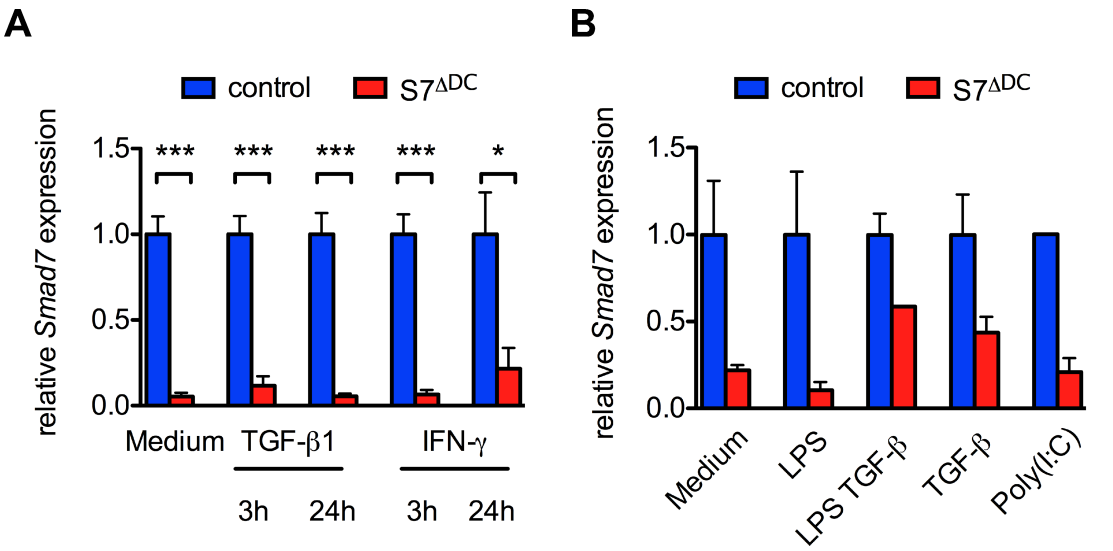

Figure 2: Smad7 deletion efficiency in $S7^{\Delta DC}$ derived DCs

(A) Real time analysis for Smad7 expression of splenic CD11c MACs purified DCs from control (n=4) and $S7^{\Delta DC}$ (n=4) mice either untreated or treated with 10ng/ml TGF-β or 10ng/ml IFN-γ for the indicated time points. Shown is one representative of five independent experiments. **(B)** Real time analysis of GMCSF derived BMDCs from control (n=2) and $S7^{\Delta DC}$ mice **(**n=3) either untreated or treated with 10ng/ml TGF-β, 1µg/ml LPS or 100µg/ml

Poly(I:C) for12h. Bar graphs depict mean value ± SEM. Statistical significance was assessed using Student's t-Test (*p ≤0.05, **p ≤ 0.005, ***p ≤ 0.0005).

3.2 Impact of DC specific Smad7 deletion during DC homeostasis

DCs are important regulators of the immune system and as professional antigen presenting cells (APCs) induce immunity versus tolerance decisions to foreign and self- antigens (Steinman et al., 2003). DCs can be subdivided into diverse subsets including the conventional DCs (cDCs), plasmacytoid DCs (pDCs), monocyte derived DCs and the skin resident Langerhans cells. DC lineage commitment is controlled by the hematopoetic growth factor granulocyte-macrophage colony-stimulating factor (GM-CSF), and cytokines such as fms-like tyrosine kinase 3 ligand (FLt3l) as well as selected transcription factors (Merad et al., 2013). TGF-β signaling plays an important role during DC development and differentiation. TGF-β signaling is crucial for the development of Langerhans cells *in vivo* (Borkowski et al., 1996). Similarly, exposure of DC progenitors to TGF-β1, led to enhanced expression of their relevant transcription factors along with cDCs development (Felker et al., 2010).
Hence, experiments were designed to investigate whether loss of Smad7 during steady state might impact DC development and DC lineage commitment.

3.2.1 Development and homeostasis of skin- resident DC subsets following DC-specific Smad7 deletion

The skin serves as a physical barrier comprising a sophisticated immune surveillance system serving as a first line of defense against external pathogens. The skin consists of the exterior epidermis and the interior dermis. Both epidermal and dermal DCs, constantly survey the skin for presence of pathogens. Langerhans cells are located in the epidermis and can be characterized based on the high expression levels of the c-type II lectin receptor Langerin (CD207; (Valladeau et al., 1999; Valladeau et al., 2000)). Langerin expression can also be found on a dermal DC subset, that unlike Langerhans cells, does not co-express the adhesion marker EpCAM (Nagao et al., 2009).
As already mentioned, Langerhans cell development is strongly dependent on TGF-β1, since TGF-$\beta1^{-/-}$ mice are devoid of Langerhans cells (Borkowski et al., 1996).

However, the development of langerin$^+$ dermal DCs is not affected by the deletion of TGF-β1, since TGF-β1 knockout mice harbor normal frequencies of dermal langerin$^+$ DCs (Merad et al., 2008).

When analyzing skin of naïve S7$^{\Delta DC}$ mice, there was no significant difference in the percentages or total cell counts of Langerhans cells or Langerin positive dermal DCs as compared to control animals. This data suggests that loss of Smad7 does not affect their development or homeostasis and it could be speculated that prolonged TGF-β signaling does reach a point of saturation at which increased signaling does not result in increase in Langerhans cells.

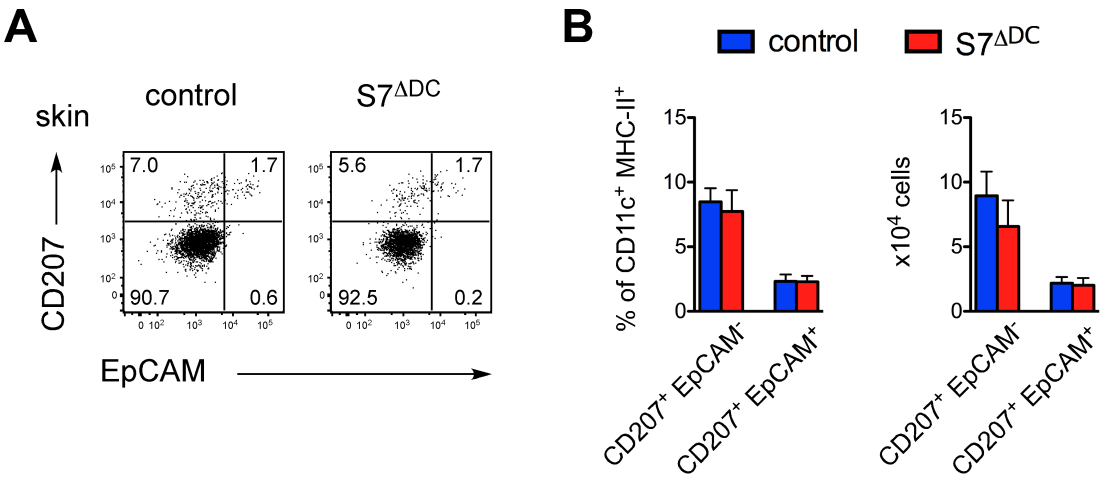

Figure 3: Comparable skin-resident dermal DC and Langerhans cells populations during steady state

(A) Representative FACs blots of Langerhans cells (CD11c$^+$ MHC-II$^+$ CD207$^+$ EpCAM$^+$) and dermal langerin positive DCs (CD11c$^+$ MHC-II$^+$ CD207$^+$ EpCAM$^-$) in the skin of 8 month old control (n=7) and S7$^{\Delta DC}$ (n=5) mice. Cells were pregated on CD11c$^+$ MHC-II$^+$ cells. Shown is one representative of two independent experiments. **(B)** Statistical analysis showing percentage and total cell counts of respective DC subsets from (A). Bar graphs depict mean value ± SEM. Statistical significance was assessed using Student's t-Test (*p ≤0.05, **p ≤ 0.005, ***p ≤ 0.0005).

3.2.2 Thymic DC development and homeostasis following DC-specific Smad7 deletion

The thymus, as a primary lymphoid organ, plays an important role in the development of T cells, which undergo various maturation steps ensuring proper rearrangement of their T cell receptor. The T cell receptor enables them to recognize antigens presented by APCs, such as DCs, on their MHC complex and to discriminate between self and foreign antigens, hence regulating tolerance and infection (Klein et al., 2014). The deletion of potentially auto-reactive T cells thus establishes central tolerance.

Proper T cell receptor formation is thus tightly regulated in order to enable recognition of pathogens without eliciting autoimmunity. Although thymocytes positive and negative selection requires recognition of antigens presented by cortical and medulla thymic epithelial cells (cTECs and mTECs, respectively), DCs have been shown to play an important role in this selection process (Bonasio et al., 2006; Brocker et al., 1997; Gallegos and Bevan, 2004; Gao et al., 1990; Proietto et al., 2008).

As DC-specific TGF-βR deletion results in premature involution of the thymus with complete loss of the thymic cortex at advanced age (Ramalingam et al., 2012)., firstly $S7^{\Delta DC}$ mice were analyzed for thymic DC subsets. Three DC subsets can be distinguished in the thymus based on the expression levels of the surface molecules CD11c, CD45RA and signal regulatory protein (Sirpα, also termed CD172a). pDCs are defined as $CD11c^{int}$ $CD45RA^{+}$, while thymic resident DCs, arising from thymic resident progenitor cells, are $CD11c^{+}$ $Sirp\alpha^{-}$,whereas thymic migratory DCs can be characterized as $CD11c^{+}$ $Sirp\alpha^{+}$ (Lahoud et al., 2006; Proietto et al., 2008; Vremec et al., 2000).

In contrast to the results previously described by Ramalingam et al., there was no significant difference in the percentage or total cell numbers of pDCs, thymic resident or thymic migratory DCs in $S7^{\Delta DC}$ as compared to control mice (Figure 4A).

TGF-β signaling on DCs in the presence of LPS *in vitro* has been associated with reduced antigen presentation and co-stimulation (Geissmann et al., 1999). However, another study using mice with a DC specific TGF-β receptor II disruption did not detect any difference in the expression of co-stimuli *in vivo* (Ramalingam et al., 2012). To test if loss of Smad7 might affect the expression of co-stimuli by thymic DCs during steady state, FACS stainings for the surface expression of CD40, CD80 and CD86 of thymi from $S7^{\Delta DC}$ and controls were performed. Yet, there was no difference in the expression levels of CD40, CD80 or CD86 between DCs derived from $S7^{\Delta DC}$ and controls (Figure 4B).

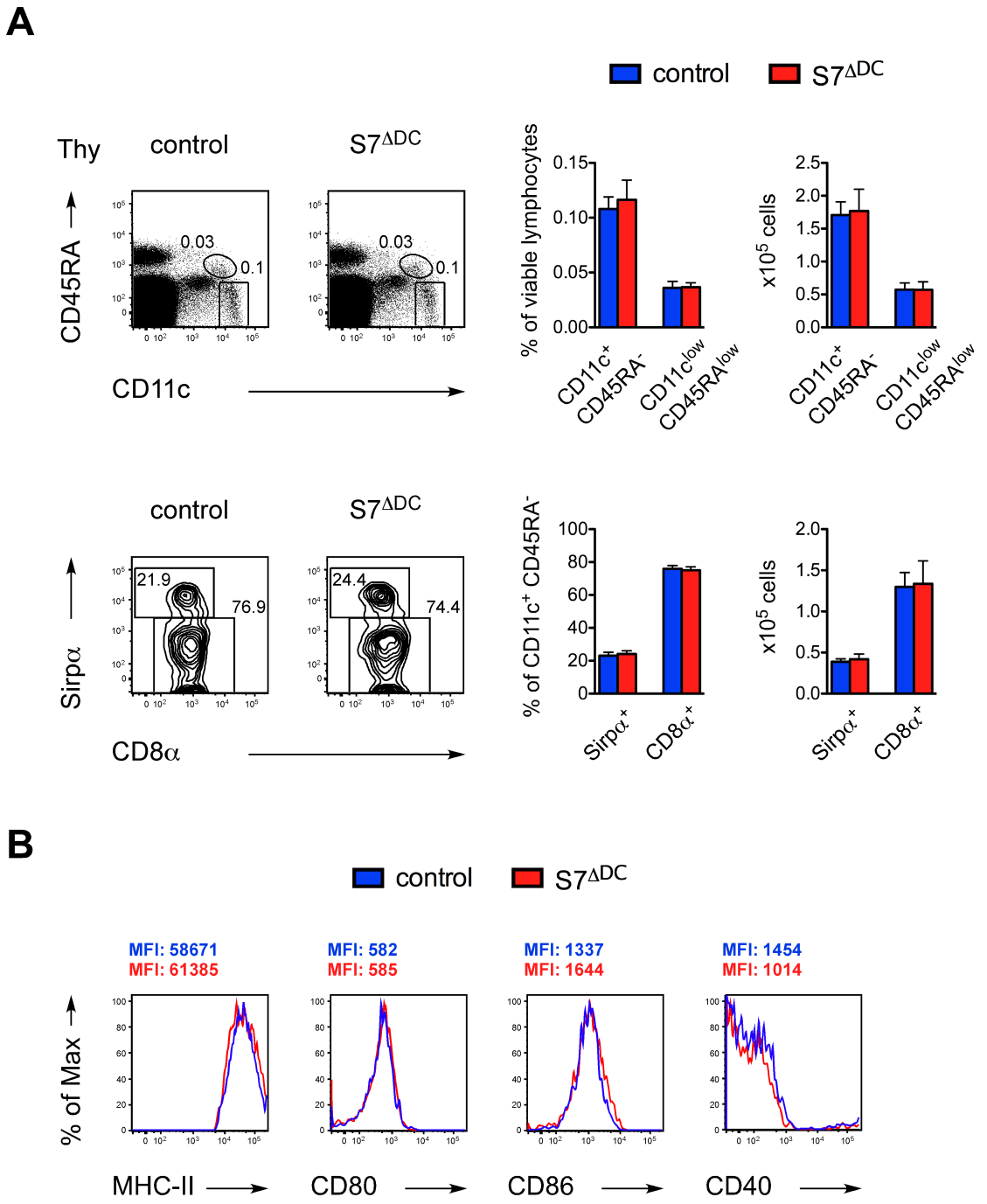

Figure 4: Smad7 does not affect DC subsets and their activation status in the thymus

(A) Representative FACs blots of thymic DC subsets in control (n=3) and $S7^{\Delta DC}$ (n=3) mice. In the upper panel representative FACs blots and the corresponding frequencies as well as total cell counts of pDCs ($CD11c^{low}$ $CD45RA^{low}$) and conventional DCs ($CD11c^{+}$ $CD45RA^{-}$) all gated on viable cells are shown. In the lower panel migratory $CD11c^{+}$ $CD8^{+}$ $Sirp\alpha^{-}$ DCs and thymic resident $CD11c^{+}$ $CD8a^{-}$ $Sirp\alpha^{+}$ DCs are shown as gated on viable $CD11c^{+}$ $CD45RA^{-}$ cells. **(B)** Representative FACS blots and mean fluorescence intensity (MFI) of MHC-II, CD80, CD86 and CD40 expression levels gated on $CD11c^{+}$ $MHC\text{-}II^{+}$ cells are shown. Bar graphs depict mean value ± SEM. Statistical significance was assessed using Student's t-Test (*p ≤0.05, **p ≤ 0.005, ***p ≤ 0.0005).

3.2.3 Smad7 deletion affects splenic DC subset commitment during steady state

The spleen and lymph nodes as secondary lymphoid organs play an important role as sites of antigen presentation and consequently induction of tolerance or immune response. When peripheral tissue DCs encounter antigens such as exogenous, commensal- or food antigens, they migrate to the draining lymph nodes (dLNs) and present these antigens to $CD4^+$ or $CD8^+$ T cells. In this way DCs regulate peripheral tolerance, while upon infection or injury mediate immunity (Belz et al., 2002).

3.2.3.1 Smad7 deletion does not affect the amount of overall DCs in peripheral lymphoid organs

It was next examined if DC specific Smad7 deletion might affect the total amounts of conventional DCs present in the peripheral lymphoid organs during steady sate.
The analysis of conventional splenic DCs in naïve $S7^{\Delta DC}$ mice revealed no significant difference in frequencies or total cell counts of overall DCs compared to controls, as based on the surface co-expression of CD11c and MHC-II (Figure 5A). Likewise, DC frequencies and total cell counts of iLN resident ($CD11c^{high}$ $MHC\text{-}II^+$) and migratory ($CD11c^+$ $MHC\text{-}II^{high}$) DCs were comparable between naïve $S7^{\Delta DC}$ mice and controls (Figure 5B).
Furthermore it was tested, whether loss of Smad7 might affect the activation status of overall splenic and iLN conventional $CD11c^+$ $MHC\text{-}II^+$ DCs. Analysis of MHC-II expression as well as expression of the co-stimulatory molecules CD80, CD86 and CD40 on the splenic $CD11c^+$ $MHC\text{-}II^+$ DCs was not significantly altered by deletion of Smad7 as compared to controls (Figure 5C). Similarly, DC specific Smad7 deletion did not affect MHC-II, CD80, CD86 and CD40 expression in migratory and iLN resident conventional DCs (Figure 5D).

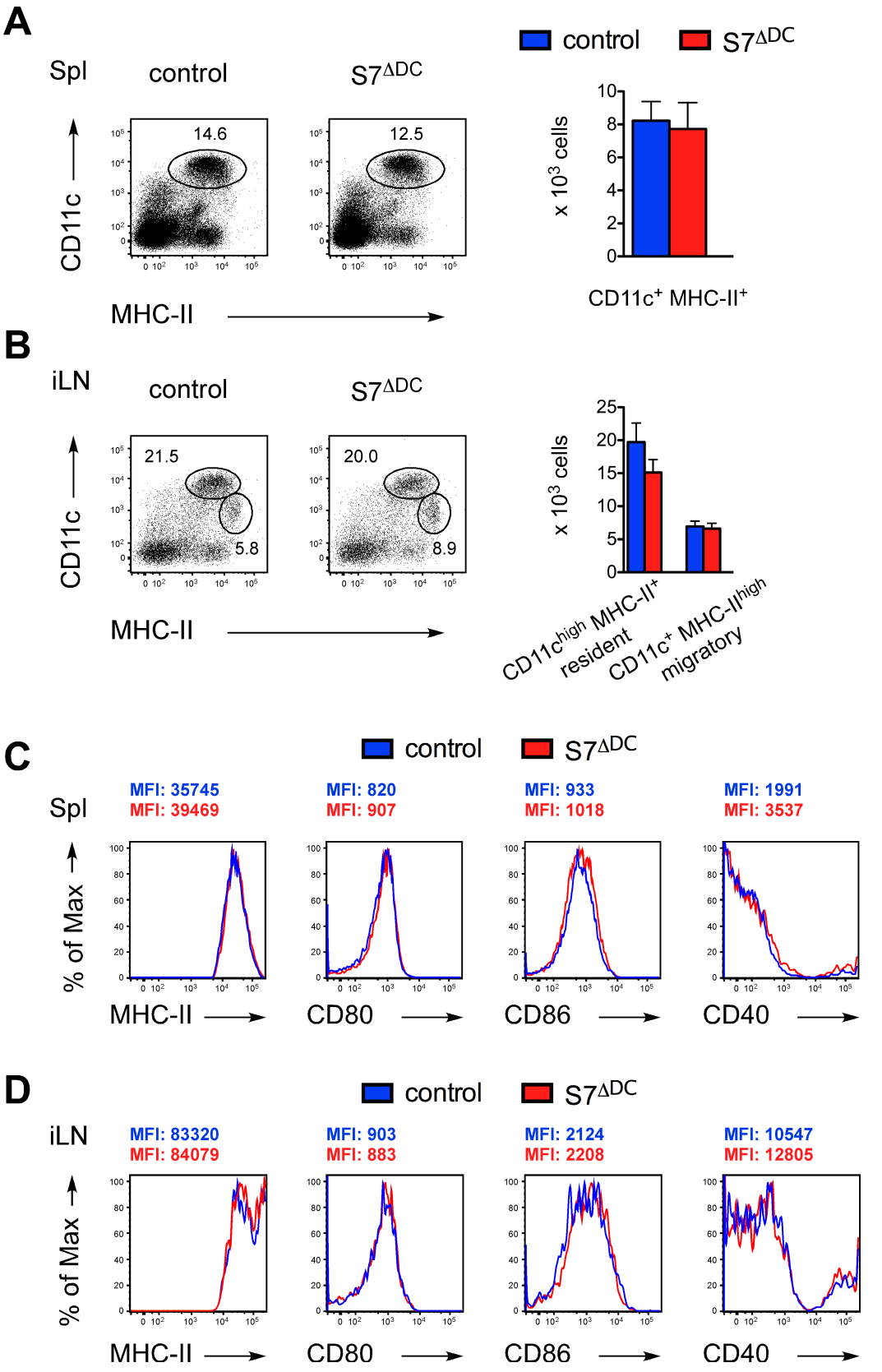

Figure 5: Total dendritic cell frequencies and DC activation status in naïve mice are not affected by Smad7 deletion

(A) FACs analysis of splenic DCs in control (n=6) and $S7^{\Delta DC}$ (n=7) mice as gated on $CD90.2^-$ $B220^-$ cells. **(B)** FACs analysis of iLN DCs in control (n=6) and $S7^{\Delta DC}$ (n=7) mice as gated on $CD90.2^-$ $B220^-$ cells. **(C)** Representative FACs blots illustrating MHC-II, CD80, CD86 and CD40 expression levels of splenic and **(D)** iLN DCs of naïve control (n=3) and $S7^{\Delta DC}$ (n=3) mice as gated on viable $CD11c^+$ $MHC\text{-}II^+$ cells. Bar graphs depict

mean value ± SEM. Statistical significance was assessed using Student's t-Test (*p ≤0.05, **p ≤ 0.005, ***p ≤ 0.0005).

Since the overall DC amounts were not affected by the deletion of Smad7, it was next assessed whether the absence of Smad7 might affect the composition of conventional DC subsets such as the $CD8^+$, $CD11b^+$ and $CD103^+$ in the iLN and spleen during steady state. An *in vitro* study using common DC progenitors stimulated with TGF-β1 reported increased differentiation towards conventional DCs. However, CD11c specific TGF-βRII deletion did not result in altered conventional DC frequencies (Felker et al., 2010; Ramalingam et al., 2012).

Analysis of iLN of naïve $S7^{\Delta DC}$ mice revealed no significant difference in the frequencies of $CD8^+$ or $CD11b^+$ cDCs as compared to controls (Figure 6A). Among the $CD8^+$ DCs, the frequencies of $CD8^+$ $CD103^+$ cDCs were increased by 1,7 –fold, however did not reach significance due to high individual heterogeneity (Figure 6B). TGF-β1 induces CD103 expression in human $CD8^+$ T cells (Mokrani et al., 2014). To assess whether the increased levels of $CD8^+$ $CD103^+$ cells might be attributed to an increased expression of CD103 on the respective DCs, the mean CD103 fluorescence intensity was assessed. Yet, the CD103 expression levels of $CD8^+$ $CD103^+$ cDCs were not significantly increased by the DC specific Smad7 deletion (Figure 6C).

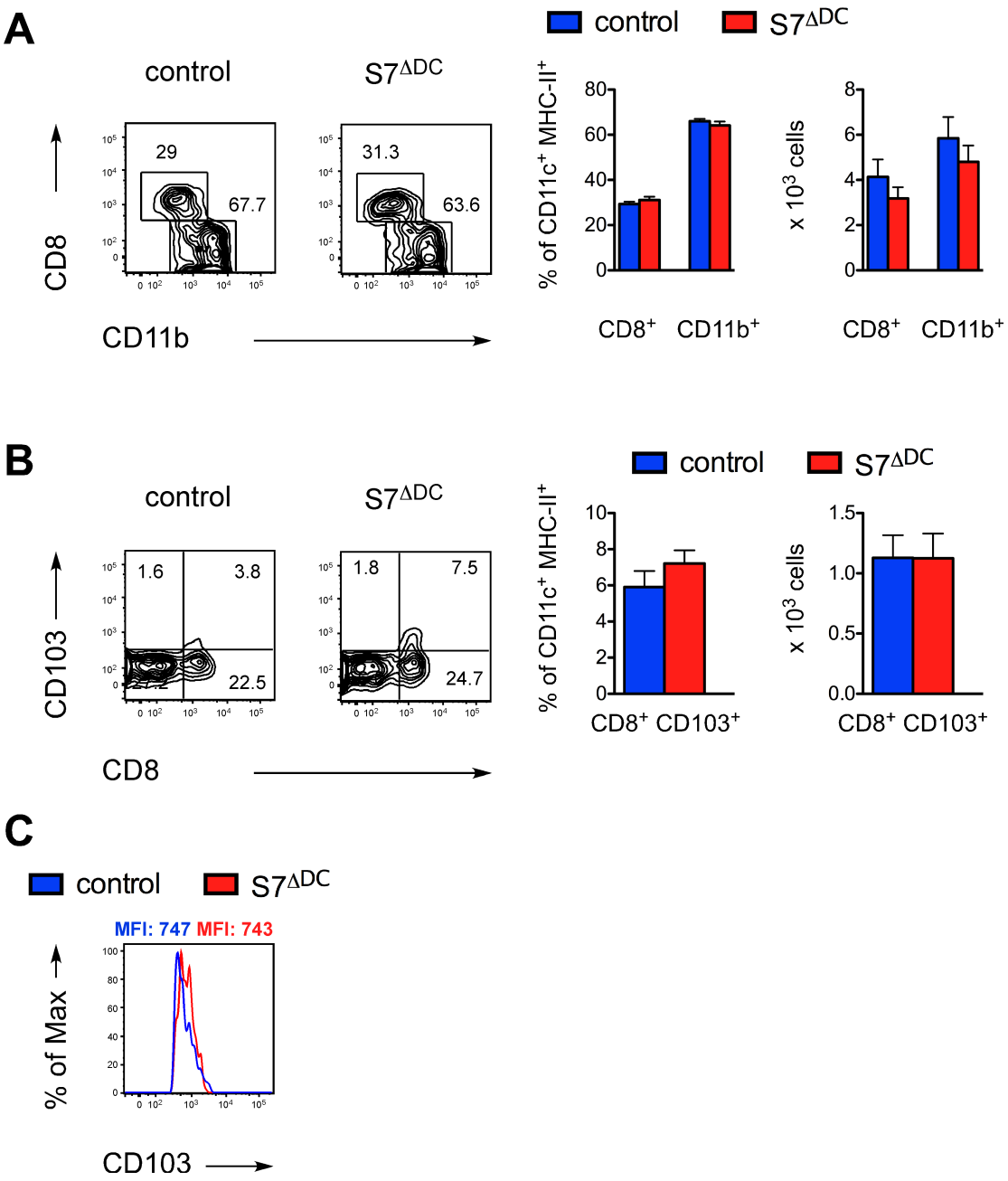

Figure 6: iLN cDC subsets are not affected by the loss of Smad7 during steady state

Representative dot blots and cell counts of iLN **(A)** $CD8^+$, $CD11b^+$ as well as **(B)** $CD8^+$ $CD103^+$ DCs in control (n=6) and $S7^{\Delta DC}$ (n=7) mice. **(C)** $CD103^+$ mean fluorescence intensity (MFI) of $CD8^+$ DCs from iLN of naïve control (n=6) and $S7^{\Delta DC}$ (n=7) mice as gated on $CD11c^+$ $MHC\text{-}II^{high}$ resident DCs. Bar graphs depict mean value ± SEM. Statistical significance was assessed using Student's t-Test (*p ≤0.05, **p ≤ 0.005, ***p ≤ 0.0005).

In contrast to the results obtained from the iLN, analysis of the splenic cDCs subsets in $S7^{\Delta DC}$ mice during steady state however, revealed a significant increase of $CD8^+$ DCs (1.3-fold) and consequently a reduction of the $CD11b^+$ cDCs as compared to control mice. Furthermore, lack of Smad7 in DCs resulted in a 1.7-fold increase in

splenic CD103$^+$ expressing CD8$^+$ cDCs without affecting the CD103$^+$ mean fluorescence intensity (Figure 7).

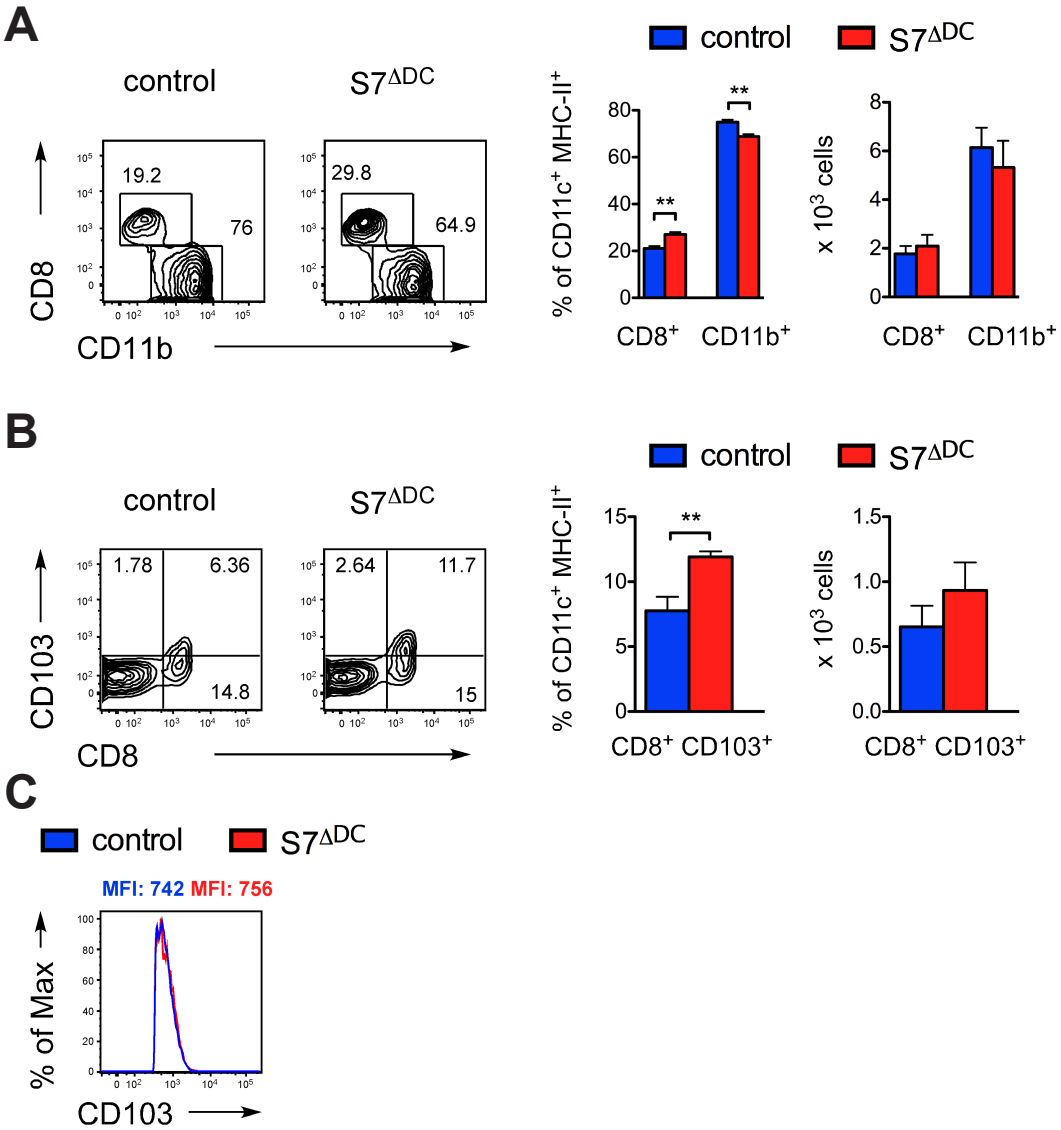

Figure 7: Smad7 increases CD8$^+$ CD103$^+$ DCs in the spleen during steady state

Representative dot blots and cell counts of splenic **(A)** CD8$^+$, CD11b$^+$ as well as **(B)** CD8$^+$ CD103$^+$ DCs in control (n=6) and S7$^{\Delta DC}$ (n=7) mice. **(C)** CD103$^+$ mean fluorescence intensity (MFI) of CD8$^+$ DCs from naïve control (n=6) and S7$^{\Delta DC}$ (n=7) mice as gated on CD11c$^+$ MHC-II$^+$ DCs. Bar graphs depict mean value ± SEM. Statistical significance was assessed using Student's t-Test (*p ≤0.05, **p ≤ 0.005, ***p ≤ 0.0005).

Besides conventional DCs lymphoid tissues also comprise pDCs, which express lower levels of CD11c and MHC-II than conventional DCs. An in *vitro study* in which common DC progenitors were stimulated with TGF-β reported an upregulation of transcription factors relevant for conventional DC development and inhibiting pDC instructive factors (Felker et al., 2010) Yet, mice lacking TGF-βRII specifically on

DCs did not display differences in the amounts of pDCs *in vivo* (Ramalingam et al., 2012). It was therefore next examined if loss of Smad7 might affect pDCs in the iLN and spleen of $S7^{\Delta DC}$ mice during steady state.

Analysis of pDCs ($B220^+$ $Ly6c^+$ $PDCA\text{-}1^+$ $Siglec\text{-}H^+$) from $S7^{\Delta DC}$ mice versus control animals revealed no significant difference in percentage or total cell counts of pDCs in the spleen or iLN (Figure 8).

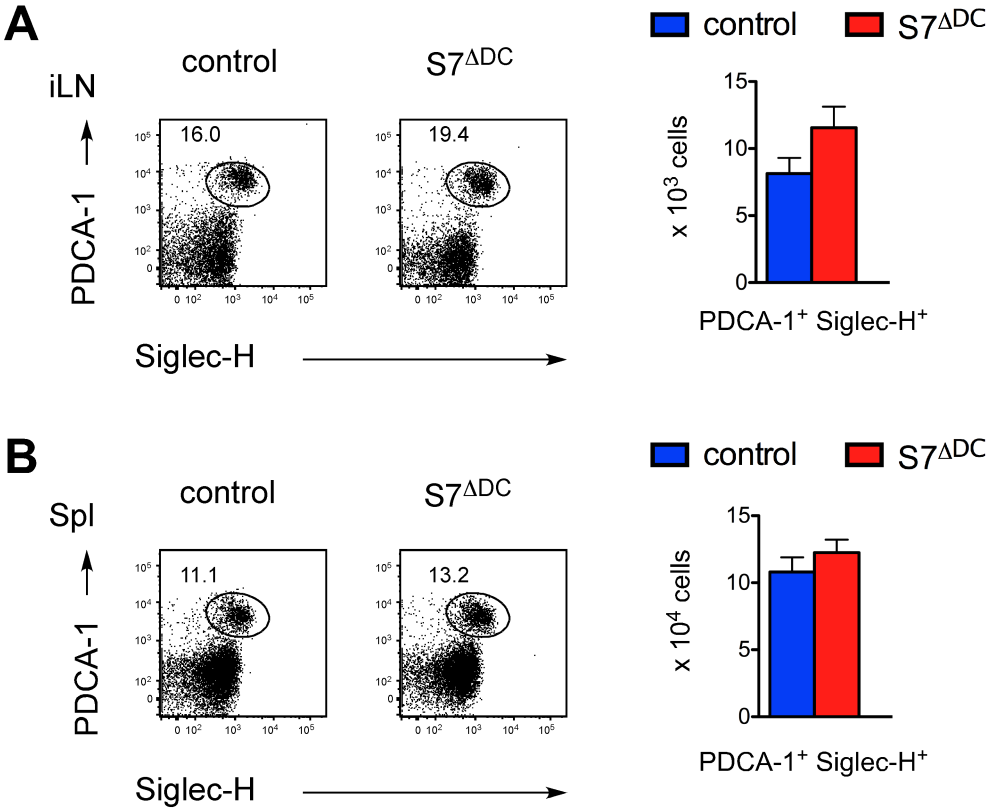

Figure 8: DC specific Smad7 deletion does not affect pDC development in steady state

(A) FACs analysis of pDCs of conrol (n=4) and $S7^{\Delta DC}$ (n=6) mice in the iLN, and **(B)** spleens as gated on live $B220^+$ $Ly6c^+$ cells. Total cell counts of pDCs are shown in the right panel. Bar graphs depict mean value ± SEM. Statistical significance was assessed using Student's t-Test (*p ≤0.05, **p ≤ 0.005, ***p ≤ 0.0005).

3.2.3.2 Smad7 deletion results in increased expression of transcription factors important for DC lineage commitment

Development of DCs is in part controlled by the expression of specific transcription factors. The transcription factors IRF8, Batf3 and ID2 have previously been reported to play a crucial role in the development of $CD8^+$ $CD103^+$ DCs (Belz and Nutt, 2012). Since mice devoid of Smad7 show an increase in the $CD8^+$ $CD103^+$ DC frequencies in the spleen, it was next examined whether the loss of Smad7 might affect the expression of IRF8, Batf3 and ID2. To this end real time analysis was performed, assessing the expression levels of IRF8, Batf3 and ID2 in MACS purified $CD11c^+$ splenic DCs derived from naïve $S7^{\Delta DC}$ mice and control mice either left untreated or treated with TGF-β or IFN-γ (Figure 9).

In comparison to non-stimulated cells, both TGF-β or IFN-γ stimulation significantly increased IRF8 relative expression in both, control and Smad7 deficient DCs. Yet, 24hrs post stimulation Smad7 deletion resulted in a significantly higher up-regulation of IRF8 transcripts under both stimuli tested as compared to controls (Figure 9A). Similarly, also Batf3 expression was elevated following these stimuli in both control and Smad7-deficient DCs. Smad7-deficient DCs displayed enhanced Batf3 levels 24hrs post IFN-γ, but not TGF-β stimuli (Figure 9B).

In contrast, stimulation with TGF-β or IFNγ for 24h significantly increased the expression of ID2 transcripts, but did not result in a significant difference between controls and Smad7 deficient DCs (Figure 9C).

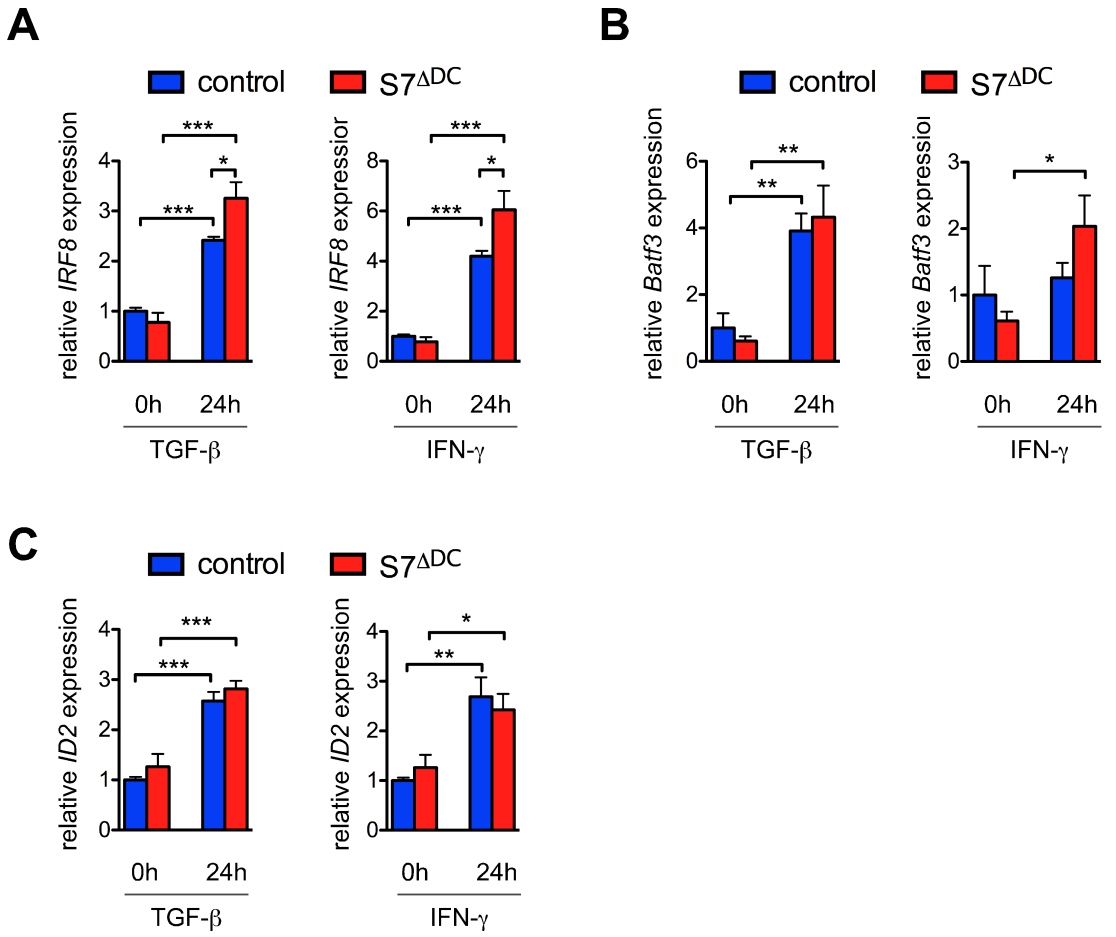

Figure 9: Smad7 deficiency increases expression the transcription factors IRF8 and Batf3 important for CD8$^+$ CD103$^+$ DC lineage commitment

(A) Real time analysis for *IRF8*, **(B)** *Batf3* and **(C)** *ID2* transcripts of control (n=4) and S7$^{\Delta DC}$ (n=4) mice in splenic DCs, either un-stimulated or stimulated with TGF-β or IFN-γ for 12h or 24h. Bar graphs depict mean value ± SEM. Statistical significance was assessed using two- way ANOVA and Bonferroni posttests (*p ≤ 0.05, **p ≤ 0.005, ***p ≤ 0.0005).

3.2.3.3 Macrophages, neutrophils and granulocytes remain unaffected by Smad7 deletion in CD11c$^+$ cells during steady state

Splenic metallophillic macrophages are important regulators of immune responses and can express low levels of CD11c on their surface (Probst et al., 2005). To assess if deletion of Smad7 in CD11c$^+$ cells might affect macrophages, neutrophils or monocytes during steady state, iLN and spleens of naïve S7$^{\Delta DC}$ mice and control animals were examined for these cells.

Analysis of naïve S7$^{\Delta DC}$ mice revealed no difference in frequencies of neutrophils, monocytes or macrophages as compared to controls in both the spleen as well as the iLN despite a minute, yet significant increase in splenic macrophage numbers (Figure 10).

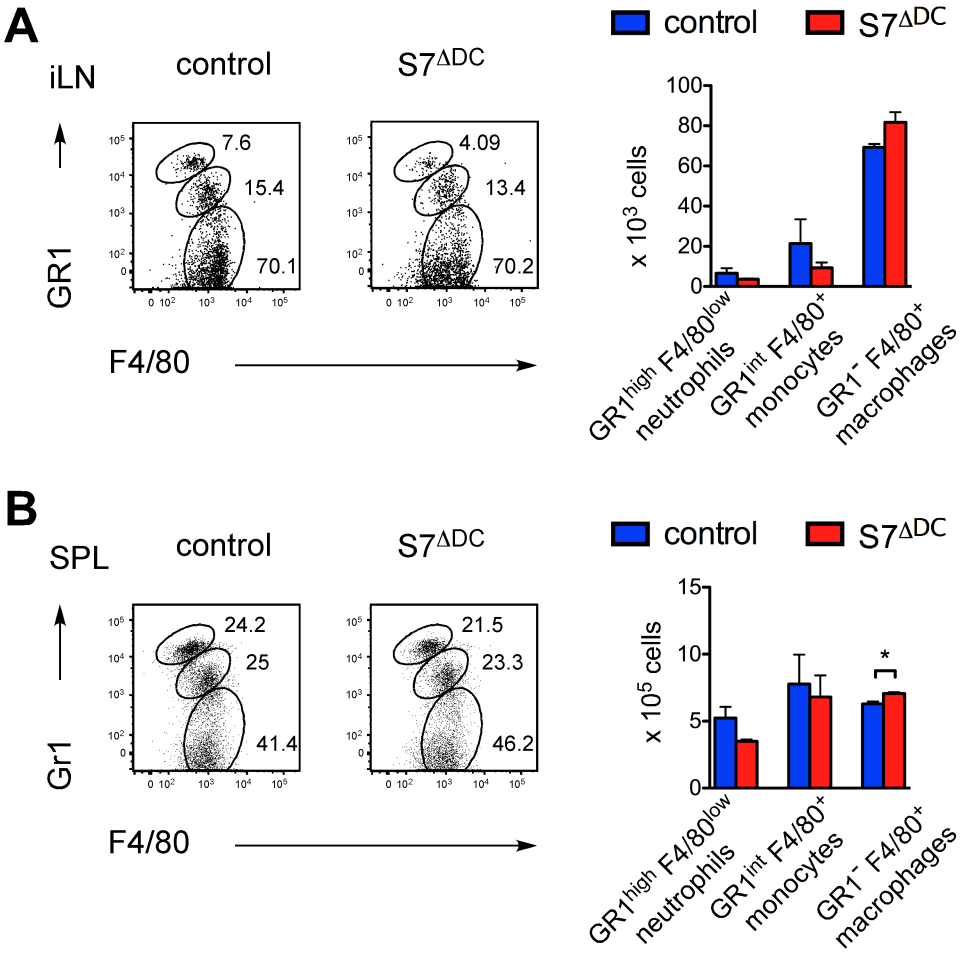

Figure 10: Neutrophils, macrophages and monocytes remain largely unaffected by Smad7 deletion in CD11c$^+$ cells.

Representative FACS blots and total cell counts of neutrophils (GR1^{high} F4/80^{low}), monocytes (GR1^{int} F/480$^+$) and marophages (GR1$^-$ F/480$^+$) in the **(A)** iLN and **(B)** spleen of naïve S7$^{\Delta DC}$ (n=3) and control (n=3) mice. Cells were gated on viable CD90.2$^-$ B220$^-$ CD11b$^+$ cells. Bar graphs depict mean value ± SEM. Statistical significance was assessed using Student's t-Test (*p ≤0.05, **p ≤ 0.005, ***p ≤ 0.0005).

3.2.3.4 Smad7 deficiency in DCs does not affect thymic T cell development

DCs along with cTECs and mTECs in the thymus shape the T cell repertoire by positive and negative selection, thus establishing central tolerance. As previously shown (Figure 4), loss of Smad7 did not affect the activation status or amounts of thymic DC subsets during steady state. It was next assessed whether loss of Smad7 in DCs might alter thymic T cell development. As already mentioned, T cells undergo various differentiation steps in the thymus resulting in functional TCR arrangement. The first step in T cell development comprises the CD4$^-$ CD8$^-$ double negative (DN)

stage that can be further subdivided into four stages based on the surface expression of CD44 and CD25. Analysis of thymi from $S7^{\Delta DC}$ mice revealed no difference in the total cell counts of DN1 ($CD25^{-}$ $CD44^{+}$), DN2 ($CD25^{+}$ $CD44^{+}$), DN3 ($CD25^{+}$ $CD44^{-}$) or DN4 ($CD25^{-}$ $CD44^{-}$) T cells as compared to control animals (Figure 11B).
The DN stage is followed by the double positive (DP) stage characterized by co-expression of both CD4 and CD8, which ultimately leads to the single positive (SP) stage in which the T cells are solely expressing CD4 or CD8 on their surface and egress the thymus. DC specific loss of Smad7 however, did not affect the total cell counts of DN, DP, CD4 SP and CD8 SP stage (Figure 11A).

In addition to the major conventional TCRαβ T cells, a subset of innate T cells called TCRγδ develops during DN3-4 stage.
Flow cytometric analysis of thymic TCRγδ T cell of naïve $S7^{\Delta DC}$ mice revealed no significant difference in total cell numbers, as compared to thymic TCRγδ T cell of control mice (Figure 11C).

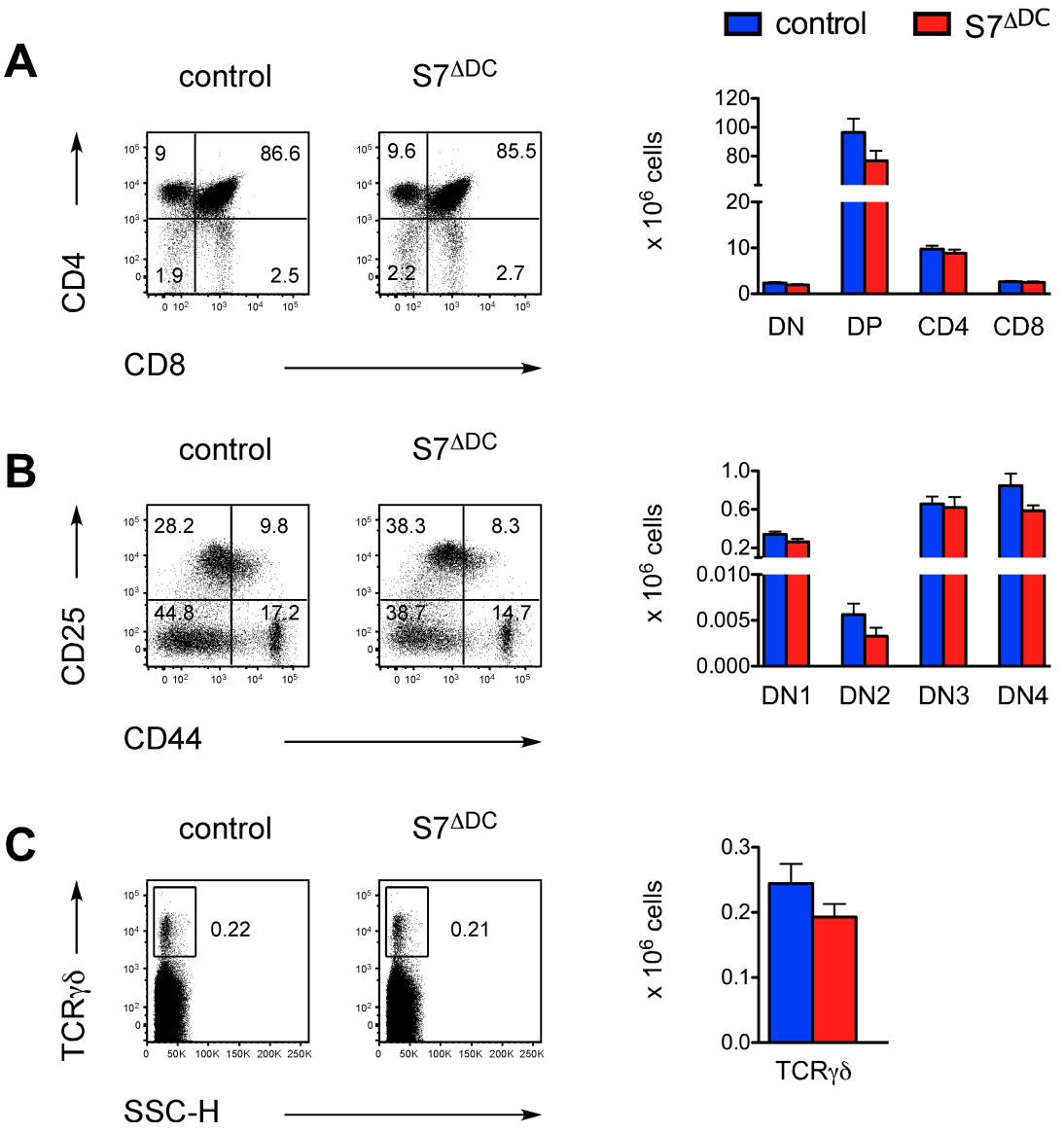

Figure 11: Normal thymic T cell development in S7$^{\Delta DC}$ mice

(A) Representative FACs blots and statistical analysis showing T cell development of control n=7 and S7$^{\Delta DC}$ n=5 mice. DN=double negative, DP=double positive **(B)** Analysis of double negative (DN)1 (CD25^{-} CD44^{+}), DN2 (CD25^{+} CD44^{+}), DN3 (CD25^{+} CD44^{-}) as well as DN4 (CD25^{-} CD44^{-}) T cell developmental stages in the thymus of control n=7 and S7$^{\Delta DC}$ n=5 mice as gated on CD4^{-}CD8^{-}B220^{-} cells. **(C)** TCRγδ T cells in the thymus of S7$^{F/F}$ n=7, S$^{F/D}$ n=4 and CD11c Cre$^{+/-}$ S7$^{F/D}$ n=5 mice. Bar graphs depict mean value ± SEM. Statistical significance was assessed using Student's t-Test (*p ≤0.05, **p ≤ 0.005, ***p ≤ 0.0005).

DCs are furthermore involved in the generation of natural occurring T regulatory cells (nTregs) in the thymus (Kushwah and Hu, 2011). Regulatory T cells are an important suppressive T cell subset, which is characterized by the expression of forkhead box P3 (Foxp3) and the IL-2 receptor CD25 and develop at the DP stage of T cell development during positive selection to self-antigens (Zheng and Rudensky, 2007). Additionally, these thymic- derived nTregs were shown to express transcription factor Helios (Thornton et al., 2010). In general, DCs can secrete TGF-β which induces

FoxP3 expression in responding T cells, resulting in the differentiation of naïve T cells towards Tregs. Plasmacytoid DCs in the thymus have been shown to participate in the generation of Tregs in humans (Martin-Gayo et al., 2010), however the relative contribution of cDC subset- derived TGF-β in thymic T cell development remains to be elucidated.

To assess whether the loss of Smad7 in DCs might have an impact on the generation of nTregs, thymi of $S7^{\Delta DC}$ mice and control animals were examined.

Flow cytometric analysis of thymocytes from $S7^{\Delta DC}$ mice revealed no significant difference in the total cell counts of $CD4^+$ $FoxP3^+$ $CD25^+$ cells (Figure 12A) as well as $CD4^+$ $FoxP3^+$ $Helios^+$ cells (Figure 12B) in $S7^{\Delta DC}$ mice as compared to controls, suggesting that nTreg differentiation is not affected by the loss of Smad7 in DCs.

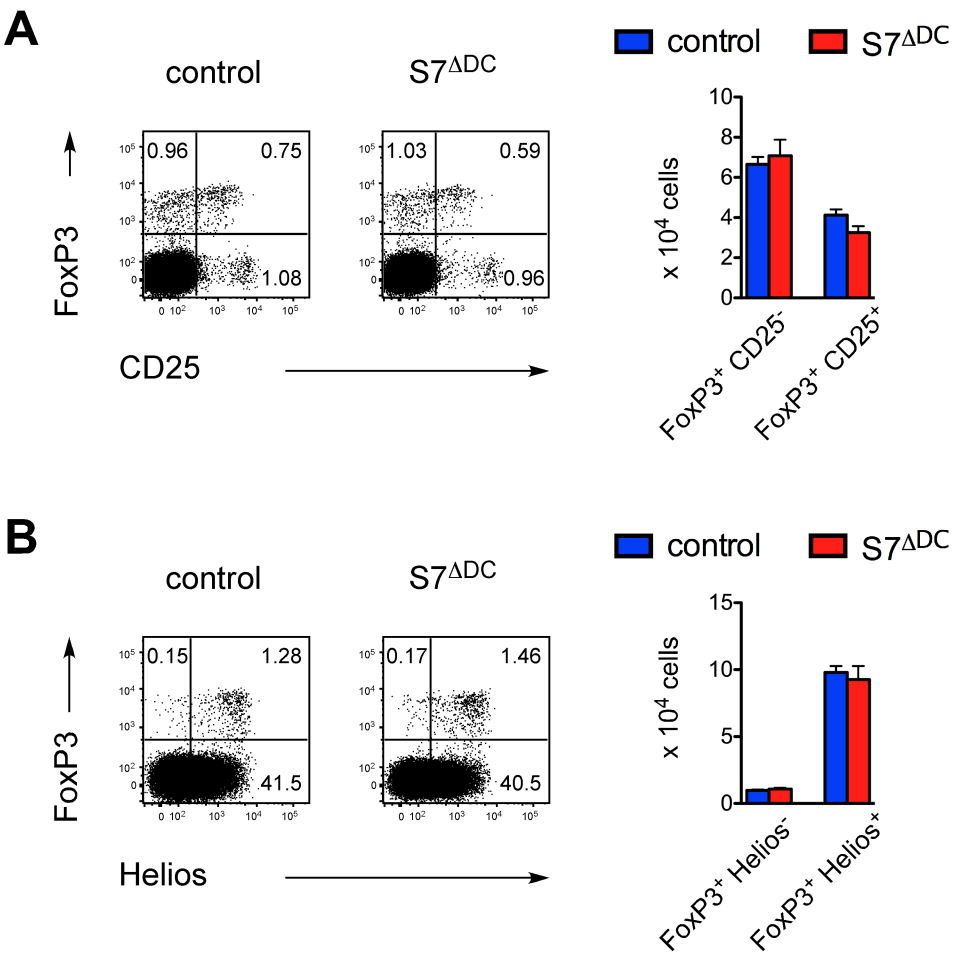

Figure 12: DCs specific Smad7 deletion does not affect the development of thymic nTregs

(A) FACs analysis of thymi from control (n=7) and $S7^{\Delta DC}$ (n=5) mice for nTregs based on the expression of FoxP3 and CD25 as well as **(B)** FoxP3 and Helios as gated on CD4 single positive cells is shown. Bar graphs depict mean value ± SEM. Statistical significance was assessed using Student's t-Test (*p ≤0.05, **p ≤ 0.005, ***p ≤ 0.0005).

3.2.3.5 Peripheral T cells remain unaffected by DC specific Smad7 deletion during steady state

Arising in the thymus, T cells egress to the periphery, where in secondary lymphoid organs they encounter DCs and other APCs presenting antigen. T cell survival and homeostatic proliferation during steady state is dependent on a process called tonic 'tickling', in which constant low-affinity engagement of the T-cell receptor to self antigens presented by mainly DCs, but also B cells, occurs (Garbi and Kreutzberg, 2012). Peripheral tolerance is achieved by elimination of potentially self-reactive cells in different ways including anergy, activation induced cell death or insufficient antigen presentation to reach threshold necessary for T cell activation.

DC specific deletion of TGF-β RII or an abrogated TGF-βR signaling in DCs leads to a strong T cell mediated spontaneous autoimmune disease upon increasing age (Laouar et al., 2008; Ramalingam et al., 2012), suggesting that DC intrinsic TGF-β signaling mediates tolerance. To examine the role of Smad7 deficiency in DCs on T cell homeostasis and activation in the periphery during steady state, spleen and iLN of naïve $S7^{\Delta DC}$ mice were analyzed.

The frequency of T cells in the iLN and spleens, as indicated by the expression of $CD90.2^{+}$ cells, was not impaired by DC specific Smad7 deletion (Figure 13A,B).

Furthermore analysis of the $CD4^{+}$ and $CD8^{+}$ T cell frequencies in the iLN revealed no difference between naïve $S7^{\Delta DC}$ mice and control animals (Figure 13C). In the spleen however, there was a mild yet significant decrease in $CD4^{+}$ T cells and increase in $CD8^{+}$ T cells in $S7^{\Delta DC}$ mice as compared to controls (Figure 13D). Although statistically significant, this minor difference is biological irrelevant.

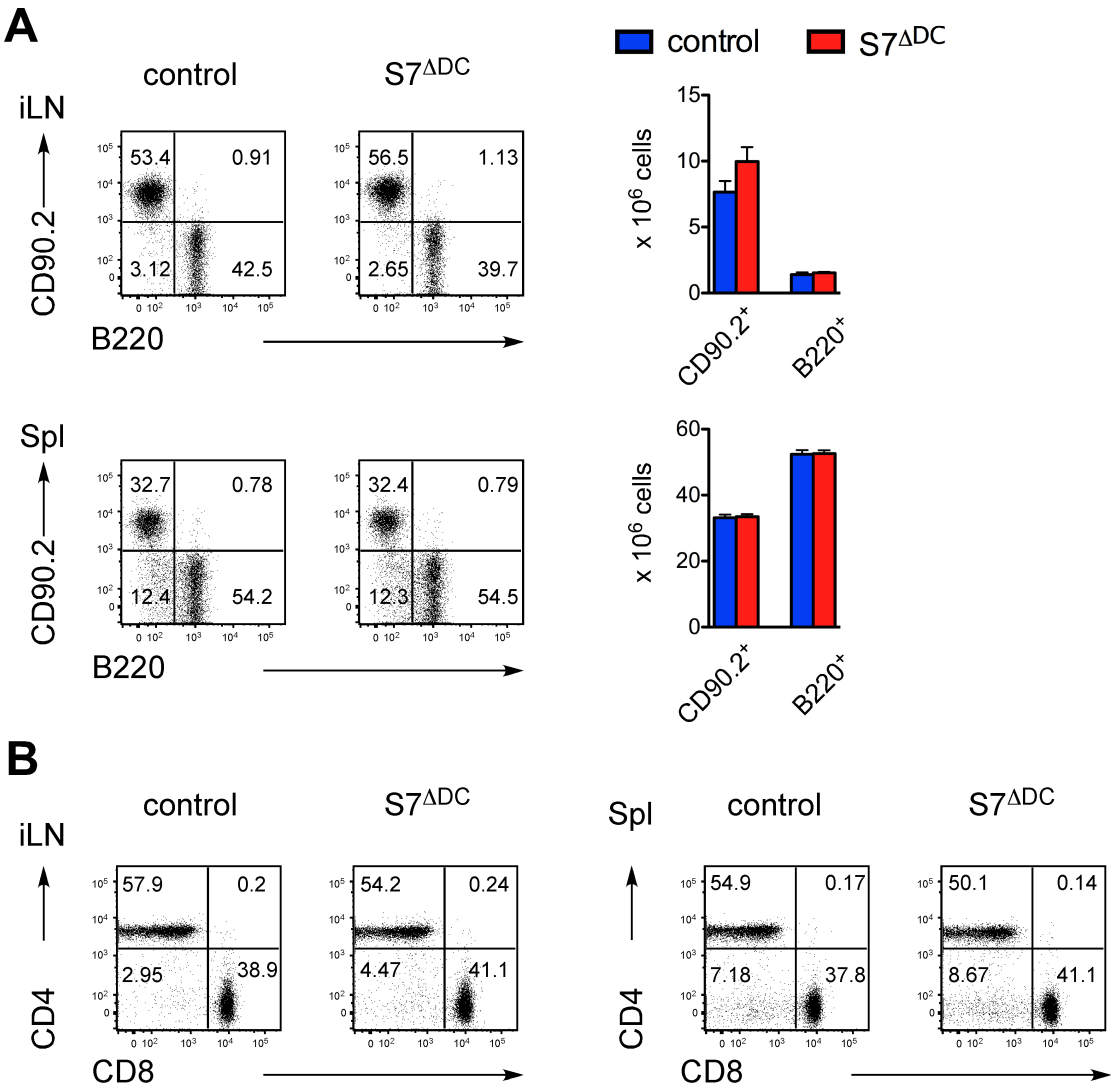

Figure 13: DC specific Smad7 deletion does not affect CD4 or CD8 T cell in the periphery during steady state

Representative FACs blots of **(A)** iLN or splenic CD90.2 T cells and $B220^+$ B cells of control (n=7) and $S7^{\Delta DC}$ (n=5) mice as gated on viable cells. **(B)** Representative FACs blots of iLN and splenic $CD4^+$ and $CD8^+$ T cells of control (n=7) and $S7^{\Delta DC}$ (n=5) mice as gated on $CD90.2^+$ viable cells. Bar graphs depict mean value ± SEM. Statistical significance was assessed using Student's t-Test (*p ≤0.05, **p ≤ 0.005, ***p ≤ 0.0005).

DCs present antigen and provide co-stimulatory signals like CD80, CD86 or CD40 that interact with CD28 or CD40L on T cells, respectively. Such signals lead to the activation of naïve T cells. Upon their activation, T cells up-regulate CD44 and subsequently down-regulate CD62L. Abrogated TGF-β signaling on DCs was suggested to enhance T cell activation, already during steady state (Ramalingam et al., 2012). To investigate whether loss of Smad7 in DCs might impact T cell activation, splenic- and iLN derived T cells of naïve $S7^{\Delta DC}$ mice were examined.

The percentage of naïve $CD4^+$ $CD62L^{high}$ $CD44^{low}$ T cells and activated $CD4^+$ $CD62L^{low}$ $CD44^{high}$ T cells as well as memory $CD4^+$ $CD62L^{high}$ $CD44^{high}$ T cells in spleen and iLN of untreated $S7^{\Delta DC}$ mice was comparable to controls (Figure 14A-C).

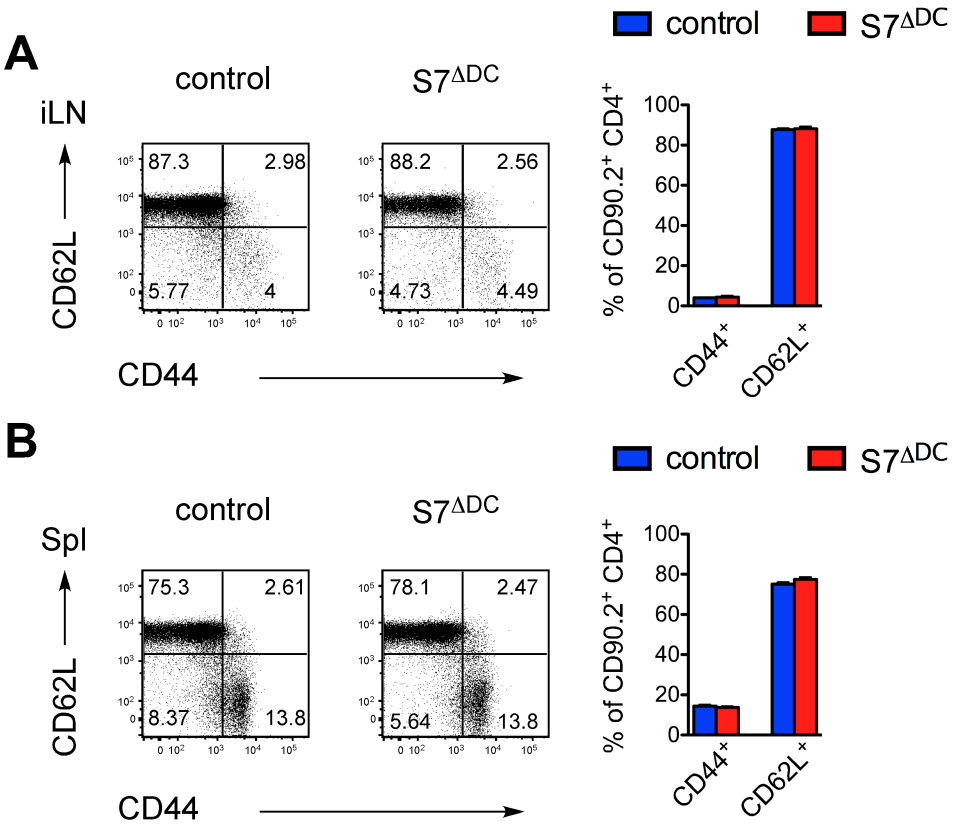

Figure 14: T cell activation is not altered by Smad7 deficient DCs

Representative FACs bots of **(A)** iLN and **(B)** splenic $CD62L^+$ and $CD44^+$ T cells in naïve control (n=7), and $S7^{\Delta DC}$ (n=5) mice as gated on viable $CD90.2^+$ $CD4^+$ cells. Bar graphs depict mean value ± SEM. Statistical significance was assessed using Student's t-Test (*p ≤0.05, **p ≤ 0.005, ***p ≤ 0.0005).

Naïve mature T cells can differentiate into diverse T cell subsets according to the stimuli that these cells are exposed to. In the periphery, induced regulatory T cells (iTregs) develop from $CD4^+$ $CD25^-$ precursors in a TGF-β dependent manner and participate in tolerance induction (Curotto de Lafaille and Lafaille, 2009).

Interestingly mice devoid of TGF-βRII specifically on DCs showed attenuated Foxp3 expression in Tregs and abnormal expansion of $CD25^+$ $Foxp3^+$ Tregs *in vivo* (Ramalingam et al., 2012). To address whether DC specific loss of Smad7 might affect Tregs in the periphery during steady state, spleen and iLN were analyzed of naïve $S7^{\Delta DC}$ mice was examined.

The percentage and total cell counts of $CD4^+$ $FoxP3^+$ Tregs in the spleen and iLN of $S7^{\Delta DC}$ mice were not altered by the DC specific Smad7 deletion as compared to controls (Figure 15A,B). Previously, it has been reported that Helios expression discriminates thymic- derived natural (nTregs) from peripheral induced Tregs (iTregs) (Thornton et al., 2010). However, the frequencies and total cell counts of $Helios^+$ and $Helios^-$ $FoxP3^+$ T cells (nTreg versus iTreg, respectively) and $CD25^-$ or $CD25^+$ $FoxP3^+$ Tregs in the iLN and spleen of naïve $S7^{\Delta DC}$ mice were not affected by the deletion of Smad7 in DCs (Figure 15A,B) Similarly, expression levels of cytotoxic T-lymphocyte antigen 4 (CTLA-4; CD152), whose expression on T cells leads to tolerance induction in both T cells and DCs was not affected in $S7^{\Delta DC}$ mice (Wing and Sakaguchi, 2010) (Figure 15D).

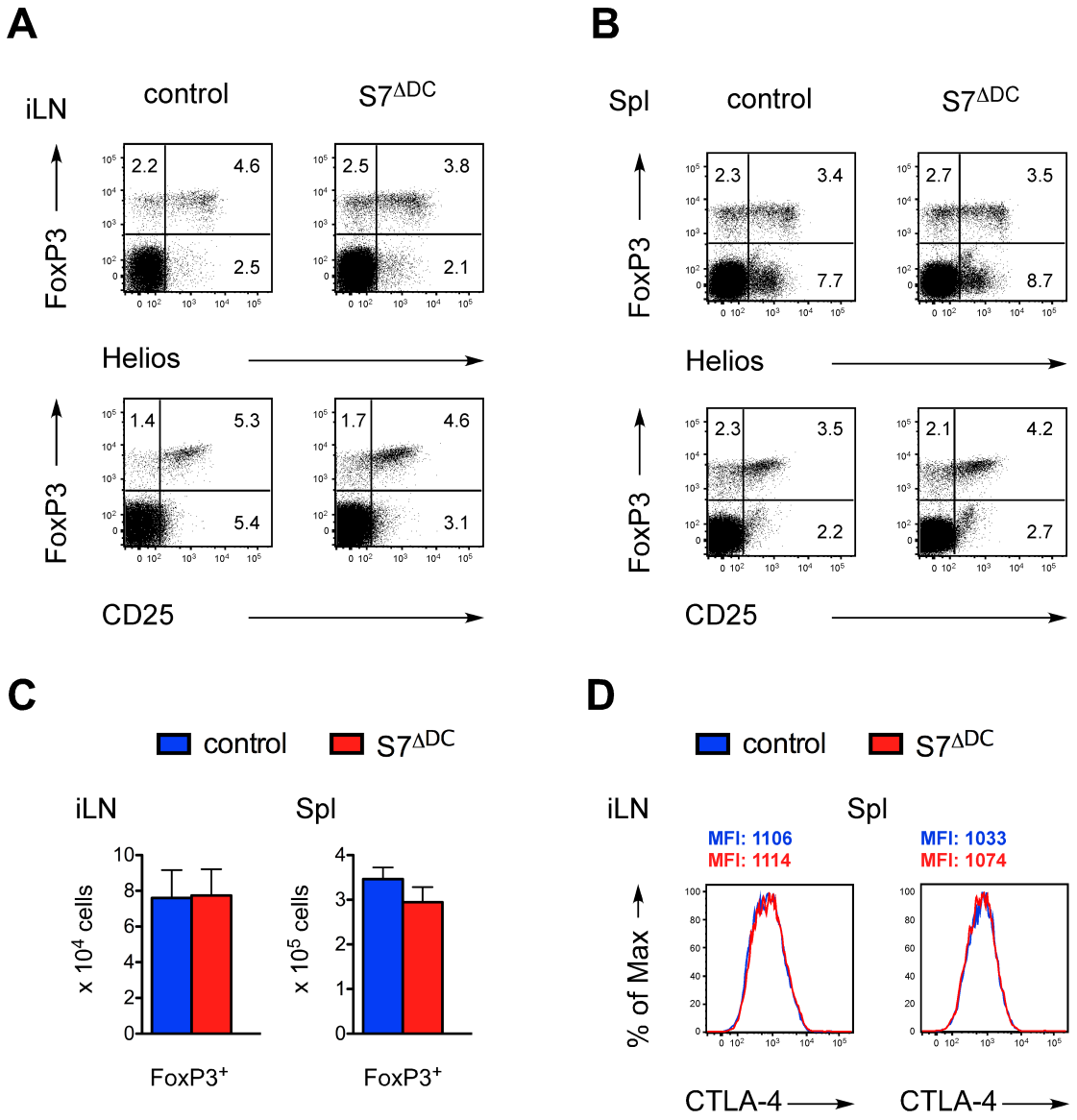

Figure 15: Normal Treg distribution in S7$^{\Delta DC}$ mice during steady state

Representative FACs blots of **(A)** splenic and **(B)** iLN Helios$^+$ and CD25$^+$ FoxP3$^+$ T cells of naïve control (n=7) and S7$^{\Delta DC}$ (n=5) mice as gated on viable CD90.2$^+$ CD4$^+$ cells. **(C)** Total FoxP3+ cell counts as gated on CD4+ viable T cells. **(D)** CTLA-4 mean fluorescence intensity (MFI) as gated on FoxP3$^+$ cells. Bar graphs depict mean value ± SEM. Statistical significance was assessed using Student's t-Test (*p ≤0.05, **p ≤ 0.005, ***p ≤ 0.0005).

3.2.4 Role of Smad7 in DCs during the autoimmune disease experimental autoimmune encephalomyelitis (EAE)

Experimental autoimmune encephalomyelitis (EAE) serves as a murine model for the demyelinating CNS autoimmune disease multiple sclerosis (MS) (Steinman and Zamvil, 2006), with which it shares many pathological and physiological features.

EAE can be induced by immunization with several different myelin antigen such as myelin oligodendrocyte glycoprotein / peptide (MOG, or MOG_{35-55} peptide), myelin basic protein (MBP) or proteolipid protein (PLP), in combination with complete Freund's adjuvans and additional administration of pertussis toxin (Mendel et al., 1995).

During EAE, autoreactive T cells which recognize these central nervous system (CNS) associated self- peptides / proteins (MOG, MOG_{35-55}, MBP, PLP) migrate to the CNS and initiate inflammation and tissue damage. The inflammation is associated with edema formation, loss of the myelin sheath, leading to paralysis, which eventually result in lethality. Primarily associated with high increase of pathogenic Th1 and Th17 effector T cells, it became evident, that the $IFN\gamma^+$ $IL17A^+$ double producing T effector cell subset is predominantly responsible for EAE as well as MS pathogenesis, while an increase in Treg cells is associated with reduced disease progression and remission (Korn et al., 2007a).

DCs, as the most prominent APCs, have been shown to play a major role during EAE. DCs not only present antigen, but also provide co-stimuli and secrete cytokines, which consequently drives the differentiation of auto-reactive T cells to the respective Teff (T effector) or Treg subsets and thus controls disease outcome. Recent findings using DC depletion models, in which EAE exacerbated, underline the tolerogenic role of DCs during EAE (Yogev et al., 2012).

Abrogated TGF-βR signaling on DCs was associated with the development of autoimmune disease (Laouar et al., 2008; Lievens et al., 2012; Ramalingam et al., 2012). However, the role of Smad7 as a negative regulator of TGF-β signaling was not addressed so far. To assess if loss of Smad7 in DCs might affect T cell mediated autoimmune disease, $S7^{\Delta DC}$ mice were subjected to EAE.

3.2.4.1 Mice deficient of Smad7 specifically in DCs are resistant to EAE

In order to assess whether Smad7 deletion in DCs has a direct impact on the outcome of EAE, $S7^{\Delta DC}$ mice were immunized with MOG_{35-55}/CFA and PTX to induce the CNS autoimmune disease EAE. The disease progression was monitored daily and disease scores were evaluated based on the scoring system 0-6 (0 = no disease; 1 = decreased tail tone; 2 = abnormal gait (ataxia) and /or impaired righting reflex; 3 = partial hind limb paralysis; 4 = complete hind limb paralysis; 5 = hind limb paralysis with partial fore limb paralysis; 6 = moribund or dead).

Following MOG_{35-55}/CFA immunization, $S7^{\Delta DC}$ mice exhibited a significantly reduced EAE susceptibility as compared to wild type controls (Figure 16). The disease severity was assessed based on the clinical signs, as well as the day of onset, the mean maximal clinical score and disease incidence (Table 6). The maximal clinical EAE score of $S7^{\Delta DC}$ mice when compared to controls was significantly reduced by 44%, from an average of 2.8 to 1.6. EAE incidence in $S7^{\Delta DC}$ mice was reduced by 31%, from 85% in the controls to below 60% in the knockout group. Notably, the day of EAE onset however, was not affected by the DC specific Smad7 deletion.

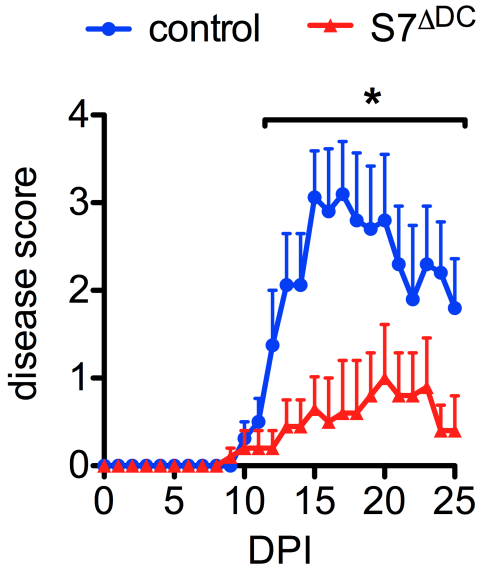

Figure 16: DC-specific Smad7 deletion renders mice resistant to EAE

EAE disease course of $S7^{\Delta DC}$ mice (n=10) and control animals (n=8) after MOG_{35-55}/CFA and PTX immunization. Shown is one representative out of five independent experiments. Data are shown as mean value ± SEM. Statistical significance was assessed using EAE area under curve (AUC) followed by Student's t- Test (*p ≤ 0.05, **p ≤ 0.005, ***p ≤0.0005).

genotype	control	$S7^{\Delta DC}$
amount of mice per group	n=68	n=60
day of onset	11.46 ± 0.24	11.97 ± 0.39
maximal clinical score	2.77 ± 0.20	1.55 ± 0.21
incidence	85.07 ± 4.39	58.33 ± 6.42

Table 6: EAE in $S7^{\Delta DC}$ mice

During EAE inflammation, reactive oxygen species (ROS) are produced and contribute to CNS tissue damage during EAE (Fischer et al., 2012). ROS can be formed in a direct process catalyzed by nicotinamide adenine dinucleotide phosphate-(NADPH) oxidase that catalyzes oxygen to superoxide. DC harbor NOX2 (Rybicka et al., 2012; Savina et al., 2006) and TGF-β was reported to induce NOX2 and NOX4 expression (Bondi et al., 2010).

Hence, it was assessed if $S7^{\Delta DC}$ mice subjected to EAE disease would have altered amounts of ROS in the blood, which would contribute to the reduced disease progression and target tissue damage observed in $S7^{\Delta DC}$ mice.

Whole blood of untreated control mice, EAE immunized $S7^{\Delta DC}$ or control mice on day 14 post immunization was assessed for the presence of ROS using the chemiluminescence dye 8-amino-5-chloro-7-phenylpyridol [3,4-*d*] pyridazine-1,4-(2H,3H) dione sodium salt (L-O12). Following EAE induction, control mice displayed significant increased ROS levels (1.8- fold) in their circulation. Yet, $S7^{\Delta DC}$ mice showed a significant (1.4-fold) reduction in circulating ROS levels when compared to blood of EAE immunized control animals, correlating with the disease resistance observed in these mice (Figure 17A).

Furthermore, the production of ROS in whole blood of the above-mentioned samples was assessed upon stimulation with phorbol 12,13-dibutyrate (PDBU). PDBU is a stimulator of the protein kinase C, which in turn activates the NADPH oxidase that catalyzes oxygen to superoxids. PDBU treatment strongly enhanced ROS production, as seen when comparing the values obtained from naïve mice (Figure 17A) to PDBU-unimmunized controls (Figure 17B). Similarly, PDBU increased circulating ROS production in samples obtained from both MOG_{35-55}/CFA immunized wild type, or $S7^{\Delta DC}$ mice by approximately 15- fold, as compared to the respective non-PDBU challenged controls. However, PDBU stimulated blood samples of $S7^{\Delta DC}$ MOG_{35-}

$_{55}$/CFA immunized mice showed significantly reduced ROS levels (1.4-fold) when compared to the respective immunized and PDBU treated controls (Figure 17B).

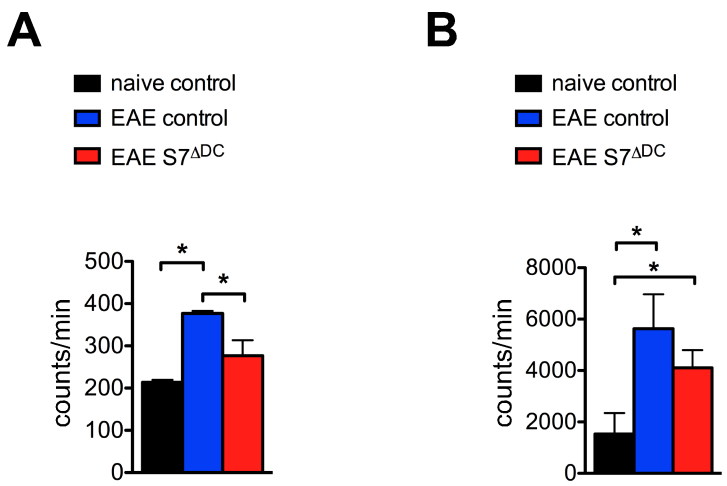

Figure 17: Reduced reactive oxygen species levels in S7$^{\Delta DC}$ mice during EAE

(A) Detection of reactive oxygen species (ROS) as measured in whole blood of unimmunized wild type (n=5) as well as EAE immunized control (n=5) and S7$^{\Delta DC}$ (n=5) mice on day 14 post MOG$_{35-55}$/CFA immunization using the chemiluminescent dye L-012. **(B)** ROS measurement in PDBU treated whole blood of unimmunized wild type (n=5) as well as EAE subjected wildtype control mice (n=5) and S7$^{\Delta DC}$ (n=5) mice on day 14 post EAE induction using the chemiluminescent dye L-012. Bar graphs depict mean value ± SEM. Statistical significance was assessed using Student's t-Test (*p ≤ 0.05, **p ≤ 0.005, ***p ≤ 0.0005).

During EAE, effector T cells infiltrate into the CNS and mediate tissue damage. Since mice with a DC specific Smad7 deletion showed a significantly reduced EAE disease progression, the composition of the CNS infiltrates with focus on the CD4$^+$ T helper cells was analyzed.

Analysis of CNS infiltrates on the peak of disease revealed a significantly reduced CD90.2$^+$ T cell infiltration in S7$^{\Delta DC}$ mice as compared to control mice (37% reduction in percentage and 41% reduction in total cell counts) (Figure 18A). Among these CD90.2$^+$ T cells, the percentages and total cell counts of CD4$^+$ T helper cells were significantly reduced in S7$^{\Delta DC}$ mice by 50%, as compared to control animals (Figure 18B).

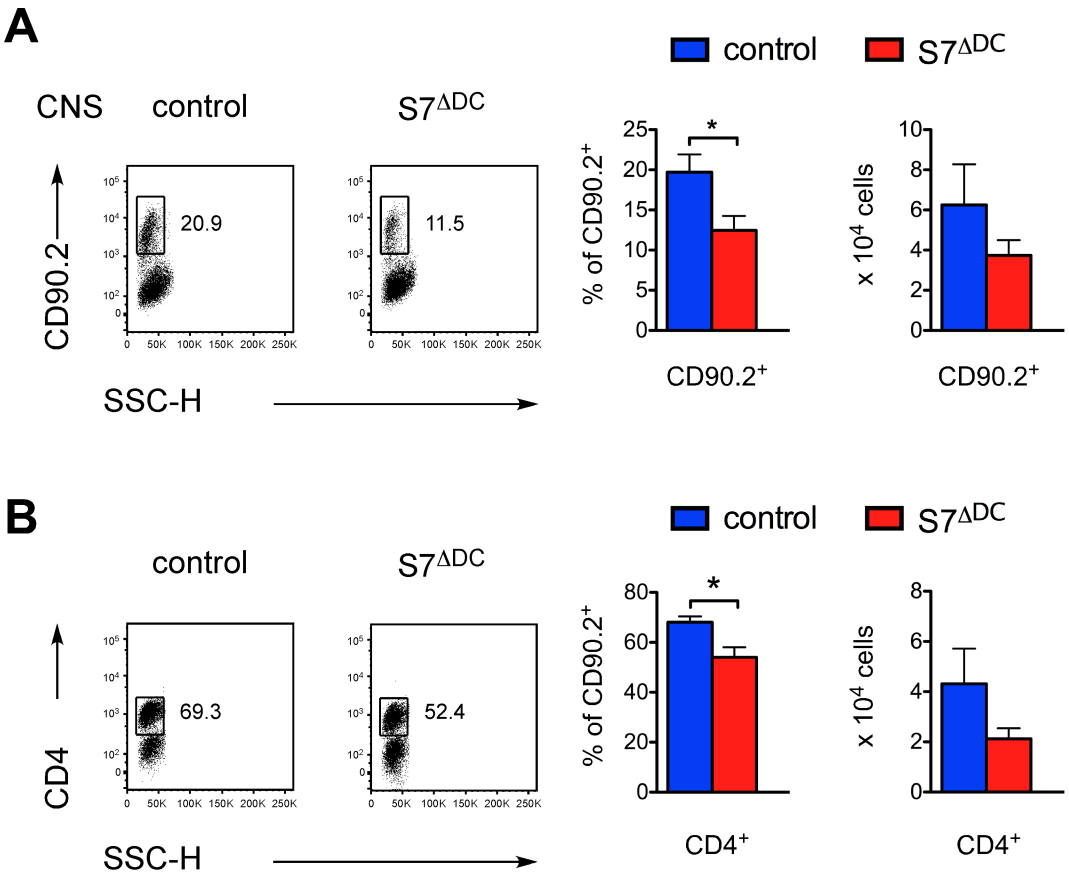

Figure 18: Reduced infiltration of Tcells to the CNS in S7$^{\Delta DC}$ mice

(A) Flow cytometric analysis of CNS infiltrating CD90.2$^+$ T cells from S7$^{\Delta DC}$ (n=8) and control mice (n=7) at the peak of disease (day15). Cells were gated on live cells. Depicted is one representative out of four independent experiments. **(B)** FACS blots of CNS infiltrating CD4$^+$ T cells from S7$^{\Delta DC}$ (n=8) and control mice (n=7) at the peak of disease (day15). Cells were gated on live CD90.2$^+$ cells. Bar graphs depict mean value ± SEM. Statistical significance was assessed using Student's t-Test (*p ≤ 0.05, **p ≤ 0.005, ***p ≤0.0005).

Since DC specific loss of Smad7 resulted in significantly reduced infiltration of T cells to the CNS, it was therefore next assessed which of the different CD4$^+$ T helper cell subsets known to play a role in EAE pathology, might be altered in S7$^{\Delta DC}$ mice upon MOG$_{35-55}$/CFA immunization. Hence, CNS infiltration of IFN-γ producing Th1 cells, IL-17A producing Th17 cells and IFN-γ$^+$ IL-17A$^+$ double producing CD4$^+$ effector T cells was examined during the peak of disease.

To assess how many of these infiltrating T cells were antigen specific, CNS infiltrates were re-stimulated with MOG$_{35-55}$, which led to the up-regulation of CD40L on antigen experienced cells. The analysis of CNS infiltrating CD4$^+$ T cells that co-expressed CD40L and CD44 upon MOG$_{35-55}$ re-stimulation, revealed a significant reduction of MOG- specific S7$^{\Delta DC}$- derived cells (46%) as compared to those found in wild type mice (Figure 19A). These MOG$_{35-55}$- specific CD4$^+$ T cells could be further

defined as Th1, Th17 and double producing cells based on the expression of IFN-γ^+ and/or IL-17A$^+$. The percentages of all three CNS infiltrating MOG_{35-55}- specific T effector cell subsets were comparable to controls (Figure 19A). However, analysis of the total cell counts of MOG_{35-55} specific Th1, Th17 and IFN-γ^+ IL-17A$^+$ double producing MOG_{35-55}-effector CD4$^+$ T cells revealed a strong reduction in all three T effector cell subsets in S7$^{\Delta DC}$ mice as compared to control animals (Th1 50%, Th17 63%, IFN-γ^+ IL-17A$^+$ 77%) as depicted in Figure 19B.

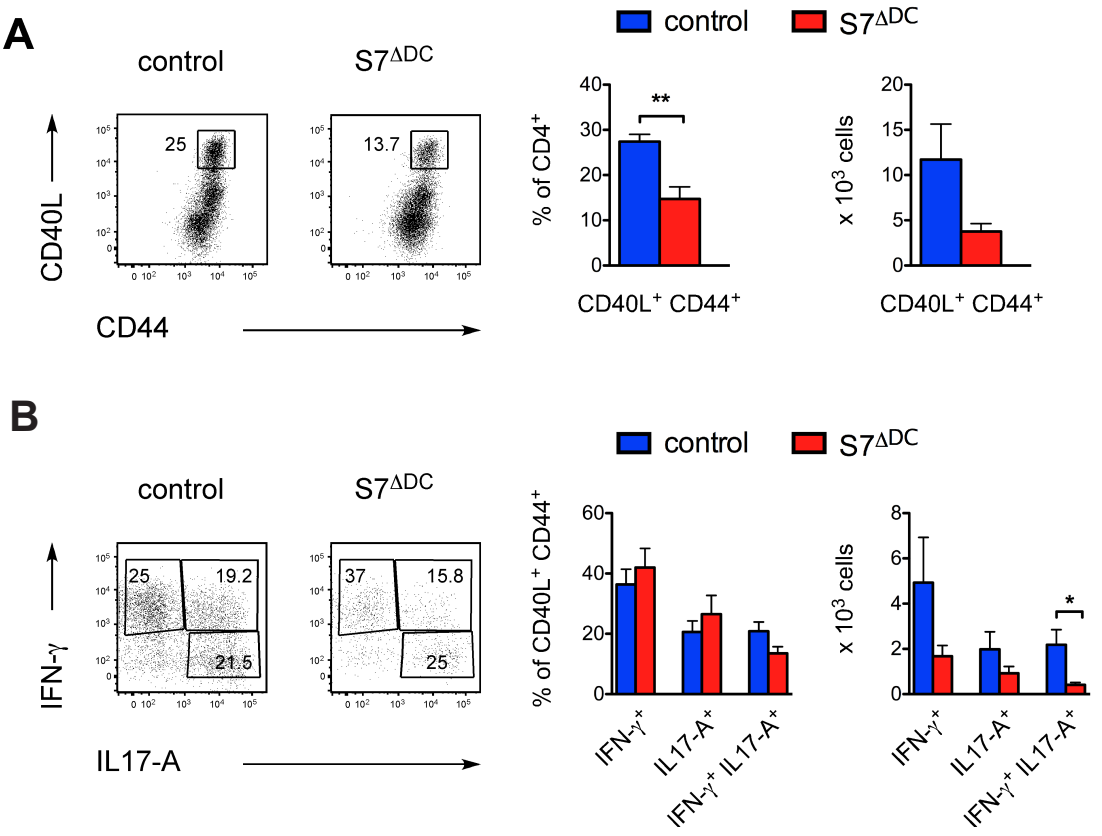

Figure 19: S7$^{\Delta DC}$ mice display reduced CNS infiltration of MOG_{35-55} specific effector Th1, Th17 and IFN-γ^+ IL-17A$^+$ T cells during EAE

(A) Representative FACs blots showing MOG_{35-55} reactive CD40L$^+$ CD44$^+$ effector T cells as gated on CD90.2$^+$ CD4$^+$ CNS infiltrates on the peak of disease. **(B)** Representative FACs blots showing MOG_{35-55} specific Th1 (IFN-γ^+) and Th17 (IL-17A$^+$) and IFN-γ· IL-17A$^+$ double producing cells infiltrating the CNS of control (n=7) and S7$^{\Delta DC}$ (n=8) mice on the peak of disease, as gated on CD90.2$^+$ CD4$^+$ CD40L^{high} CD44$^+$ cells. Bar graphs depict mean value ± SEM. Statistical significance was assessed using Student's t-Test (*p ≤ 0.05, **p ≤ 0.005, ***p ≤0.0005).

In addition to the immunogenic function of the tissue-infiltrating T effector cells, other T cell subsets such as FoxP3$^+$ CD4$^+$ Treg cells are known to infiltrate the CNS.

The regulatory functions of these cells contribute to the resolution of inflammation in this disease model.

Analysis of CNS infiltrates during the peak of disease revealed a significant 1.7-fold increase in the percentages of CNS infiltrating Treg cells in $S7^{\Delta DC}$ mice as compared to controls (Figure 20A). The total cell counts of CNS infiltrating Treg cells however, were not affected. This discrepancy could be attributed to the significant reduction of overall T cell infiltrates observed in these mice.

Tregs play a major role in autoimmune resolution by suppressing other auto-reactive T cells. During steady state, the percentages and absolute numbers of peripheral Tregs were comparable in $S7^{\Delta DC}$ mice and control mice (Figure 15). Moreover, the expression levels of FoxP3 and CTLA-4, a transcription factor and an activation marker associated with Treg suppression capacity, as well as expression of Helios (a marker for nTregs) were all comparable among these mice (Figure 15). Thus, the increase in CNS-infiltrating Tregs seen in $S7^{\Delta DC}$ mice, could account for the lower EAE susceptibility. To test whether the increased in Treg cells upon immunization was specifically localized at the target tissue or could also be detected in peripheral organs, EAE subjected mice were analyzed (Figure 20B,C).

Although Treg percentages among total iLN $CD4^+$ T cells were not altered, Treg absolute numbers in $S7^{\Delta DC}$ mice were significantly and highly increased by 3.5-fold (more than 70% increase) as compared to respective wild type controls (Figure 20B).

Similarly, when compared to controls, the percentages of Tregs among $CD4^+$ T cells as well as total Treg counts were significantly increased in the spleen of $S7^{\Delta DC}$ mice by approximately 50% and 70%, respectively (Figure 20C).

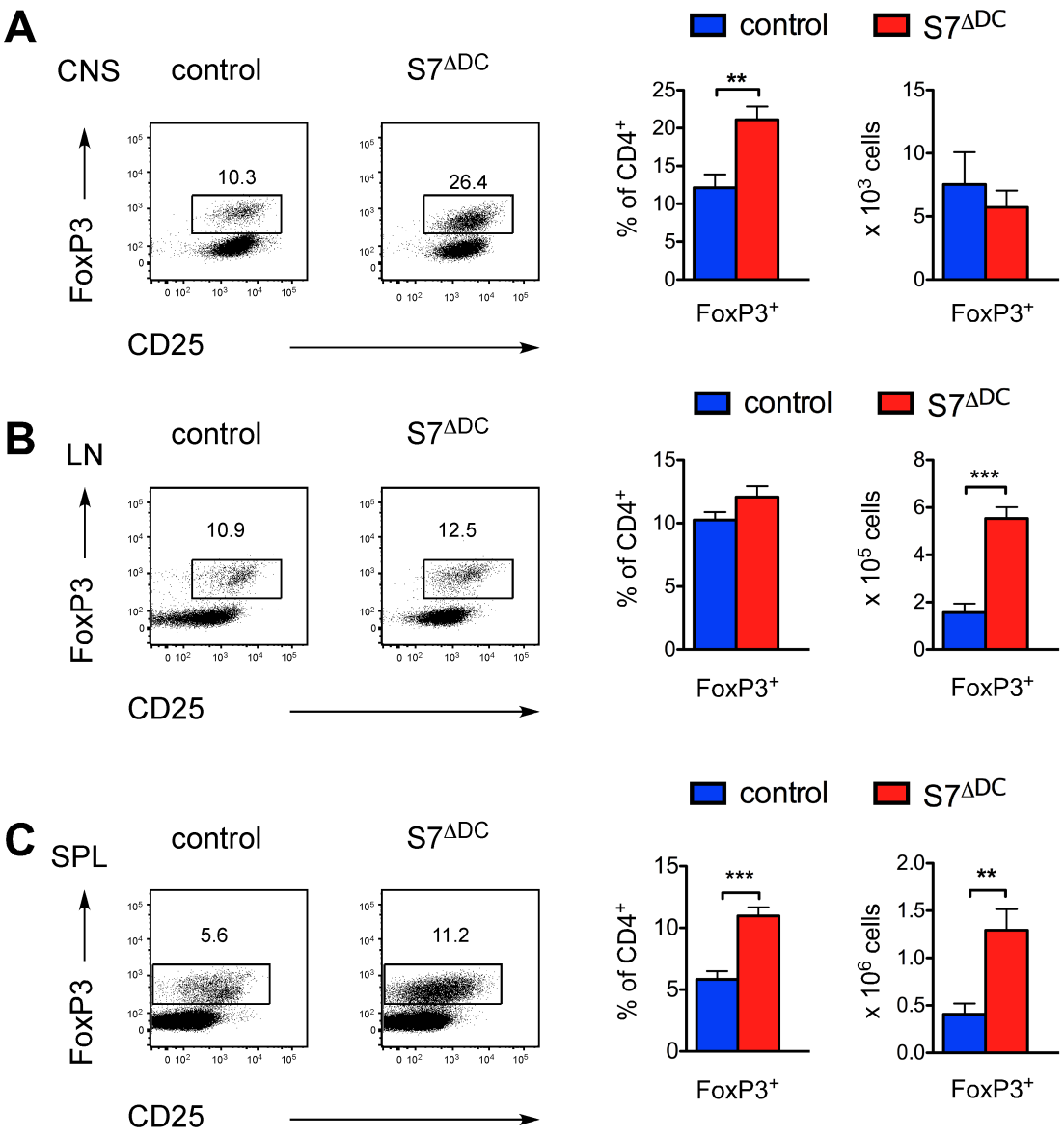

Figure 20: Increased CNS infiltration and peripheral amounts of Tregs in S7$^{\Delta DC}$ mice

(A) FACS blots as well as counts of CNS infiltrating FoxP3$^+$ Tregs and **(B)** LN as well as **(C)** splenic Foxp3$^+$ Tregs of S7$^{\Delta DC}$ (n=8) and control mice (n=7) at the peak of disease (day15). One representative out of four independent experiments is shown. Bar graphs depict mean value ± SEM. Statistical significance was assessed using Student's t-Test (*p ≤ 0.05, **p ≤ 0.005, ***p ≤ 0.0005).

Next it was assessed whether frequencies of MOG_{35-55}-specific peripheral IFN-γ producing Th1, IL-17A producing Th17 or IFN-γ/IL-17A double producing CD4$^+$ T cells were altered in the S7$^{\Delta DC}$ mice in comparison to control mice. To this end, spleen and iLNs of S7$^{\Delta DC}$ mice and controls were analyzed for the respective T cell subsets on day 15 post immunization (Figure 21).

Analysis for splenic MOG_{35-55} specific $CD40L^+$ $CD4^+$ effector T cells in $S7^{\Delta DC}$ mice on the peak of disease revealed no significant difference in percentage or absolute numbers when compared to control mice (Figure 17A). Likewise, further characterization of the MOG_{35-55} specific Th1, Th17 as well as IFN-γ/ IL-17A double producing $CD4^+$ T effector cells in the spleen of $S7^{\Delta DC}$ mice show no significant difference in percentages or absolute numbers when compared to controls (Figure 21B). Similarly, the percentages of MOG_{35-55} specific cells among the $CD4^+$ effector T cells in the iLN of $S7^{\Delta DC}$ mice were not altered as compared to controls (Figure 21 C). However, when Smad7 was absent in DCs, the total amounts of MOG_{35-55}-specific $CD4^+$ T cells in the iLN were significantly increased by 3-fold as compared to wild type mice, respectively (Figure 21C). The total amount of MOG_{35-55} specific $CD4^+$ T cells in the iLN on the peak of disease was significantly increased by 3-fold as compared to wild type mice (Figure 21C).

A comprehensive analysis of iLN derived MOG_{35-55} specific Th1, Th17 as well as IFN-γ/ IL-17A double producing $CD4^+$ T cells at the peak of disease, showed a significant reduction of 2.5-fold in the percentage of IFN-γ/ IL-17A double producers among the $CD4^+$ T cells in the $S7^{\Delta DC}$ mice (Figure 21). Concurrently, the ratios of Th1 and Th17 cells remained unaltered by the deletion of Smad7 in DCs (Figure 21D). Interestingly, when analyzing the total counts of these respective MOG_{35-55} reactive cells, no significant difference was found in regard to IFN-γ/ IL-17A double producing $CD4^+$ T cells. Instead, the total amounts of iLN Th17 cells in the $S7^{\Delta DC}$ mice were increased by 2-fold as compared to wild type (Figure 21D).

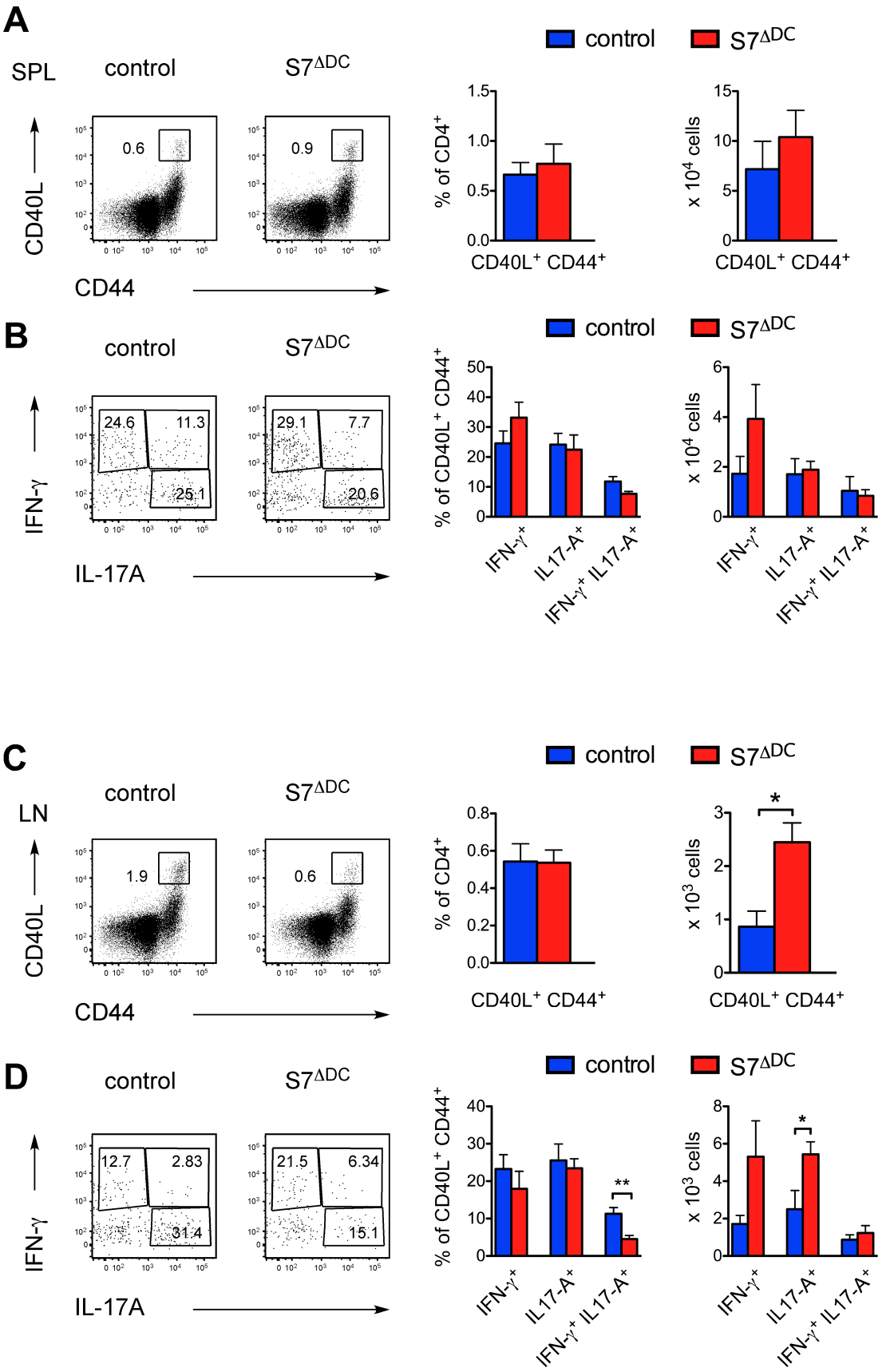

Figure 21: Characterization of MOG_{35-55} reactive T effector cells in peripheral organs of $S7^{\Delta DC}$ mice during EAE

(A+B) Flow cytometric analysis of splenic and **(C+D)** LN MOG_{35-55}- specific effector T cells ($CD40L^{high}$ $CD44^{+}$) pre-gated on $CD90.2^{+}$ $CD4^{+}$ cells from $S7^{\Delta DC}$ (n=8) and control mice (n=7) at the peak of disease (day15) and

(B+D) MOG_{35-55}-specific Th1 (IFN-γ^+), Th17 (IL-17A$^+$) and IFN-γ^+IL-17A$^+$ effector cells as pre-gated on CD90.2$^+$ CD4$^+$ CD40L^{high} CD44$^+$ cells. Bar graphs depict mean value ± SEM. Statistical significance was assessed using Student's t-Test (*$p \leq 0.05$, **$p \leq 0.005$, ***$p \leq 0.0005$).

At steady state, DCs found in the CNS are predominantly tolerogenic (Suter et al., 2003). During CNS inflammation on the other hand, activated and expanded MOG_{35-55}-specific T cells enter the CNS where they re-encounter APCs which re-present them their cognate antigen, leading to the full exertion of their pathogenic function (Greter et al., 2005). Thus, DCs play an important role in this process and therefore are able to impair the disease outcome to either immunity or tolerance. In fact deletion of DCs during EAE worsens disease progression suggesting that DCs are crucial for tolerance induction (Yogev et al., 2012).

Thus, it was investigated if the reduced susceptibility of S7$^{\Delta DC}$ mice to EAE and the reduced amount of MOG_{35-55} reactive T effector cells in the CNS might be attributed to a reduced abundance of DCs in the CNS target tissue during EAE, which would result in insufficient T cell licensing. Therefore S7$^{\Delta DC}$ mice were sacrificed on the peak of disease and the CNS infiltrating cells were isolated and thereafter were analyzed for the different DC subsets (Figure 22).

There was no significant difference in the percentages or total cell counts of CD11c$^+$ MHC-II$^+$ DCs found in the CNS of the S7$^{\Delta DC}$ mice as compared to controls during the peak of disease (Figure 22A). Likewise, the percentage and total cell counts of CD11c$^+$ CD11b$^-$ as well as CD11c$^+$ CD11b$^+$ cells in the CNS were comparable in all mice and were not affected by the deletion of Smad7 in DCs (Figure 22A, middle panel). Next, the expression levels of selected surface markers expressed by CNS-infiltrating DCs were examined. The mean fluorescence intensity (MFI) of CD103, MHC-II and PD-L1 expressed by CD11c$^+$ MHC-II$^+$ CNS cells was comparable between S7$^{\Delta DC}$ mice and controls (Figure 22B).

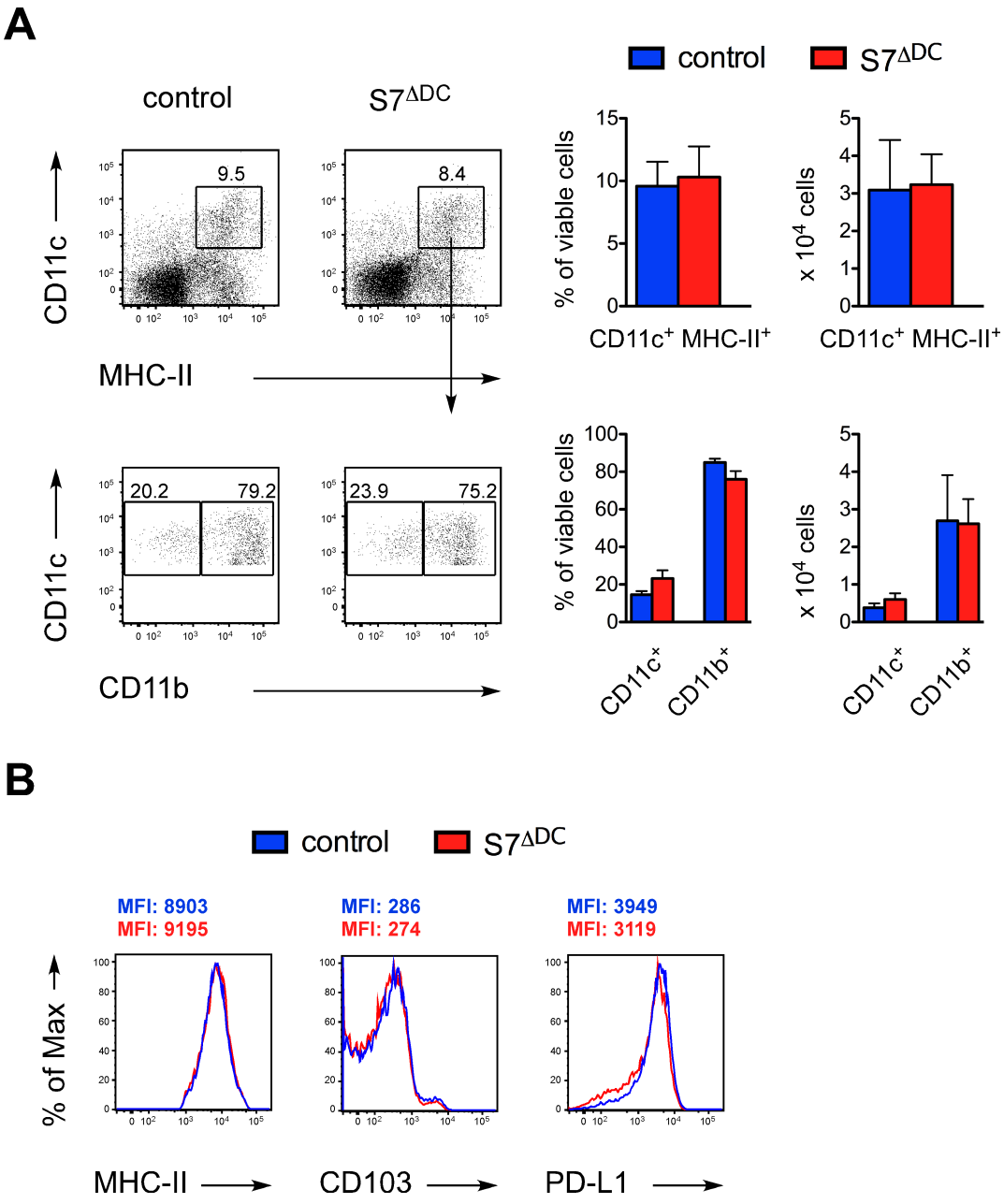

Figure 22: Smad7 deletion does not affect CD11c$^+$ MHC-II$^+$ cell homing to the CNS

(A) Representative FACs blots of CD11c$^+$ MHC-II$^+$ cells of S7$^{\Delta DC}$ (n=7) and control mice (n=3) on the peak of disease (day 17) pre-gated on viable cells (upper panel). **(B)** Histogram blots depicting CD103, MHC-II and PDL-1 expression by CD11c$^+$ MHC-II$^+$ DCs in the CNS of S7$^{\Delta DC}$ (n=7) and control mice (n=3) on the peak of disease (day 17). Bar graphs depict mean value ± SEM. Statistical significance was assessed using Student's t-Test (*p ≤ 0.05, **p ≤ 0.005, ***p ≤ 0.0005).

Next, it was examined whether DC-specific Smad7 deletion might affect splenic and LN DC substes during EAE. Therefore, S7$^{\Delta DC}$ and control mice were immunized with MOG_{35-55}/CFA+PTX and spleens as well as dLN were examined for the different DC subsets.

During steady state, $S7^{\Delta DC}$ mice had significantly elevated splenic $CD8^+$ DC frequencies, while in the LN $CD8^+$ DC frequencies remained mostly unaffected with comparable levels as those found in control animals (Figure 23; CD8, day0). In response to immunization however, $CD8^+$ DC frequencies in the spleen of wild type mice increased by 1.5 fold (Figure 23A). Although $S7^{\Delta DC}$ mice displayed significantly higher splenic $CD8^+$ DC frequencies than controls prior to immunization, this difference was no longer detectable three days post immunization (Figure 23A, day 0 vs. day 3). In the LN, $CD8^+$ DC frequencies in response to MOG_{35-55}/CFA immunization declined and were not affected by loss of Smad7 (Figure 23B, day 0 vs. day 3). The increased frequencies of splenic $CD8^+$ DCs are also reflected by the reduction of $CD11b^+$ DCs, the other major cDCs subset (Figure 23A), whereas in the LN $CD11b^+$ DCs are found in comparable occurrence (Figure 23B).

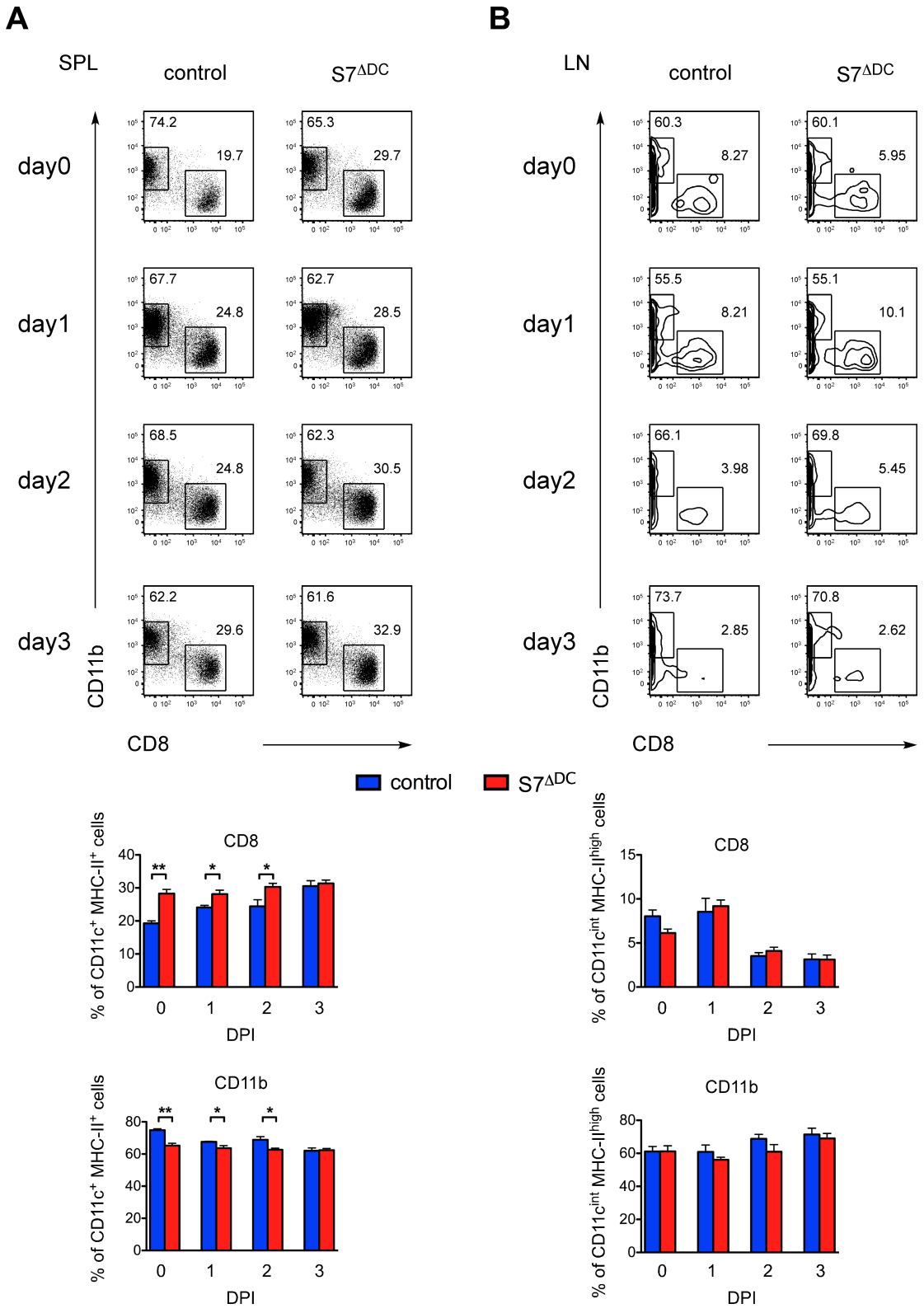

Figure 23: Evaluation of conventional CD8$^+$ and CD11b$^+$ DCs in S7$^{\Delta DC}$ mice during EAE

(A) Representative FACS blots and bar graphs depicting CD8$^+$ and CD11b$^+$ DC from spleens and **(B)** draining LN of S7$^{\Delta DC}$ (n=4) and control animals (n=4) at the indicated time points after MOG_{35-55}/CFA+PTX immunization. Cells were pre-gated on live CD90.2$^-$ B220$^-$ CD11c$^+$ MHC-II$^+$ (spleen) or CD11c^{int} MHC-II^{high} migratory DCs (LN), respectively. Bar graphs depict mean value ±SEM. Statistical significance was assessed using Student's t-Test (*$p \leq 0.05$, **$p \leq 0.005$, ***$p \leq 0.0005$).

$CD8^+$ DCs can be further subdivided into $CD103^-$ and $CD103^+$ DCs, with the latter being associated with tolerance induction. Therefore it was next investigated whether DC-specific Smad7 deletion affects $CD8^+$ $CD103^+$ DC in response to MOG_{35-55}/CFA immunization. The frequencies of splenic $CD8^+$ $CD103^+$ DCs in wild type mice increased by 3-fold following immunization (Figure 24A, day 0 vs. day 3). Similarly as seen for total $CD8^+$ splenic DCs frequencies, also $CD8^+$ $CD103^+$ DCs were strongly elevated during steady state (Figure 24A, day 0), yet three days after immunization no significant difference could be detected between $S7^{\Delta DC}$ mice and control animals (Figure 24A, day 3). In contrast, frequencies of $CD8^+$ $CD103^+$ DCs in the LNs three days post immunization were decreasing in control animals, while $S7^{\Delta DC}$ mice maintained elevated levels (Figure 24B, day 3). Though it did not reach significant difference, this was also reflected by total cell counts (Figure 24A and B).

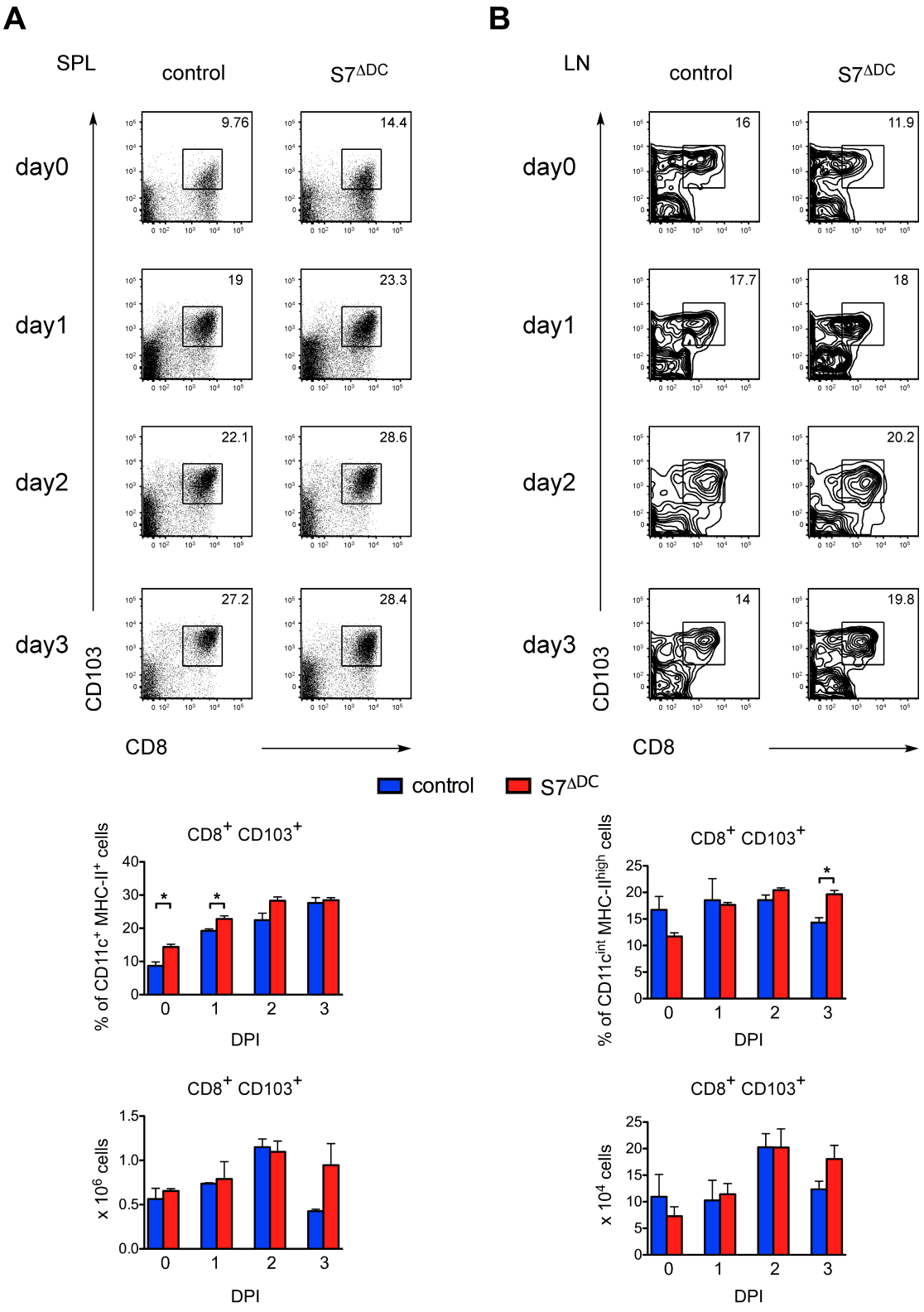

Figure 24 Evaluation of CD8$^+$ CD103$^+$ DC frequencies in S7$^{\Delta DC}$ mice during EAE

(A) Representative FACS blots and bar graphs depicting CD8$^+$ CD103$^+$ DC from spleens and **(B)** draining LN of S7$^{\Delta DC}$ (n=4) and control animals (n=4) at the indicated time points after MOG_{35-55}/CFA+PTX immunization. Cells were pre-gated on live CD90.2$^-$ B220$^-$ CD11c$^+$ MHC-II$^+$ (spleen) or CD11c^{int} MHC-II^{high} migratory DCs (LN), respectively. Bar graphs depict mean value ±SEM. Statistical significance was assessed using Student's t-Test (*p ≤ 0.05, **p ≤ 0.005, ***p ≤ 0.0005).

Next it was assessed if loss of Smad7 in DCs might affect the monocyte derived DCs (mDCs) subset during EAE. mDCs are identified based on the expression of CD24 and CD64 in addition to the classical CD11c and MHC-II cDC markers. Although upon MOG_{35-55}/CFA + PTX immunization mDC percentages and absolute numbers were increased in the spleen (1.5-fold and 3-fold, respectively), there was no difference between $S7^{\Delta DC}$ and controls mice (Figure 25A). mDCs in the LN were not enhanced upon immunization, exhibiting comparable percentages and absolute numbers of mDCs between $S7^{\Delta DC}$ and control mice (Figure 25B).

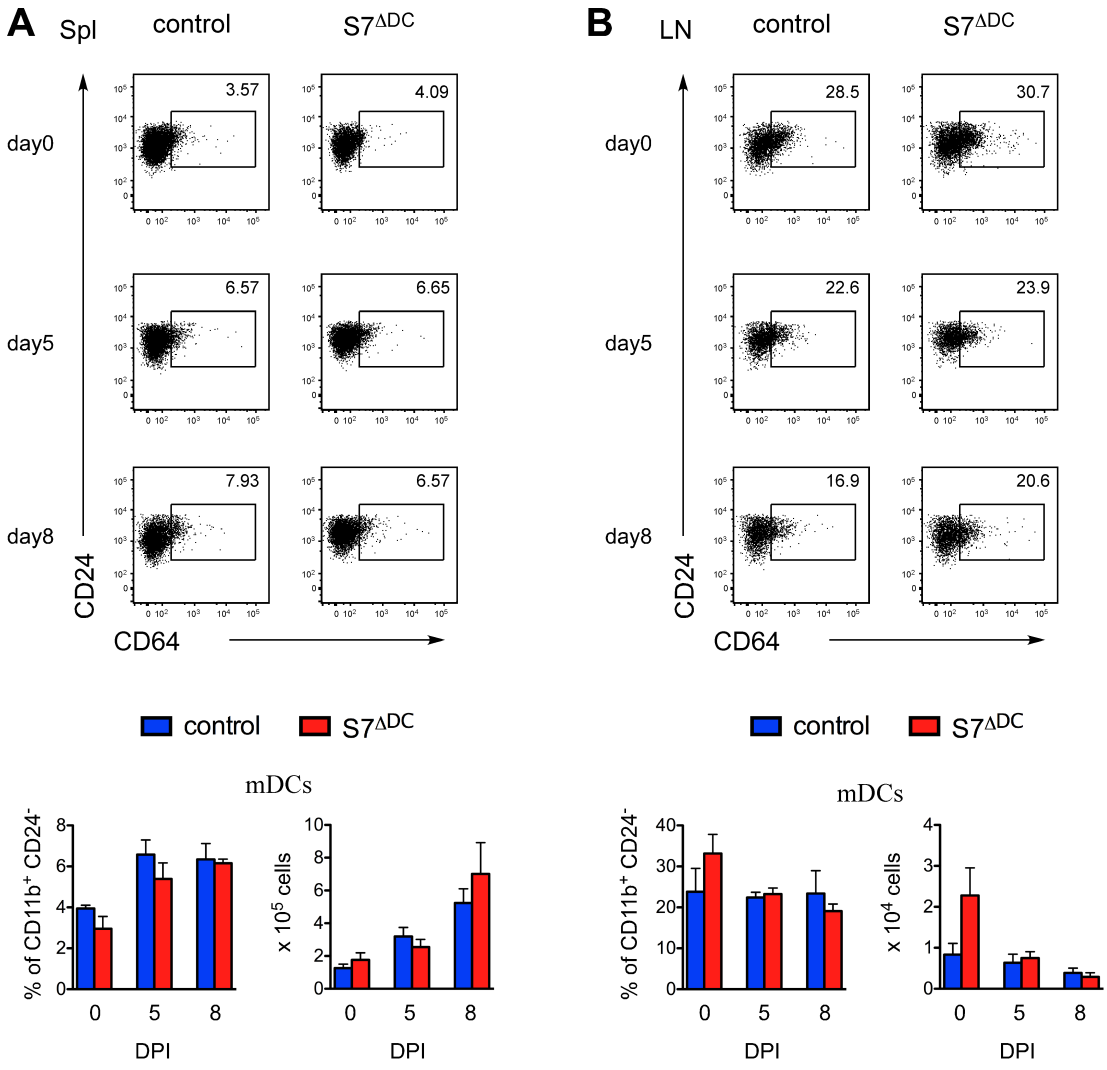

Figure 25: Frequencies and numbers of peripheral monocyte derived DCs in $S7^{\Delta DC}$ mice during EAE

(A) Splenic and **(B)** LN mDC of $S7^{\Delta DC}$ mice (n=2-4) and control (n=4-6) mice on the indicated time points after MOG_{35-55}/CFA immunization. Monocyte derived DCs were gated as viable $CD90.2^-$ $B220^-$ $CD11c^+$ $MHC\text{-}II^+$ $CD24^-$ $CD11b^+$ $CD64^+$cells. Bar graphs depict mean value ± SEM. Statistical significance was assessed using Student's t-Test (*$p \leq 0.05$, **$p \leq 0.005$, ***$p \leq 0.0005$).

3.2.4.2 Dendritic cell migration and antigen presentation by Smad7 deficient DCs during EAE

Following EAE induction, DCs take up the MOG_{35-55} antigen at the site of immunization and thereafter migrate to the lymph nodes, where they present the antigen to T cells. Since $S7^{\Delta DC}$ mice show reduced susceptibility to EAE, it was therefore next investigated whether Smad7 deficiency might affect this process, thus resulting in a lower amount of pathogenic effector T cells. To this end, mice were immunized with MOG_{35-55}/CFA emulsion containing FITC fluorescently-labeled beads. Upon antigen/beads encounter, DCs take up the antigen together with the FITC- labeled beads and migrate to the draining LN, were they can be detected based on the green fluorescence.

As early as twenty-four hours post immunization, the migration of DCs that incorporated the fluorescent-labeled beads at the site of immunization was visible in the skin-draining LNs of both groups tested (Figure 26). The maximal frequency of FITC-labeled beads incorporated DCs was detected in the dLN three days post immunization (Figure 26).

However, there was no significant difference in the percentage of fluorescent-labeled migratory DCs in both groups at any time point tested.

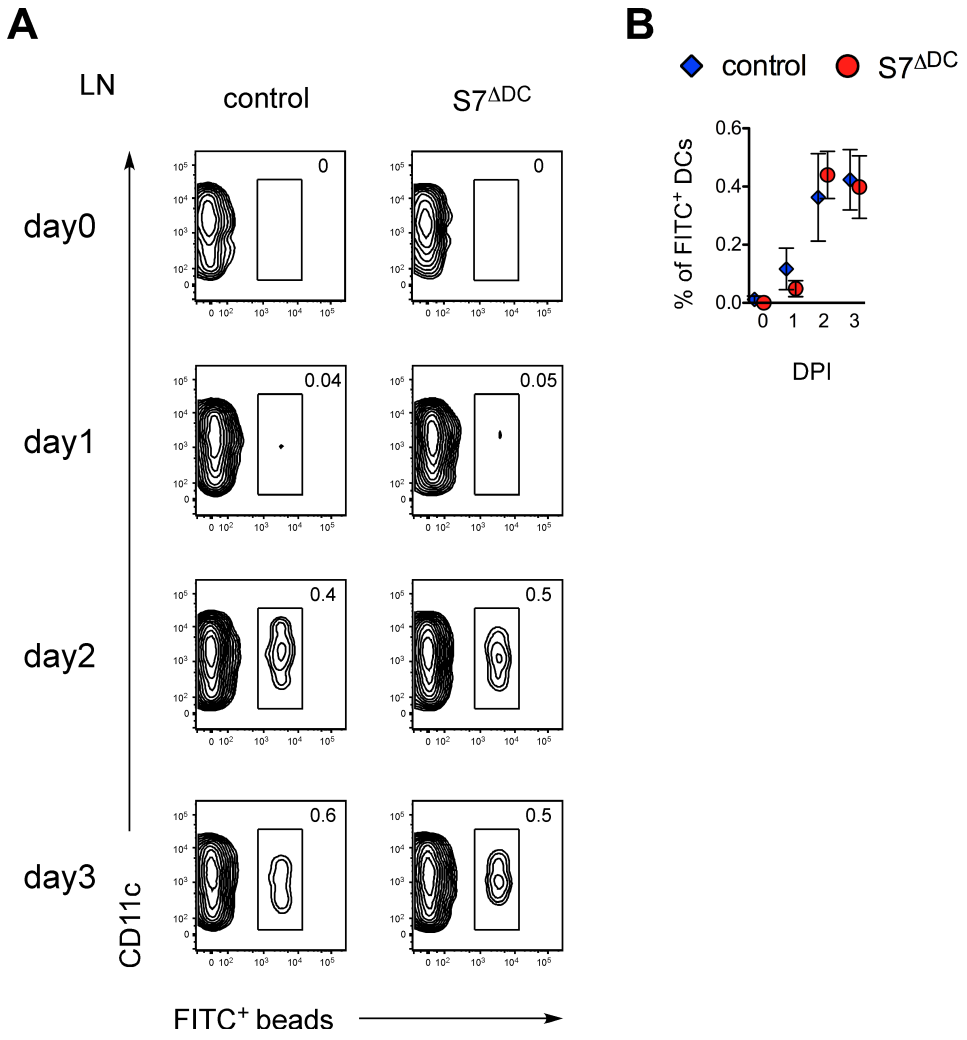

Figure 26: DC antigen uptake and migration to the LN is not affected by Smad7 deletion

(A) Representative FACS blots **(B)** and bar graphs of DCs isolated from draining LN of $S7^{\Delta DC}$ (n=4) and control animals (n=4) at the indicated time points after MOG_{35-55}/CFA+PTX immunization with emulsion containing FITC labeled beads. Cells were pre-gated on live $CD90.2^{-}$ $B220^{-}$ $CD11c^{int}$ MHC-II^{high} migratory DCs. Bar graphs depict mean value ±SEM. Statistical significance was assessed using two-way ANOVA and Bonferroni posttests (*$p \leq 0.05$, **$p \leq 0.005$, ***$p \leq 0.0005$).

Since antigen uptake and cell migration were not altered by DC-specific Smad7 deletion, it was next assessed whether Smad7-deficient DCs might have impaired antigen-presenting capacity due to altered expression of co-stimulatory molecules and thus lack the potential to activate T effector cells sufficiently.

To address this question, DCs expression of MHC-II and co-stimulatory molecules were measured during the first days post immunization.

In comparison to time point 0, the expression of the co-stimulatory molecules CD80 and CD86 on wild type DCs in the dLN increased upon immunization by 3.5-fold.

However, both Smad7-deficient and control DCs displayed similar up-regulation of CD80 and CD86 on migratory $CD11c^+$ $MHC\text{-}II^+$ DCs in the dLN upon EAE induction (Figure 27A). Next, GM-CSF derived bone marrow DCs (BMDCs) were generated from $S7^{\Delta DC}$ mice or control animals and their activation status in response to LPS stimulation was measured 24 hours later. BMDCs strongly up-regulated the expression of co-stimuli upon LPS stimulation. Yet, wild type-derived and $S7^{\Delta DC}$ mice derived BMDCs expressed similar levels of MHC-II, CD80, CD86 and CD40 upon LPS stimulation (Figure 27B).

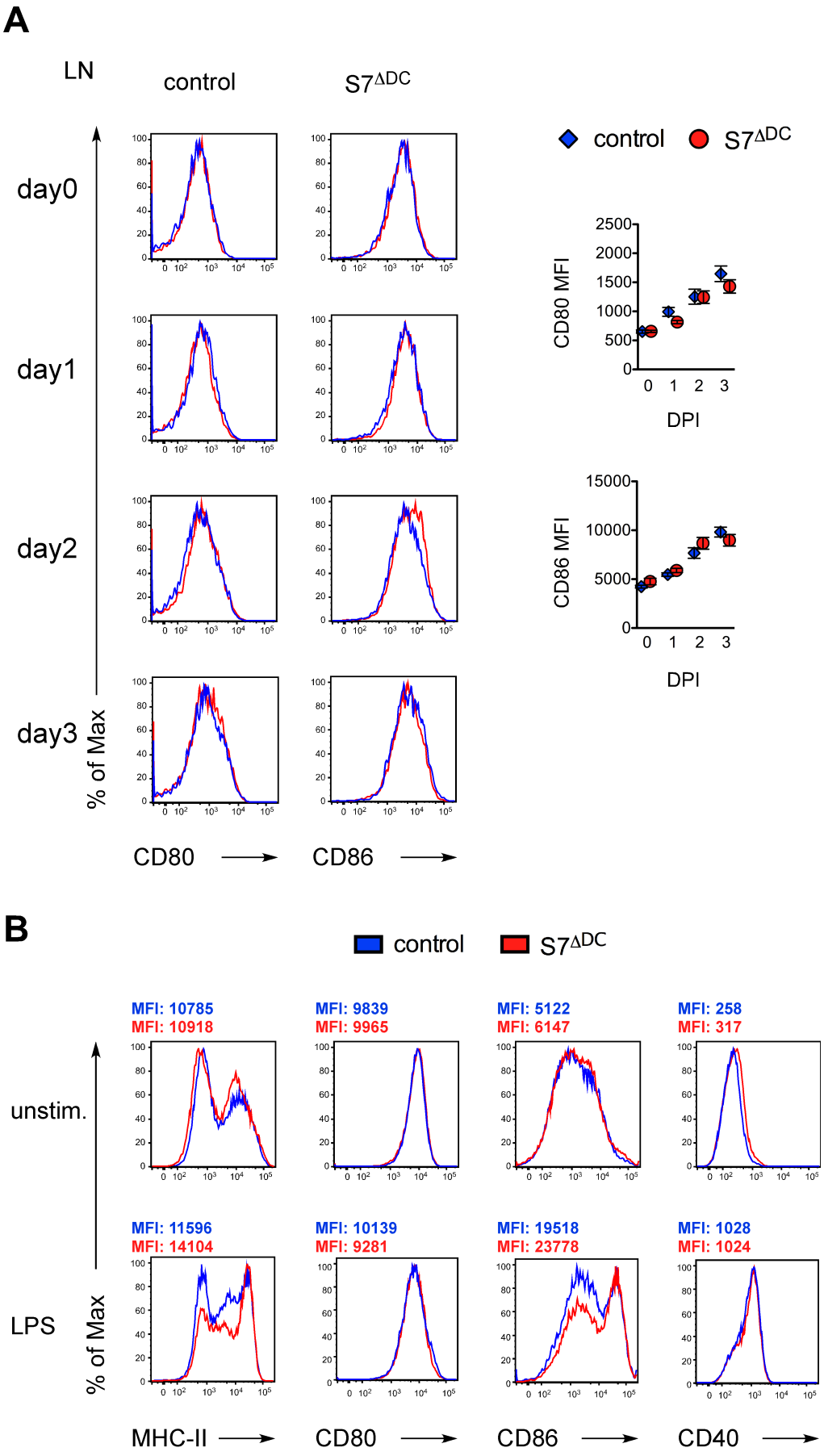

Figure 27: Expression of co-stimulatory molecules by DCs in response to inflammation is not affected by loss of Smad7

(A) Representative histogram blots (left) and MFI (right) of CD80 and CD86 expression on migratory DCs from dLNs of MOG_{35-55}/CFA+PTX immunized $S7^{\Delta DC}$ (n=4) and control animals (n=4) at the indicated time points after MOG_{35-55}/CFA+PTX immunization. Cells were gated on viable $CD90.2^-$ $B220^-$ $CD11c^{int}$ $MHC\text{-}II^{high}$ cells. **(B)** Representative histogram blots and MFI of MHC-II, CD80, CD86 and CD40 expression by GMCSF derived and LPS stimulated or un-treated BMDCs of $S7^{\Delta DC}$ (n=4) and control animals (n=5). Bar graphs depict mean value ±SEM. Statistical significance was assessed using (A) two-way ANOVA and Bonferroni posttests and (B) Student's t-Test (*$p \leq 0.05$, **$p \leq 0.005$, ***$p \leq 0.0005$).

3.2.4.3 DC- specific Smad7 deletion does not affect T cell activation and proliferation

Since the antigen up-take at the site of immunization, the migration to the dLN and the co-stimuli expression was not altered upon loss of Smad7 in DCs, it was next examined whether the reduced EAE susceptibility observed in these mice might result from reduced T cell activation by a mechanism that might have not been addressed yet. To this end, EAE was induced, mice were sacrificed several days later and the iLN as well as spleens were examined for the activation status of the T cells. On day 3 and day 8 post immunization, the percentage and total cell counts of activated $CD4^+$ T cells, based on the expression of $CD44^+$ $CD66L^+$, were comparable between $S7^{\Delta DC}$ and controls mice, suggesting that T cell activation is not affected by the DC specific Smad7 deletion (Figure 28).

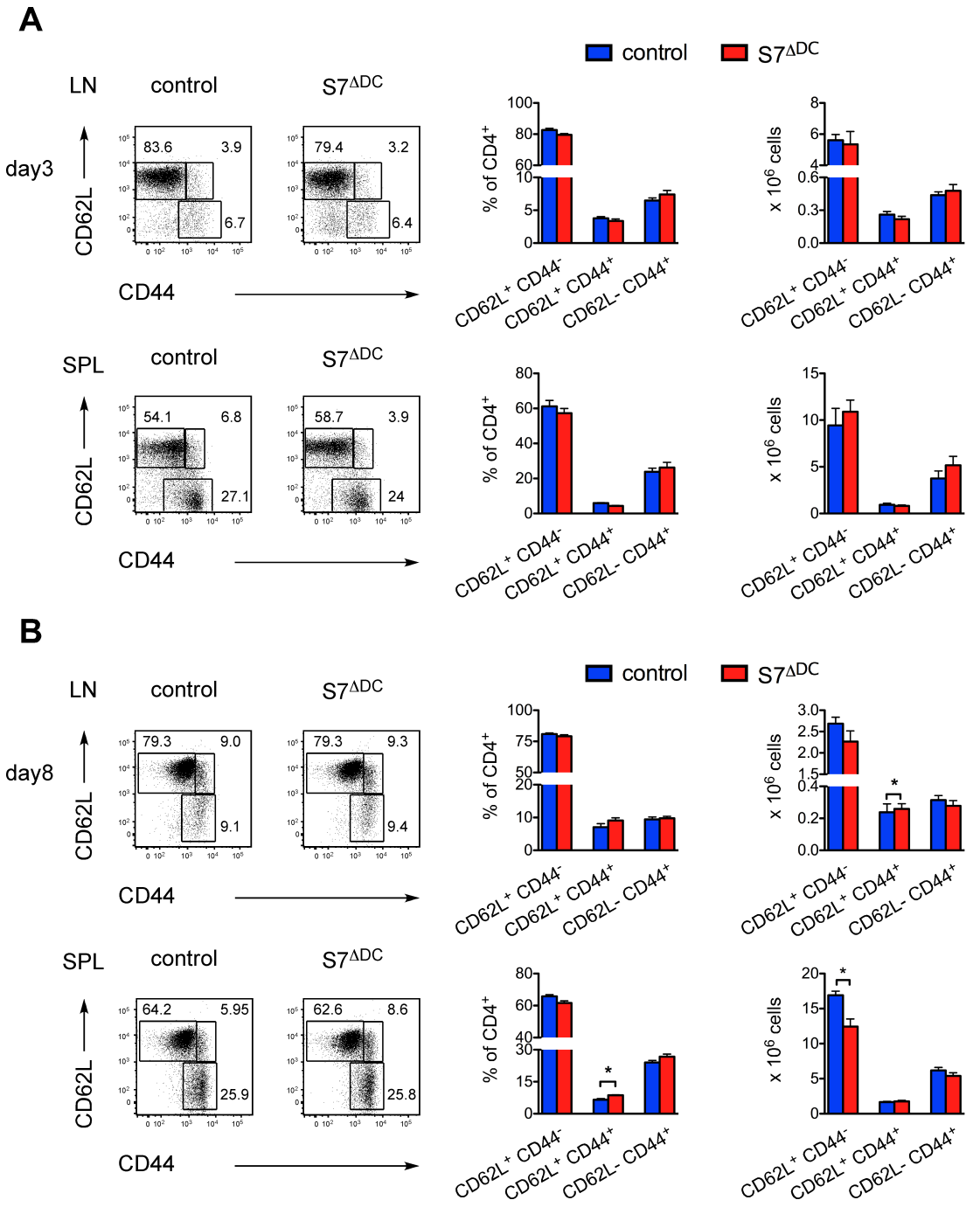

Figure 28: T cell activation during EAE is not affected by DC specific Smad7 deficiency

(A) Representative FACs blots of naïve ($CD62L^+$ $CD44^-$), central memory ($CD62L^+$ $CD44^+$) and effector memory ($CD62L^-CD44^+$) $CD4^+$ T cells in the iLN and spleen of control (n=4/3) and $S7^{\Delta DC}$ (n=4/9) mice on day 3 and **(B)** day 8 post MOG_{35-55}/CFA+PTX immunization. Gates were set on viable $CD90.2^+$ $CD4^+$ cells. Bar graphs depict mean value ± SEM. Statistical significance was assessed using Student's t-Test (*p ≤ 0.05, **p ≤ 0.005, ***p ≤0.0005).

Next it was assessed whether T cell proliferation in response to MOG_{35-55} presentation by Smad7 deficient DCs might be impaired. To this end $CD4^+$ 2D2 TCR transgenic $CD4^+$ T cells, harboring a transgenic TCR specific for MOG_{35-55}, were CFSE labeled

and co-cultured under the indicated conditions with MOG_{35-55}-pulsed splenic DCs or GM-CSF derived BMDCs, from either naïve $S7^{\Delta DC}$ or control animals (Figure 29).

The *in vitro* proliferation as seen by CFSE dilution of $CD4^+$ 2D2 TCR transgenic T cells primed by MOG_{35-55} pulsed splenic DCs, was similar and irrespective of the presence or absence of Smad7 in DCs (Figure 29A). Likewise MOG_{35-55} presentation by GM-CSF derived BMDCs generated from either naïve $S7^{\Delta DC}$ mice or control mice resulted in similar proliferation of $CD4^+$ 2D2 TCR transgenic T cells (Figure 29B).

When TGF-β was added to the culture, proliferated cell MFIs were higher than in the same condition without TGF-β, indicating that although mild, TGF-β stimulation did suppress cell proliferation. Nevertheless, when comparing the different genotypes under the same conditions, there was no significant difference in the capability of Smad7 deficient DCs and control DCs to induce T cell proliferation (Figure 29B).

Since Smad7 deficiency in DCs did not affect the T cell proliferation under the conditions tested, it was next assessed whether the reduced susceptibility to EAE might be attributed to a reduced migration of MOG_{35-55} reactive T cells to the target tissue. Therefore $S7^{\Delta DC}$ or wild type control mice were subjected to EAE and 5 days post MOG_{35-55}/CFA immunization, a MOG_{35-55} re-challenge was performed by injection of MOG_{35-55} to one ear and saline as a control to the other ear. Ear swelling was measured before re-challenge as well as for three consecutive days post injection. The MOG_{35-55} specific ear swelling was calculated by subtracting the ear swelling of the saline treated ear from the value of the MOG_{35-55} treated ear. Within 24h after MOG_{35-55} re-challenge, ear swelling was strongly increased by 7-fold and 72h post re-challenge, the swelling increased by11-fold as compared to basal levels. However, no significant difference was detected, when comparing ear-swelling of $S7^{\Delta DC}$ mice and wild-type controls (Figure 29C).

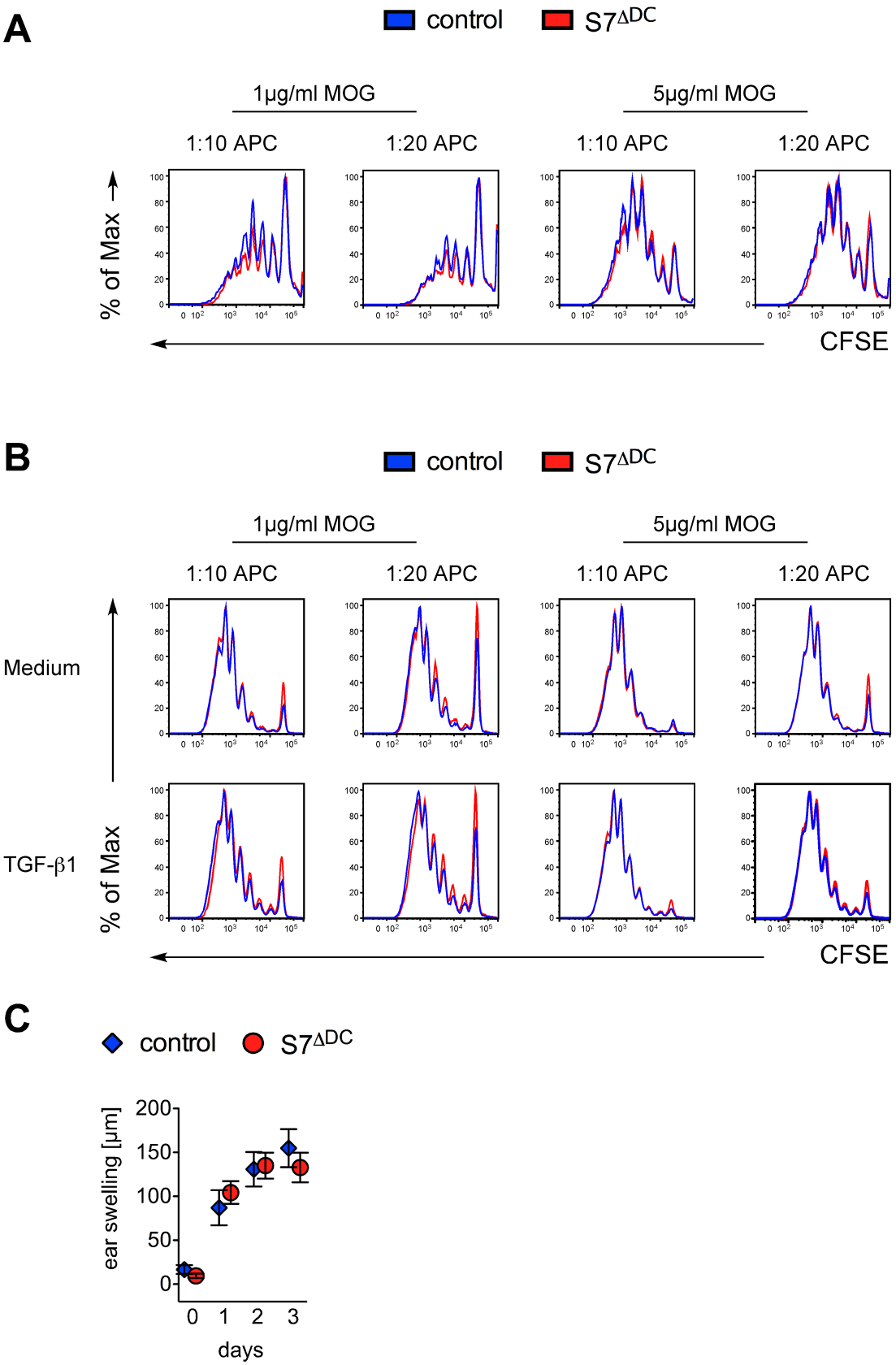

Figure 29: DC specific Smad7 expression does not affect T cell proliferation

(A) Representative proliferation of $CD4^+$ MACs purified CFSE labeled 2D2 TCR transgenic T cells co-cultured with splenic CD11c MACs purified MOG_{35-55} pulsed DCs derived from control (n=2) or $S7^{\Delta DC}$ (n=2) mice, stimulated for 5 days under indicated ratios of T cells to APCs. **(B)** Representative proliferation of $CD4^+$ MACs

purified CFSE stained 2D2 TCR transgenic T cells co-cultured with GM-CSF derived MOG_{35-55} pulsed BMDCs derived from control (n=2) or $S7^{\Delta DC}$ (n=2) mice, stimulated for 5 days under indicated ratios of T cells to APCs and under the indicated stimuli condition. **(A-B)** Results represent two independent experiments. **(C)** Ear swelling response of MOG_{35-55}/CFA + PTX immunized $S7^{\Delta DC}$ (n=10) or control mice (n=5), that were re-challenged with MOG_{35-55} or saline control *intra pinna*, into right and left ear, respectively. Ear swelling response to MOG_{35-55} was measured in comparison to the saline treated ear at the indicated time points.

Next it was tested whether loss of Smad7 might impact on the ability of DCs to differentiate T cells into the Th1 and Th17 cell subsets. Therefore GMCSF derived BMDCs (Figure 30A) or splenic purified DCs (Figure 30B) were co-cultured with $CD4^+$ T cells derived from naïve 2D2 TCR transgenic mice in presence or absence of MOG_{35-55} in combination with or without LPS and in the presence of TGF-β1. While without MOG_{35-55} almost no IL-17A or IFN-γ production could be detected (Figure 30; upper panels), the addition of MOG_{35-55} alone or in combination with LPS resulted in Th1 cell differentiation as detected by IFN-γ production. Nevertheless, in both BMDCs and splenic DC cultures there was no difference in the percentages of IFN-γ positive T cells, regardless whether the DCs derived from control or $S7^{\Delta DC}$ mice (Figure 30; second and third panel). When T cells were cultured in the presence of MOG_{35-55}, LPS and TGF-β1, the percentages of IL-17A positive T cells strongly increased. Yet, deletion of Smad7 in DCs did not affect the percentages of IL-17A positive T cells neither when BMDCs or splenic DCs were used.

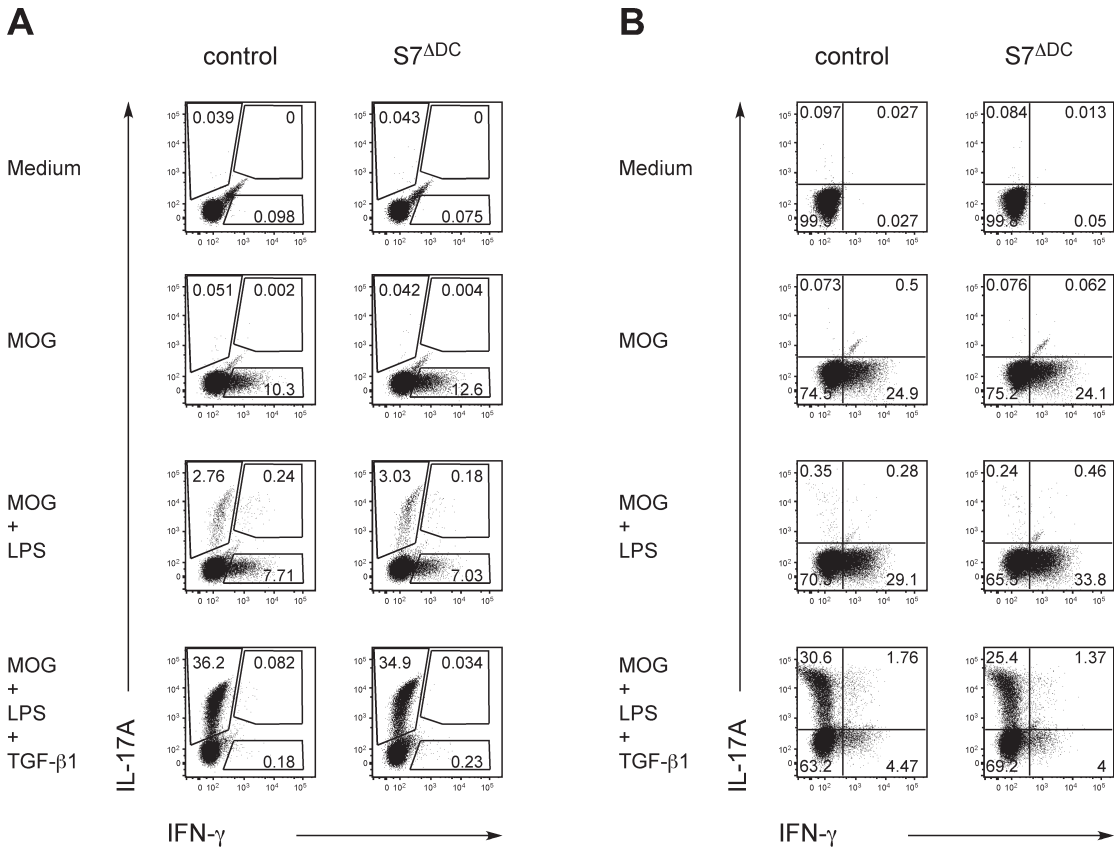

Figure 30 DC specific loss of Smad7 does not affect differentiation of Th1 and Th17 cells *in vitro*

(A) GM-CSF derived BMDCs or **(B)** splenic CD11c$^+$ MACs purified DCs of control (n=1) and S7$^{\Delta DC}$ (n=3) mice were co-cultured with CD4$^+$ MACs purified 2D2 TCR transgenic T cells under indicated conditions *in vitro*. Gates were set on CD90.1$^+$ CD4$^+$ lymphocytes. Data represents results of two independent experiments.

Next it was tested if DCs devoid of Smad7 might produce less pro-inflammatory cytokines than wild type DCs resulting in diminished inflammation during EAE. Therefore, the relative mRNA, as well as expression of cytokines prominent during EAE such as TNF-α and IL-6 was examined.

The relative IL-6 mRNA expression of *in vitro* LPS (TLR4 agonist) stimulated splenic DCs derived from naïve control S7$^{\Delta DC}$ mice was increased by 5-fold as compared to the medium control levels. However, there was no significant difference between Smad7 proficient and deficient DCs (Figure 31A). Likewise, stimulation of the TLR3 on DCs using Poly(I:C) *in vitro* resulted in 5-fold increased IL-6 mRNA expression as compared to medium controls. However, consistently the IL-6 expression level was unaltered between stimulated wild type and Smad7-deficient DCs (Figure 31A).

Further analysis of IL-6 cytokine expression upon LPS stimulation of splenic DCs derived from naïve control or S7$^{\Delta DC}$ mice *in vitro* revealed an 11-fold increase in IL-6

cytokine production as compared to medium controls (Figure 31B). LPS treated DCs deficient in Smad7 had similar IL-6 cytokine levels as control stimulated DCs. Stimulation of DCs with LPS in combination with TGF-β1 reduced the IL-6 expression levels by 50% in comparison to the IL-6 cytokine levels obtained in LPS treated DCs alone, however there was no significant difference between Smad7 proficient and deficient DCs (Figure 31B). To recapitulate the conditions present during EAE, when DCs encounter T cells in a pro-inflammatory cytokine environment, DCs were stimulated with LPS together with CD40L in the presence or absence of TGF-β1. Without TGF-β1 stimulation, IL-6 levels increased by 16-fold as compared to medium control levels. Yet, though IL-6 levels were reduced by 1.5-fold in $S7^{\Delta DC}$-derived DCs as compared to control DCs, this difference was not statistically significant. The addition of TGF-β1 along with the LPS and CD40L stimulation reduced IL-6 production by 40% as compared to LPS and CD40L treated DCs without additional TGF-β1 stimulation. DCs devoid of Smad7 expressed similar levels of IL-6 as control DCs under these conditions (Figure 31B).

Since IL-6 expression was not affected by the deletion of Smad7 under all conditions tested, it was further assessed if Smad7 might affect the production of TNF-α, another pro-inflammatory cytokine expressed by DCs and known to be involved in immediate inflammatory response. Splenic DCs isolated from naïve control or $S7^{\Delta DC}$ mice were therefore stimulated with LPS or PolyIC *in vitro* and real time analysis for TNF-α transcripts was performed. The expression of TNF-α mRNA in response to both tested stimuli was comparable between DCs devoid of Smad7 and wild type control DCs, resulting in 3-fold increase by both stimuli as compared to medium controls (Figure 31C). Analysis of TNF-α cytokine expression by splenic DCs isolated from naïve control or $S7^{\Delta DC}$ mice, either stimulated with LPS or LPS in combination with CD40L in the presence or absence of TGF-β1, revealed no significant difference between DCs devoid of Smad7 and wild type DCs under any tested conditions, despite a 4-fold increase in all tested conditions when compared to medium controls (Figure 31D).

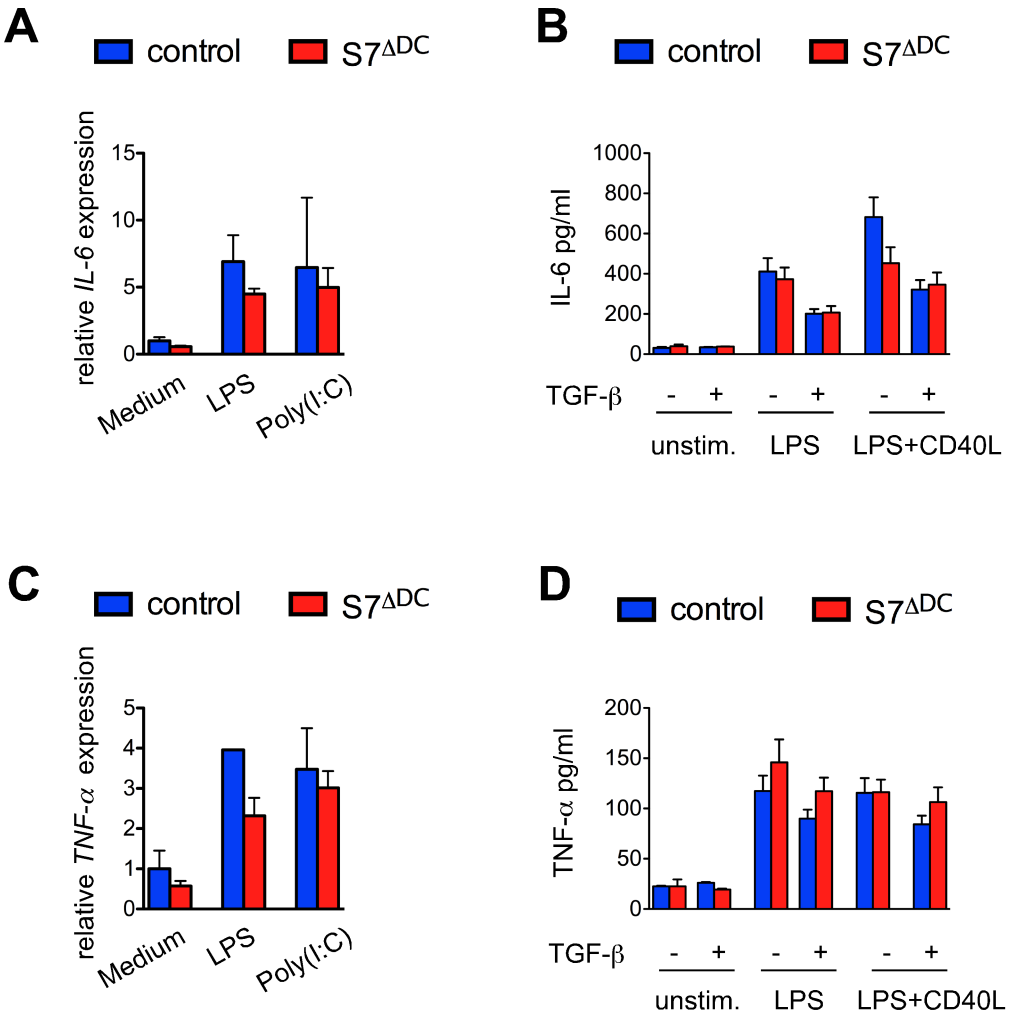

Figure 31: Smad7-deficiency does not affect DC derived IL-6 and TNF-α production

(A) Real time analysis showing relative IL-6 expression by splenic DCs derived from naïve control (n=2) and $S7^{\Delta DC}$ (n=3) mice stimulated for 4h with LPS, PolyIC or left untreated. **(B)** Cytokine bead array showing IL-6 cytokine expression of splenic DCs derived from naïve control (n=5) and $S7^{\Delta DC}$ (n=5) mice stimulated 24h with the indicated conditions. **(C)** Real time analysis showing relative TNF-α expression by splenic DCs derived from naïve control (n=2) and $S7^{\Delta DC}$ (n=3) mice stimulated for 4h with LPS, PolyIC or left untreated. **(D)** Cytokine bead array showing TNF-α cytokine expression of splenic DCs derived from naïve control (n=5) and $S7^{\Delta DC}$ (n=5) mice stimulated 24h with the indicated conditions. Bar graphs depict mean value ± SEM. Statistical significance was assessed using Student's t-Test (*$p \leq 0.05$, **$p \leq 0.005$, ***$p \leq 0.0005$).

As DC secretion of prominent pro-inflammatory cytokines was not altered by the loss of Smad7, it was next assessed whether Smad7-deficient DCs exhibit an altered expression of anti-inflammatory cytokines such as IL-10 or TGF-β1.

Analysis of either LPS or Poly(I:C) stimulated as well as untreated splenic DCs isolated from naïve control or $S7^{\Delta DC}$ mice revealed no significant difference in IL-10 mRNA expression levels between Smad7 deficient and control DCs (Figure 32A). LPS stimulation increased IL-10 expression by 4-fold, while Poly(I:C) stimulation increased the IL-10 expression by 2-fold as compared to the IL-10 mRNA expression

levels in the medium control. However, loss of Smad7 in DCs had no effect on IL-10 expression in these conditions tested (Figure 32A). Measurement of IL-10 cytokine production by splenic DCs, isolated from naïve control or $S7^{\Delta DC}$ mice in response to *in vitro* stimulation with or without LPS in combination with CD40L in presence or absence of TGF-β1, revealed no significant difference between Smad7-deficient DCs and wild type DC controls (Figure 32B).

When stimulated with LPS, the IL-10 cytokine levels increased by 10-fold as compared to medium controls in both groups tested, whereas when stimulated with TGF-β1 in addition, the IL-10 production was reduced by 50% in both groups (Figure 32B). The combination of LPS and CD40L stimulation increased IL-10 expression by 2.6-fold compared to LPS treatment alone, and by 30-fold compared to the medium control. Both groups, when stimulated additionally with TGF-β1, exhibit 50% reduction in IL-10 expression as compared to the values obtained in the absence of TGF-β1.

Previously, it was suggested that an autocrine TGF-β1 loop exists (Kim et al., 1989a; Kim et al., 1989b; Kim et al., 1989c). Therefore, it was next assessed whether under pro-inflammatory conditions Smad7 deletion might affect TGF-β1 production by DCs. To this end, splenic DCs from naïve control and $S7^{\Delta DC}$ mice were stimulated with LPS or Poly(I:C) and mRNA transcripts for TGF-β1 were measured (Figure 32C). Interestingly, both conditions did not show any elevation in TGF-β1 mRNA expression compared to medium controls. Furthermore, there was no difference in TGF-β1 expression between DCs lacking Smad7 and wild type control DCs. Further analysis of TGF-β1 production *in vitro* upon LPS or LPS in combination with CD40L stimulation of splenic DCs derived from control and $S7^{\Delta DC}$ mice revealed no difference in TGF-β1 expression. However, LPS as well as LPS and CD40L stimulation did not induce TGF-β1 expression as both TGF-β1 mRNA transcripts and cytokine levels upon stimulation were comparable to the medium controls (Figure 32D).

In vitro stimulation of splenic DCs with TGF-β1, induced the expression of TGF-β1 transcripts by 2-fold already within 3h post stimulation as compared to medium controls. Whereas 24h post stimulation, TGF-β1 transcripts levels were back at basal levels. This was independent of Smad7 presence or absence on DCs, as both groups

showed comparable expression levels of TGF-β1 transcripts (Figure 32E). The stimulation with IFN-γ did not induce TGF-β1 expression, but rather blocked expression of TGF-β1 transcripts after stimulation for 24h irrespective of the genotype (Figure 32F).

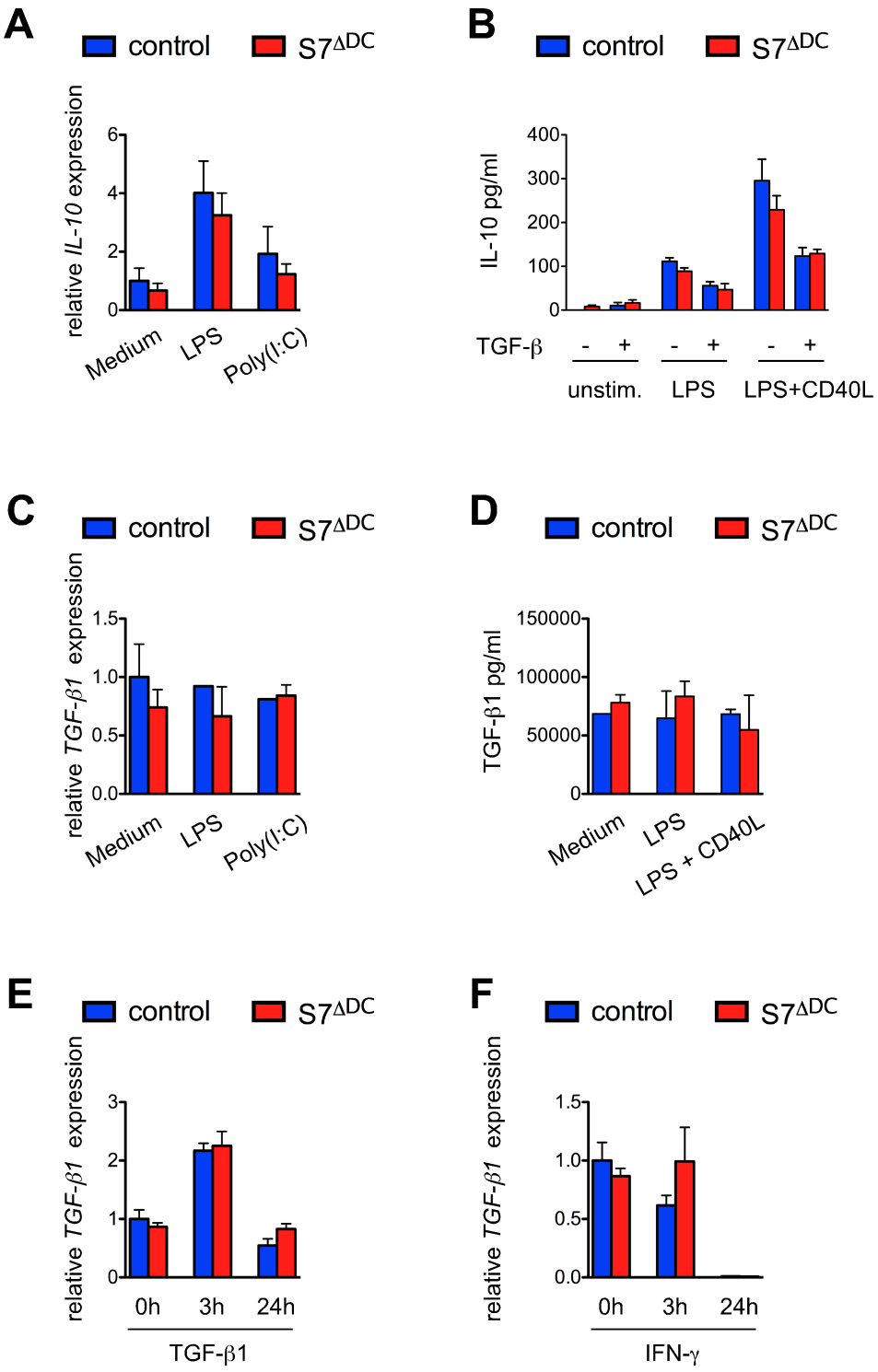

Figure 32: DC specific Smad7 deletion does not affect expression of TGF-β and IL-10

(A) Real time analysis showing relative IL-10 expression by splenic DCs derived from naïve control (n=2) and $S7^{\Delta DC}$ (n=3) mice stimulated for 4h with LPS, Poly(I:C) or left untreated. **(B)** Cytokine bead array showing IL-10 cytokine expression of splenic DCs derived from naïve control (n=5) and $S7^{\Delta DC}$ (n=5) mice stimulated 24h with the indicated conditions. **(C)** Real time analysis showing relative TGF-β1 expression by splenic DCs derived from naïve control (n=2) and $S7^{\Delta DC}$ (n=3) mice stimulated for 4h with LPS, Poly(I:C) or left untreated. **(D)** Cytokine bead array showing TGF−β1 cytokine expression of splenic DCs derived from naïve control (n=5) and $S7^{\Delta DC}$ (n=5) mice stimulated 24h with the indicated conditions. **(E)** Real time analysis for relative TGF-β1 expression by TGF-β1 or **(F)** IFN-γ stimulated splenic DCs from control (n=3) and $S7^{\Delta DC}$ (n=3) mice. Bar graphs depict mean value ± SEM. Statistical significance was assessed using Student's t-Test (*p ≤ 0.05, **p ≤ 0.005, ***p ≤0.0005).

3.2.4.4 Smad7 deletion increases IDO expression

Mice lacking Smad7 specifically in DCs showed reduced susceptibility to EAE, which was accompanied by decreased infiltration of MOG_{35-55} reactive effector T cells and increased Tregs during EAE. However, the loss of Smad7 did not alter DC antigen uptake, migration, expression of co-stimulatory molecules or the production of prominent pro- and anti-inflammatory cytokines. Since DCs deficient in Smad7 showed increased expression of IRF8 transcripts in response to both TGF-β or IFN-γ stimulation (Figure 9A), it was thus hypothesized that the expression of indoleamine-2,3 dioxygenase (IDO), a direct target of IRF8, might be likewise affected by Smad7 deletion.

Indoleamine-2,3 dioxygenase 1 and 2 (IDO) are enzymes involved in the tryptophan catabolism, that also exert anti-inflammatory functions. IDO was reported to both suppress effector T cells and induce Tregs, which might account for reduced disease progression during EAE in $S7^{\Delta DC}$ mice.

To test whether lack of Smad7 in DCs might result in higher IDO expression levels under TGF-β1 and IFN-γ stimulation, real time analysis for IDO1 and IDO2 transcripts of splenic purified DCs derived from naïve control and $S7^{\Delta DC}$ mice treated with TGF-β1 and IFN-γ *in vitro* was performed.

DCs deficient in Smad7 had slightly increased IDO1 expression levels already at steady state (Figure 33A and C), while IDO2 expression was absent in all samples tested (Figure 33B and D). Stimulation of splenic DCs derived from naïve control and $S7^{\Delta DC}$ mice with IFN-γ for 12h and 24h strongly increased IDO1 expression when compared to control DCs (Figure 33A). The expression of IDO2 transcripts upon 12h of IFN-γ stimulation was strongly increased by 4-fold in Smad7-deficient DCs as compared to wild type stimulated controls (Figure 33B). IDO1 expression in response

to 24h stimulation with IFN-γ was 2,5 fold higher in Smad7-deficient DCs when compared to the respective control (Figure 33B).

Stimulation of splenic DCs derived from naïve control and $S7^{\Delta DC}$ mice with TGF-β1 *in vitro* revealed a 3-fold increase after 3h stimulation while only a small increase of 1.3-fold was visible after 24h stimulation in DCs devoid of Smad7 as compared to control DCs (Figure 33C). IDO2 expression levels of splenic DCs derived from naïve control and $S7^{\Delta DC}$ mice with TGF-β1 *in vitro* revealed a 3-fold decrease after 3h and a small increase of 1.3-fold after 24h stimulation in DCs devoid of Smad7 as compared to control DCs (Figure 33D).

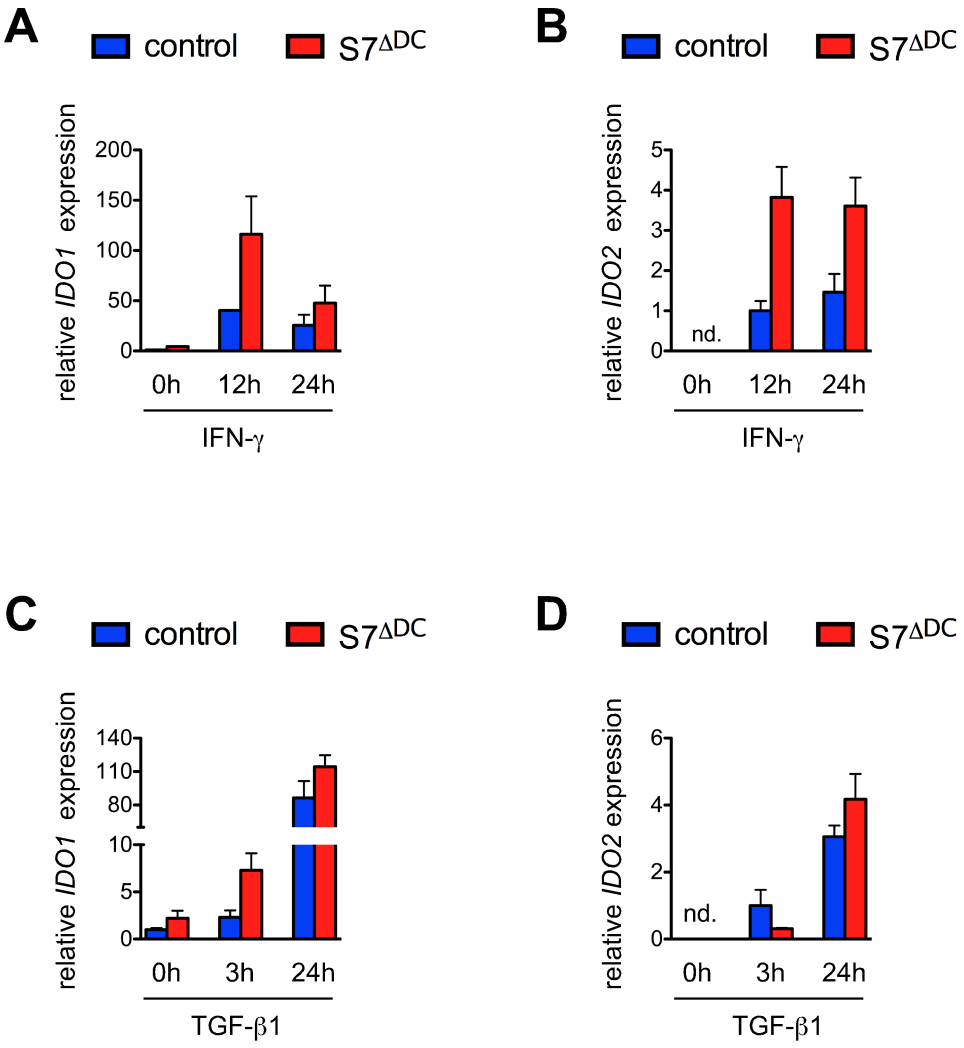

Figure 33: Smad7 deficiency results in increased IDO expression

(A) Real time PCR analysis for IDO1 and **(B)** IDO2 mRNA expression by splenic purified DCs of naïve control (n=2) or $S7^{\Delta DC}$ (n=2) mice, stimulated with IFN-γ for indicated time points. Expression of IDO1 and IDO2 transcripts were measured relative to the housekeeping gene HPRT and normalized to the controls 0h time point in case of IDO1, the 12h time point of IFN-γ stimulated control DCs in case of IDO2 expression. **(C)** Real time PCR analysis for IDO1 and **(D)** IDO2 mRNA expression by splenic DCs of naïve control (n=4) and $S7^{\Delta DC}$ (n=4) mice stimulated with TGF-β1 for the indicated time points. Expression of IDO1 and IDO2 transcripts were measured

relative to the housekeeping gene HPRT and normalized to the controls 0h time point in case of IDO1 expression or to the 3h time point in case of IDO2 expression. Bar graphs depict mean value ± SEM. Statistical significance was assessed using Student's t-Test (*p ≤ 0.05, **p ≤ 0.005, ***p ≤0.0005).

In order to assess which DC subsets are potent IDO producers during steady state and upon MOG_{35-55}/CFA immunization, spleens and dLNs of wild type animals during steady state were analyzed (Figure 34A-E).
In general all DC subsets expressed significantly more IDO than T and B cells. Among the splenic and LN DC subsets tested during steady state, pDCs expressed the highest IDO levels, followed by $CD8^+$ $CD103^+$ cDCs and $CD8^+$ cDCs, whereas mDCs and $CD11b^+$ DCs had the lowest IDO expression during steady state (Figure 34A, and B).

Since all DC subsets expressed IDO at steady state, it was further assessed which DC subsets in general increase upon MOG_{35-55}/CFA immunization. Therefore the total cell counts of splenic DC subsets during steady state and upon MOG_{35-55}/CFA immunization in wild type mice were quantified (Figure 34C). MOG_{35-55}/CFA immunization increased the amounts of all DC subsets tested. However, the total cell counts of $CD8^+$ $CD103^+$ cDCs (15-fold) and pDCs (7-fold) increased to the highest extent in response to MOG_{35-55}/CFA immunization when compared to the other DC subsets tested.

Next, the IDO expression by cDCs, pDCs and mDCs in the spleen and dLN 8 days post MOG_{35-55}/CFA immunization was analyzed (Figure 34D). IDO expression by splenic $CD8^+$, $CD11b^+$ and $CD8^+$ $CD103^+$ cDCs was not affected by MOG_{35-55}/CFA immunization. Although pDCs expressed the highest IDO levels during steady state, IDO expression by pDCs was significantly reduced following MOG_{35-55}/CFA immunization. In contrast to pDCs, splenic mDCs responded with the highest increase of IDO expression following MOG_{35-55}/CFA immunization, compared to all tested DC subsets. Due to high variability of IDO expression in the analyzed groups, the result was not statistically significant.
Eight days post MOG_{35-55}/CFA immunization, total dLN-derived $CD11c^+$ MHC-II^+ cells, and in particular the $CD8^+$ cDCs revealed significantly increased IDO expression levels when compared to steady state (Figure 34E). IDO expression likewise increased in $CD11b^+$ cDCs, but due to a high variability within the groups,

failed to reach significance. pDCs and $CD8^+$ $CD103^+$ cDCs maintained their high levels of IDO expression detected during steady state. mDCs showed the highest increase of IDO expression in response to MOG_{35-55}/CFA immunization, although due to high variability within the groups, these results did not reach statistical significance.

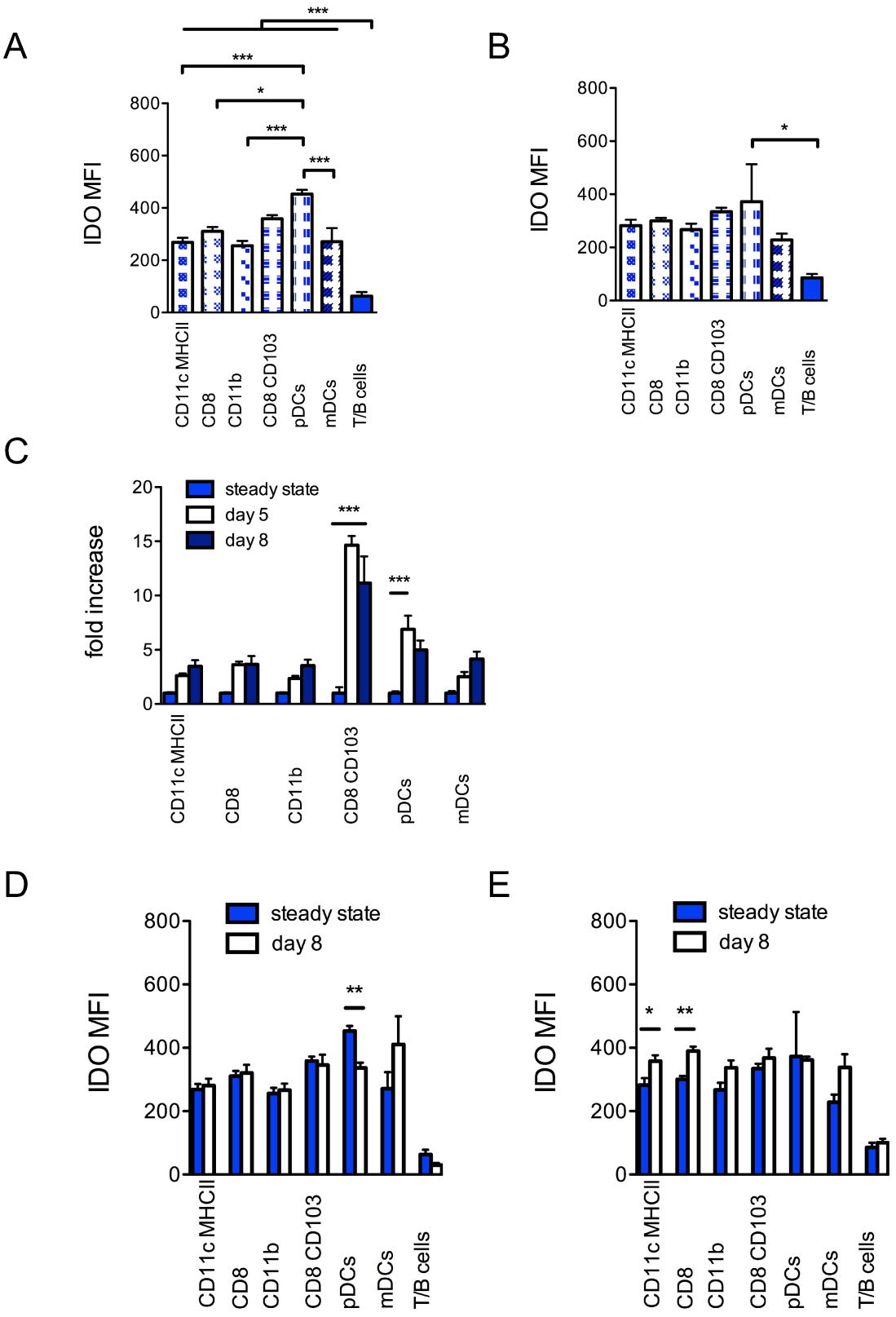

Figure 34: Characterization of IDO expression by different DC-subsets during steady state and EAE

(A) IDO1 mean fluorescence intensity (MFI) of splenic and **(B)** dLN DC subsets derived from naïve wild type mice (n=4). **(C)** Fold increase of indicated splenic DC-subset cell counts on day 5 (n=6) and day 8 (n=4) post MOG_{35-55}/CFA immunization. Values of day 5 and day 8 were normalized to the steady state values obtained for each DC subset. **(D)** IDO1 MFI of dLN and **(E)** splenic DC subsets derived from naïve (n=4) wild type mice or MOG_{35-55}/CFA + PTX immunized wild type mice (n=6) five days post immunization. (**A-E**) Conventional DC

subsets were pregated on viable CD90.2$^-$ B220$^-$ CD11c$^+$ MHC-II$^+$ and further on either CD8$^+$, CD11b$^+$ or CD8$^+$ CD103$^+$ cDCs. For pDCs gates were set on viable CD90.2$^-$ B220$^+$ Ly6c$^+$ PDCA1$^+$ cells. For monocyte derived DCs (mDCs) gates were set on viable CD90.2$^-$B220$^-$ CD11c$^+$ MHC-II$^+$ CD24$^-$ CD11b$^+$CD64$^+$. Bar graphs depict mean value ± SEM. Statistical significance was assessed using Student's t-Test (*p ≤ 0.05, **p ≤ 0.005, ***p ≤0.0005).

Since DCs devoid of Smad7 expressed increased IDO mRNA levels, it was next examined if DCs from S7$^{\Delta DC}$ mice have altered IDO1 expression during EAE. Therefore IDO1 protein expression in DCs derived from spleen and iLN of S7$^{\Delta DC}$ mice and control mice on day 5 post MOG$_{35-55}$/CFA immunization was assessed by intracellular FACs staining.

While splenic S7$^{\Delta DC}$-derived cDCs, pDCs and mDCs had similar IDO expression level as that of control mice (Figure 35A), in the dLNs, S7$^{\Delta DC}$ mice had significantly increased IDO1 expression in CD11c$^+$ MHC-II$^+$, CD8$^+$, CD11b$^+$ and CD8$^+$ CD103$^+$ cDCs as compared to the respective controls (Figure 35B).

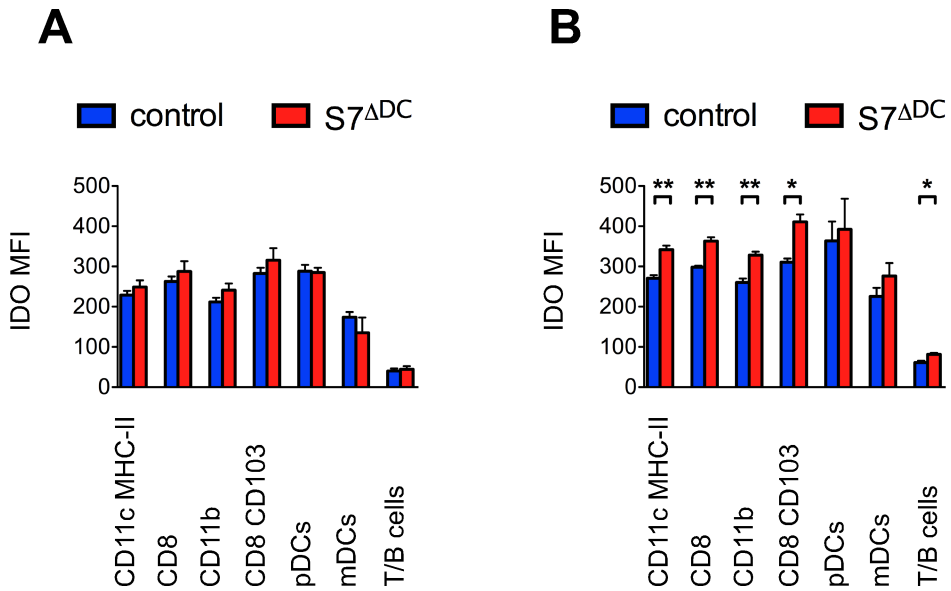

Figure 35: Smad7-deficient DCs express higher levels of IDO during EAE

(A) Splenic and **(B)** dLNs DC subsets of S7$^{\Delta DC}$ (n=4) and control (n=6) mice on day 5 post MOG$_{35-55}$/CFA immunization. **(A-B)** cDC subsets gates were pregated on viable CD90.2$^-$ B220$^-$ CD11c$^+$ MHC-II$^+$, CD8$^+$, CD11b$^+$ or CD8$^+$ CD103$^+$ cells. For pDCs gates were set on viable CD11c$^+$ B220$^+$ PDCA1$^+$ Ly6c$^+$ cells. mDCs were gated as viable CD90.2$^-$ B220$^-$ CD11c$^+$ MHC-II$^+$ CD24$^-$ CD11b$^+$ CD64$^+$cells. Bar graphs depict mean value ± SEM. Statistical significance was assessed using Student's t-Test (*p ≤ 0.05, **p ≤ 0.005, ***p ≤0.0005).

As DCs devoid of Smad7 expressed increased levels of IDO during EAE, it was next tested whether the reduced susceptibility of $S7^{\Delta DC}$ mice to EAE might be attributed to the increased expression of IDO. To test this, EAE was induced by MOG_{35-55}/CFA and PTX immunization along with simultaneous treatment with 1-Methyl-D-tryptophan (1-MT), a competitive inhibitor of IDO, or the respective vehicle control (Cady and Sono, 1991; Hou et al., 2007; Mellor and Munn, 2004; Munn, 2006).

Wild type control mice treated with the vehicle developed normal EAE disease progression, while $S7^{\Delta DC}$ mice were less susceptible to EAE with delayed onset, reduced mean maximum clinical scores and reduced incidence as documented previously (Figure 36A; Table 7). Inhibition of IDO activity by injection of 1-MT on the day of EAE induction significantly restored the susceptibility of $S7^{\Delta DC}$ mice to EAE as compared to vehicle treated mice (Figure 36B; Table 7). The day of disease onset in 1-MT treated $S7^{\Delta DC}$ mice was 2 days earlier as compared to vehicle treated $S7^{\Delta DC}$ mice, and the mean maximum scores as well as disease incidence were both increased when IDO was inhibited (Figure 36B; Table 7). 1-MT treatment of wild type control animals resulted in slightly increased mean maximum scores and an increased EAE incidence.

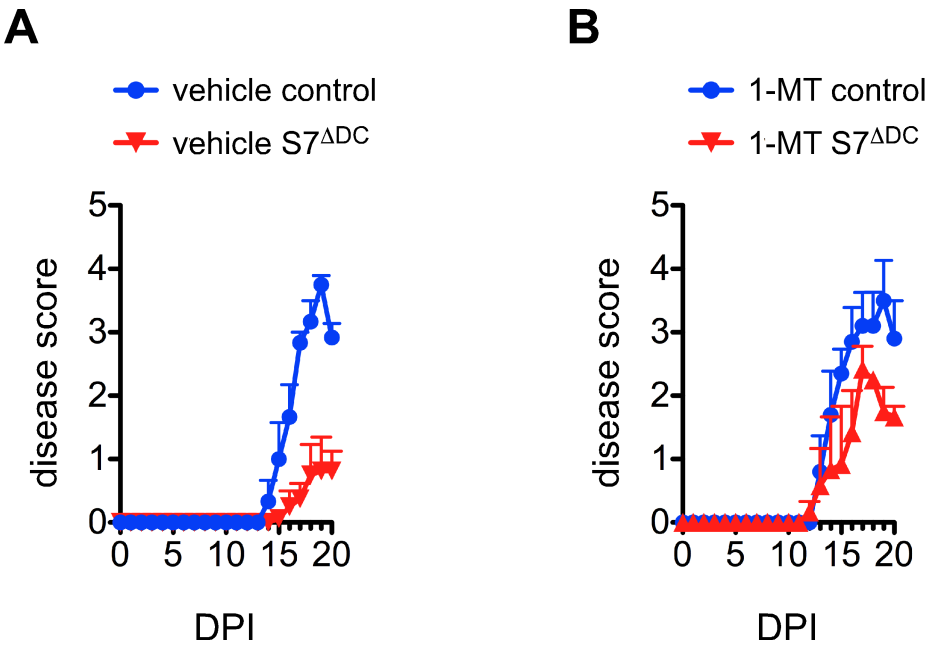

Figure 36: Inhibition of IDO by treatment with 1-MT restores susceptibility of $S7^{\Delta DC}$ mice to EAE

(A) EAE disease progression in vehicle treated control (n=3) or $S7^{\Delta DC}$ (n=4) mice and **(B)** 1-MT treated control (n=5) or $S7^{\Delta DC}$ (n=3) mice. Vehicle or 1-MT treatment was performed once on the day of MOG_{35-55}/CFA immunization. Shown is one representative out of two independent experiments. Bar graphs depict mean value ± SEM. Statistical significance was assessed using EAE area under curve (AUC) followed by two-way ANOVA and Bonferroni posttests (*$p \leq 0.05$, **$p \leq 0.005$, ***$p \leq 0.0005$

genotype	control	$S7^{\Delta DC}$	control	$S7^{\Delta DC}$
treatment	vehicle	vehicle	1-MT	1-MT
amount of mice per group	n=9	n=9	n=7	n=9
day of onset	14.13 ± 1.47	17.25 ± 2.06	14.00 ± 2.00	15.00 ± 2.38
maximal clinical score	2.81 ± 1.19	0.5 ± 0.76	3.25 ± 1.39	2.03 ± 1.36
incidence	87.5 ± 17.68	47.5 ± 38.89	100 ± 0.00	77.5 ± 3.54

Table 7: Inhibition of IDO restores the susceptibility of $S7^{\Delta DC}$ mice to EAE

Since the susceptibility of $S7^{\Delta DC}$ mice to EAE was increased by a single injection of the IDO inhibitor 1-MT at the day of MOG_{35-55}/CFA immunization, it was further analyzed how this treatment affects the CNS infiltration in general and especially the CNS infiltration of $CD4^+$ T effector and Treg cells. To this end, mice were subjected to EAE and treated with either vehicle or 1-MT on the day of immunization. Thereafter, the mice were sacrificed on day 20 post EAE induction and single cell suspensions of the spinal cords as well as brains were analyzed.

In accordance with the clinical scores, $S7^{\Delta DC}$ mice treated with vehicle control showed reduced amounts of $CD45.2^+$ $CD11b^+$ cells in percentage and absolute numbers as compared to vehicle treated control mice (Figure 37). 1-MT treatment increased the percentage and amounts of CNS infiltrating $CD45.2^+$ $CD11b^+$ cells in $S7^{\Delta DC}$ mice to comparable levels like in 1-MT treated controls (Figure 37A). Analysis of the CNS infiltrates for $CD4^+$ $CD90.2^+$ T cells in $S7^{\Delta DC}$ mice treated with the vehicle revealed a strong reduction in percentage and total cell counts of infiltrating $CD4^+CD90.2^+$ T cells as compared to the vehicle treated control group (Figure 37B). 1-MT treatment of $S7^{\Delta DC}$ mice resulted in increased $CD4^+$ $CD90.2^+$ T cell infiltration to the CNS in percentage and total cell counts to comparable levels as in 1-MT treated control mice. Further analysis for MOG_{35-55} specific effector T cells, based on CD40L and CD44 co-expression on CNS infiltrating $CD4^+$ lymphocytes, revealed as expected a strong decrease in the vehicle treated $S7^{\Delta DC}$ mice as compared to the vehicle treated control group (Figure 37C). IDO inhibition with 1-MT reverted this difference to similar levels as observed in 1-MT treated controls. Subsequent analysis of MOG_{35-55} specific effector Th1, Th17 and IL-$17A^+$ IFN-γ^+ T cells in the vehicle treated group displayed no difference in the ratios among these cells, but as previously shown, a

strong reduction in the total cell counts of all three subsets was detected when Smad7 was absent in DCs. This difference observed in vehicle treated $S7^{\Delta DC}$ mice was reverted by 1-MT treatment, resulting in comparable amounts of CNS infiltrating Th1, Th17 and IL-17A$^+$ IFN-γ^+ T cells as that in 1-MT treated control mice.

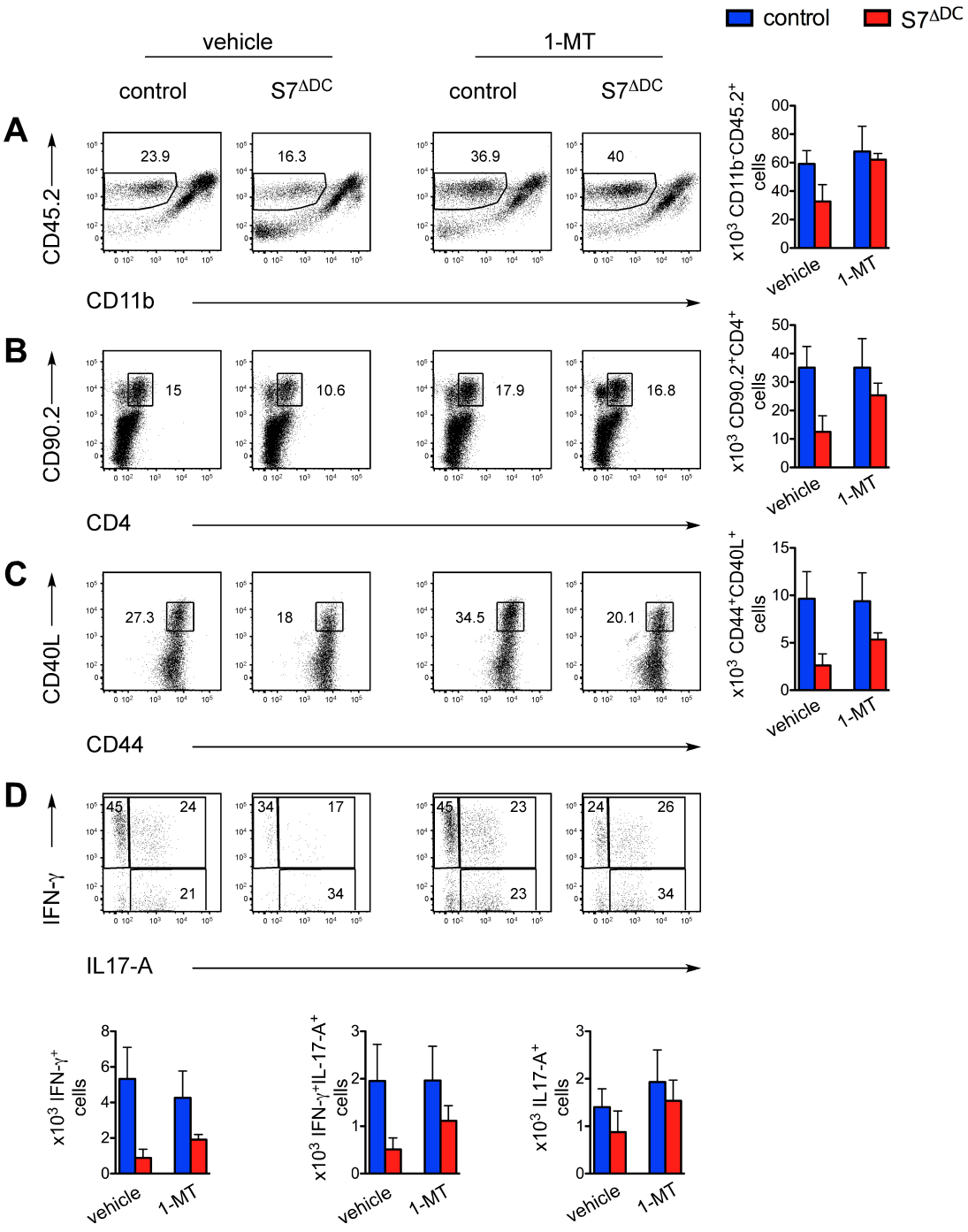

Figure 37: Inhibition of IDO by 1-MT increases CNS infiltration of effector T cells in $S7^{\Delta DC}$ mice during EAE

(A) Analysis of CNS infiltrates on day 20 post EAE induction in vehicle treated control (n=3) or $S7^{\Delta DC}$ (n=4) mice and 1-MT treated control (n=5) or $S7^{\Delta DC}$ (n=3) mice. FACS blots and bar graphs illustrating CNS infiltrating CD45.2$^+$CD11b$^-$ lymphocytes pre-gated on viable cells, **(B)** CD90.2$^+$ CD4$^+$ cells pre-gated on viable cells, **(C)**

MOG-specific $CD40L^+$ $CD44^+$ effector T cells pre-gated on viable $CD90.2^+$ $CD4^+$ cells and **(D)** MOG-specific Th1, Th17 and IL-$17A^+$ IFN-γ^+ double producing cells as gated on viable $CD90.2^+$ $CD4^+$ $CD40L^+$ $CD44^+$ cells. Bar graphs depict mean value ± SEM. Statistical significance was assessed using two-way ANOVA and Bonferroni posttests (*$p \leq 0.05$, **$p \leq 0.005$, ***$p \leq 0.0005$).

As inhibition of IDO by a single 1-MT injection partially restored disease progression, it was next assessed whether loss of Smad7 in DCs might induce the generation of iTregs and whether this could be reverted by 1-MT treatment. Therefore, $S7^{\Delta DC}$ or control MACS purified splenic DCs were pulsed with MOG_{35-55}, stimulated with TGF-β1 with or without additional 1-MT treatment and co-cultured with naïve sorted $CD4^+$ T cells derived from 2D2 TCR transgenic FoxP3-GFP mice. Detection of *de novo* generated iTregs was performed based on the GFP expression of cultured T cells. DCs isolated from $S7^{\Delta DC}$ mice had a strong tendency to induce higher amounts of iTregs than controls (Figure 38A). Addition of 1-MT to the co-culture reduced the total amounts of Tregs in $S7^{\Delta DC}$ mice by 50% when compared to vehicle treated $S7^{\Delta DC}$ mice. At the same time, 1-MT treatment in the control group resulted in a strong induction of Tregs (Figure 38A and B).

Next, it was assessed whether the increased amounts of Tregs detected in $S7^{\Delta DC}$ mice during an ongoing CNS inflammation result from increased IDO levels, and accordingly, whether 1-MT treatment would revert this increase. For this purpose, $S7^{\Delta DC}$ and controls mice were subjected to EAE and treated with 1-MT or vehicle on the day of MOG_{35-55}/CFA injection. Treg numbers in the LNs of EAE subjected mice were assessed 10 days after MOG_{35-55}/CFA immunization and revealed a strong increase in response to immunization when compared to naïve controls, suggesting that the immunization was successful and the time point of analysis was suitable to assess iTreg generation in response to EAE induction. Vehicle treated $S7^{\Delta DC}$ mice had significantly higher amounts of Tregs in the LN when compared to vehicle treated controls, yet 1-MT treatment completely abolished this significant difference (Figure 38C).

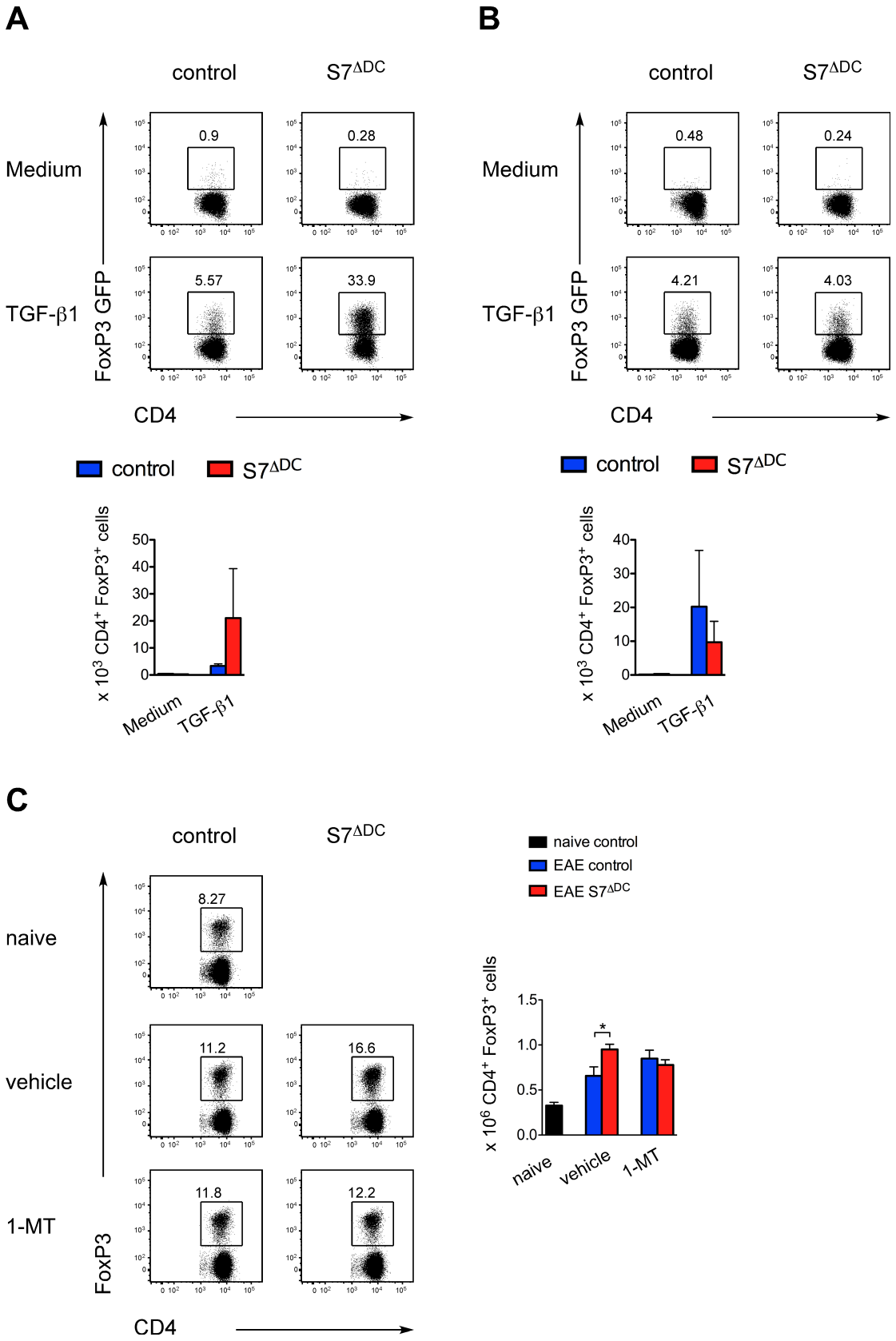

Figure 38: DCs devoid of Smad7 enhance IDO mediated iTreg differentiation

(A) FACS blots and absolute cell numbers of *in vitro* generated iTregs from $CD4^+$ $CD44^-$ $CD62L^+$ naïve FACS sorted T cells derived from 2D2 TCR transgenic FoxP3-GFP mice in response to TGF-β1 stimulated MACS purified splenic DCs of $S7^{\Delta DC}$ mice (n=4) or control mice (n=4) MOG_{35-55} pulsed with or **(B)** without additional stimulation with 1-MT. **(C)** Analysis of $CD4^+$ $FoxP3^+$ Treg numbers in LNs from naïve control mice (n=3) as well

as EAE immunized mice 10 days after immunization either treated with vehicle (control (n=8); $S7^{\Delta DC}$ (n=8)) or 1-MT (control (n=5); $S7^{\Delta DC}$ (n=6)) on the day of EAE immunization. Cells were gated on viable $CD90.2^{+}$ $CD4^{+}$cells. Bar graphs depict mean value ± SEM. Statistical significance was assessed two-way ANOVA and Bonferroni posttests (*$p \leq 0.05$, **$p \leq 0.005$, ***$p \leq 0.0005$).

IDO not only plays a role in the tryptophan catabolism but has also been reported to suppress effector T cells and induce Tregs. Hence, it was subsequently important to clarify if the reduced EAE susceptibility observed in $S7^{\Delta DC}$ mice results from increased Treg induction or from a reduction of T effector cells mediated by high levels of IDO. In order to address this, $S7^{\Delta DC}$ and control mice were treated with either αCD25 depleting antibody (PC61), or with an isotype control antibody (Mock) prior to MOG_{35-55}/CFA immunization and disease progression was monitored daily (Figure 39A and B). As expected, isotype-treated wild type mice exhibited although mild but full-blown disease progression, whereas isotype-treated $S7^{\Delta DC}$ mice were resistant to EAE as previously described (Figure 39A). Of note, wild type mice developed a 2 score stronger EAE when treated with PC61 as compared to isotype treatment (Figure 39B). Furthermore, PC61 treated wild type mice failed to resolve EAE, while isotype treated mice recovered from EAE. Interestingly, Treg depletion restored EAE susceptibility of $S7^{\Delta DC}$ mice. Disease progression of PC61 treated $S7^{\Delta DC}$ mice was characterized by comparable mean clinical scores to PC61 treated wild type mice. Likewise, EAE lack of remission observed in PC61 treated $S7^{\Delta DC}$ mice, was similar to that found in PC61 treated control mice (Figure 39B).

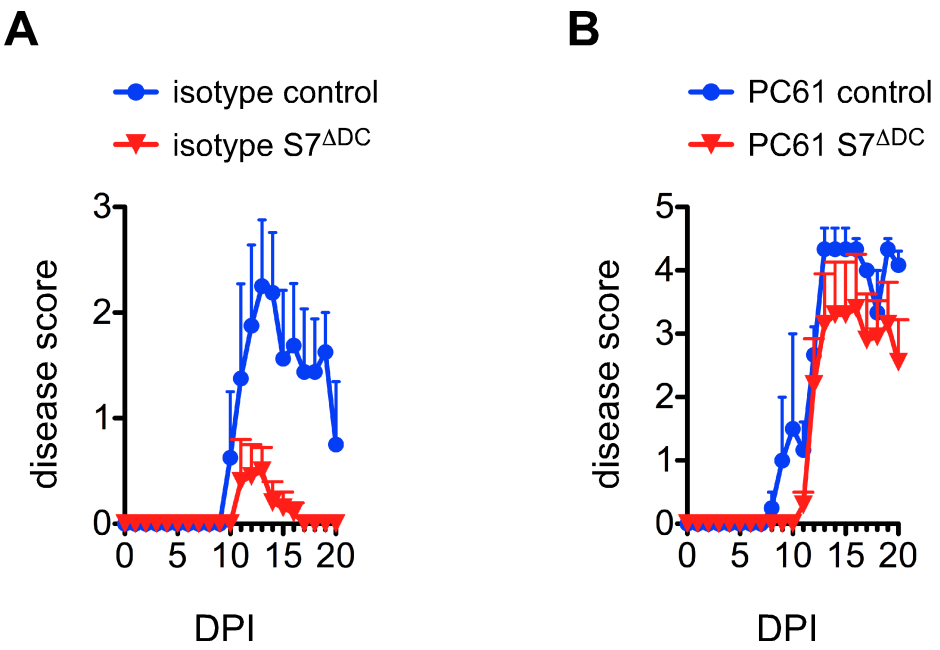

Figure 39: Treg depletion restores EAE susceptibility in S7$^{\Delta DC}$ mice

(A) EAE disease scores of either isotype or **(B)** PC61 treated S7$^{\Delta DC}$ mice (n=5/4 respectively; left panel) and control animals (n=5/4 respectively; right panel). Shown is one representative of two independent experiments. Bar graphs depict mean value ± SEM. Statistical significance was assessed using EAE area under curve (AUC) followed by two- way ANOVA and Bonferroni posttests (*p ≤0.05, **p ≤ 0.005, ***p ≤ 0.0005).

In addition to the disease evaluation based on the clinical scores, immunohistochemical analysis of spinal cords derived from isotype or PC61 treated S7$^{\Delta DC}$ mice and control animals on day 23 post EAE induction was performed. S7$^{\Delta DC}$ mice treated with the isotype control showed significantly reduced demyelination as compared to isotype treated controls (Figure 40A upper panels; B first bar graph). PC61 treatment significantly increased demyelination in wild type mice as compared to isotype treated wild type control mice and significantly restored the degree of demyelination in S7$^{\Delta DC}$ mice to comparable levels as observed in PC61 treated wild type control mice.

The infiltration of T cells to the CNS, as visualized by staining for CD3^{+} cells, was diminished in S7$^{\Delta DC}$ mice as compared to the respective controls, while upon PC61 treatment T cell infiltration was restored to comparable levels as detected in PC61 treated control mice (Figure 40A second panel; B second bar graph). Similarly, S7$^{\Delta DC}$ mice showed reduced infiltration of macrophages to the CNS, which significantly increased followed by PC61 treatment, resulting in comparable levels of macrophages in the CNS as detected in PC61 treated control mice (Figure 40A third panel; third bar graph). PC61 treatment likewise increased B cell infiltration to the CNS in S7$^{\Delta DC}$

mice as compared to the levels detected in vehicle treated $S7^{\Delta DC}$ mice, but had little effect on B cell infiltration observed in wild type mice as compared to vehicle treated wild type mice (Figure 40A fourth panel; B fourth bar graph). Amyloid precursor protein (APP) staining revealed reduced axonal damage in vehicle treated $S7^{\Delta DC}$ mice, which could be significantly increased upon PC61 treatment to comparable levels like wild type PC61 treated mice (Figure 40A last panel; B last bar graph).

Taken together, depletion of Tregs in $S7^{\Delta DC}$ mice resulted in increased infiltration of effector cells to the CNS leading to tissue damage and thus restored the susceptibility of these mice to EAE. These results implicate that induction of Tregs by Smad7-deficient DCs is a dominant mechanism involved in the reduced EAE disease susceptibility detected in $S7^{\Delta DC}$ mice.

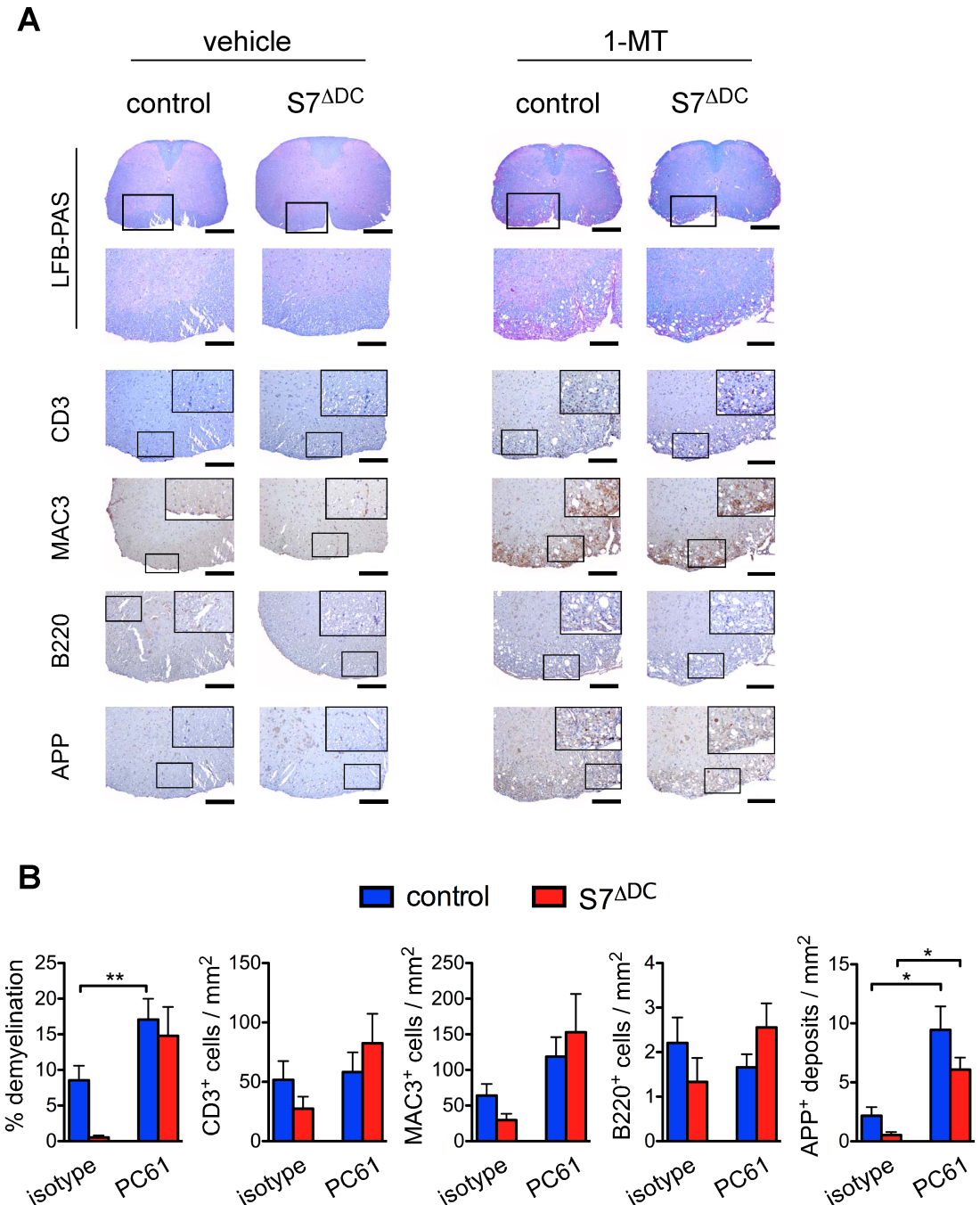

Figure 40: Deletion of Tregs in S7$^{\Delta DC}$ mice reverts EAE resistance

(A) Histological quantification of spinal cords 23 days post EAE induction from S7$^{\Delta DC}$ mice (n=4-5) or control mice (n=4-5) either treated with isotype or PC61. Spinal cord sections were stained with LFB-PAS (Luxol fast blue-periodic acid Schiff) to reveal the degree of demyelination, for CD3^{+} infiltrates, Mac3^{+} and B220^{+} infiltrates and amyloid precursor protein (APP)$^{+}$ deposits exposing axonal damage as indicated. Respective infiltrating cells/deposits were calculated per mm^{2}. Bar represents 50 µm. **(B)** Bar graphs depict quantification of results obtained in **(A)** and are shown as mean value ±SEM. Statistical significance was assessed by two-way ANOVA and Bonferroni posttests (*p ≤ 0.05, **p≤ 0.005, ***p ≤ 0.0005).

DC specific loss of Smad7 resulted in reduced EAE susceptibility presumably mediated by increased IDO levels leading to high amounts of protective Tregs. As IDO expression can be induced upon both TGF-β and IFN-γ signaling, it was next analyzed which of the two signaling cascades might be predominantly responsible for the increased IDO levels and resistance of $S7^{\Delta DC}$ mice during the course of EAE. Therefore, $S7^{\Delta DC}$ mice were crossed to IFN-γ$R2^{\Delta DC}$ mice, which lack the IFN-γR2 specifically on DCs. In these mice the TGF-β signaling on the DCs remains intact, whereas the IFN-γ signaling is completely abrogated. When subjected to EAE, these IFN-γ$R2^{\Delta DC}S7^{\Delta DC}$ mice (black triangle) developed significantly higher clinical disease progression than $S7^{\Delta DC}$ mice, which, as previously demonstrated, remained resistant to disease development (Figure 41). Deletion of both Smad7 and IFN-γR2 on DCs resulted in a significantly delayed disease onset and a slightly milder disease progression when compared to controls. Yet, the mean maximum scores of IFN-γ$R2^{\Delta DC}S7^{\Delta DC}$ mice and wild type controls were comparable (Table 8). Furthermore, IFN-γ$R2^{\Delta DC}S7^{+/-\Delta DC}$ mice are fully susceptible to EAE and display a similar disease progression like wild type controls (Figure 41). These data suggest that EAE resistance in $S7^{\Delta DC}$ mice is mediated by a pathway mostly independent of TGF-β signaling as this signaling is still intact in IFN-γ$R2^{\Delta DC}S7^{\Delta DC}$ mice.

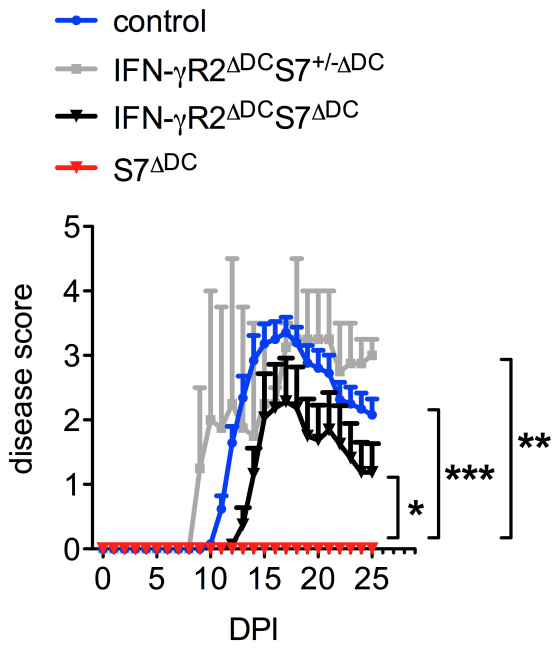

Figure 41 DC specific ablation of IFN-γR2 restores susceptibility of $S7^{\Delta DC}$ mice to EAE

Disease score of EAE subjected wild type control (n=19), $S7^{\Delta DC}$ (n=4), IFN-γ$R2^{\Delta DC}S7^{+/-\Delta DC}$ (n=2) and IFN-γ$R2^{\Delta DC}S7^{\Delta DC}$ (n=8) mice is shown. Graph depicts mean value ± SEM. Statistical significance was assessed using AUC followed by 1way ANOVA and Newman-Keuls Multiple Comparison Test (*p ≤0.05, **p ≤ 0.005, ***p ≤ 0.0005).

genotype	control	$S7^{\Delta DC}$	IFN-γ$R2^{\Delta DC}S7^{+/-\Delta DC}$	IFN-γ$R2^{\Delta DC}S7^{\Delta DC}$
amount of mice per group	n=19	n=4	n=2	n=8
day of onset	11.79 ± 1.44	nd.	12.00 ± 4.24	13.83 ± 1.33
maximal clinical score	3.75 ± 0.99	nd.	4.5 ± 0	2.69 ± 1.99
incidence	100%	0%	100%	75%

Table 8: DC specific IFN-γR2 deletion in $S7^{\Delta DC}$ mice restores EAE susceptibility

4 Discussion

Smad7 is a prominent negative regulator of TGF-β signaling, which once expressed in response to TGF-β or e.g. IFN-γ stimulation, inhibits Smad2 and Smad3 binding to the TGF-βR and together with Smurf targets the TGF-βR complex for ubiquitination followed by proteasomal degradation (Hayashi et al., 1997; Nakao et al., 1997; Yan and Chen, 2011). Studies using genetically modified mice described a prominent role for TGF-β in anti-inflammatory responses, important for the maintenance of immune homeostasis and the establishment of tolerance (Dang et al., 1995; Kulkarni et al., 1993a; Letterio and Bottinger, 1998; Li et al., 2006a; Shull et al., 1992; Yaswen et al., 1996). However, little is known on the function of the TGF-β negative regulator Smad7 in DCs. As deletion of Smad7 is embryonic lethal due to cardiovascular defects (Chen et al., 2009; Li et al., 2006d; Snider et al., 2009), mice with a DC-specific deletion of Smad7 ($S7^{\Delta DC}$) were analysed and the role of Smad7 during DC homeostasis and function, in particular, its impact on the outcome of CNS autoimmunity was characterized.

Except for an increase in $CD8^+$ $CD103^+$ DCs in the spleen, no other obvious differences between $S7^{\Delta DC}$ and control animals under steady state conditions were observed. When stimulated with IFN-γ or TGF-β, Smad7 deficient DCs expressed elevated levels of the transcription factors IRF8 and Batf3, respectively. Following IFN-γ stimulation, loss of Smad7 led to higher IDO production by DCs, and consequently an increased percentage and absolute number of Tregs *in vivo*. In line, $S7^{\Delta DC}$ mice were resistant to the induction of EAE by MOG_{35-55}-immunization, which could be reverted by both treatment with the IDO inhibitor 1-MT or Treg depletion using the CD25 depleting antibody PC61. Intriguingly, DC specific deletion of the IFN-γR2 in $S7^{\Delta DC}$ mice restored EAE incident as well as enhanced disease severity.

4.1 The role of Smad7 in DC during steady state

4.1.1 Efficiency of Smad7 deletion in dendritic cells

When evaluating DCs-specific Smad7 expression, *ex vivo* DCs and *in vitro* BMDCs displayed high deletion variability. CD11c-Cre mediated recombination in MACS purified splenic DCs was highly efficient (80-90%), yet in BMDCs Smad7 deletion efficiency in response to TGF-β signaling reached 50%. These differences may result from the heterogeneous population consistent not only of cDCs but also monocytes and macrophages in GM-CSF stimulated bone marrow cultures. In addition, CD11c Cre-mediated recombination in GM-CSF derived BMDCs is less efficient than *in situ* and increases over time due to increasing CD11c-promoter activity, as shown by the cross of CD11c-Cre mice to a *R26*-EYFP^{+} reporter strain (Caton et al., 2007). Thus, *in vitro* BMDCs have less time to excise the loxP sites, resulting in minor deletion efficiency as compared to splenic DCs.

4.2 Impact of DC specific Smad7 deletion during DC homeostasis

4.2.1 Development and homeostasis of skin- resident DC subsets following DC-specific Smad7 deletion

TGF-β signaling is mandatory for Langerhans cell development as shown by the absence of Langerhans cells in TGF-β knockout mice and conditional TGFβ-R knockout mice (Borkowski et al., 1996; Geissmann et al., 1998; Strobl et al., 1997; Zahner et al., 2011). Therefore it was hypothesized that deletion of an TGF-β signaling inhibitor might lead to increased amounts of Langerhans cells. However, although Langerhans cell yields were low due to increased age of experimental mice used in both groups (Cumberbatch et al., 2002; Rittman et al., 1987; Schwartz et al., 1983; Sprecher et al., 1990), loss of Smad7 in CD11c^{+} cells did not affect Langerhans cell frequencies nor dermal DCs during steady state, suggesting that lack of Smad7 might be compensated by another inhibitory mechanism. Alternatively exacerbated TGF-β signaling might reach a threshold at which Langerhans cell development would be saturated. Moreover another study suggested that although TGF-β signaling

is mandatory for Langerhans cell development, the classical Smad dependent TGF-β signaling is not involved in Langerhans cell development, as Smad3 knockout mice developed comparable amounts of Langerhans cells like controls (Xu et al., 2012). Smad-independent TGF-β signaling can occur via phosphatidylinositol-3-kinase PI3K (Yi et al., 2005; Zhang, 2009). In fact, another study suggested, that Langerhans cell homeostasis is dependent on mTORC1 function, a direct target of PI3K (Kellersch and Brocker, 2013).

4.2.2 Thymic DC development and homeostasis following DC-specific Smad7 deletion

DC-specific Smad7 deletion did not affect pDCs, resident CD8α$^+$ DCs or migratory Sirpα$^+$ DCs in the thymus, nor did it affect the expression of co-stimulatory molecules on thymic DCs during steady state. In contrast, DC-specific TGF-βR deletion results in premature involution of the thymus with complete loss of the thymic cortex at advanced age (Ramalingam et al., 2012), yet the role of TGF-β on the thymic DC subsets development and homeostasis was not addressed in this study (Ramalingam et al., 2012). Furthermore, Ramalingam et al suggested that the phenotype observed in the thymus of mice with DC-specific TGF-βR deletion might result from increased infiltration of peripheral CD4$^+$ T cells to the thymus as a result of autoimmunity.
As S7$^{\Delta DC}$ mice had increased frequencies of splenic CD8$^+$ DCs it was thus hypothesized, that thymic CD8$^+$ DC frequencies might also be increased. However, the micoenvironment during development might be different in the thymus as compared to peripheral lymphoid organs. In addition, stimuli like TGF-β or IFN-γ that would activate Smad7 might not be present in the thymus in sufficient amounts. Alternatively it might be possible, that in contrast to splenic CD8$^+$ DCs the development and homeostasis of thymic CD8$^+$ DCs might be dependent on different factors. In line, splenic and thymic CD8$^+$ DCs, despite similar surface phenotype, were suggested to have a different capacity to express chemokines and cytokines, indicating that the microenvironment might be an important factor in shaping DC specification (Proietto et al., 2008). This might likewise be the case for DC lineage defining microenvironments.

4.2.3 Smad7 deletion does not affect the amount of overall DCs in peripheral lymphoid organs but augments splenic $CD8^+$ $CD103^+$ DCs frequencies and corresponding transcription factors

In the steady state, DC-specific Smad7 deletion resulted in a shift in splenic DC populations, favouring the differentiation of $CD8^+$ $CD103^+$ DCs. This bias was accompanied by increased expression of the corresponding lineage defining transcription factors IRF8 and Batf3 upon TGF-β or IFN-γ stimulation, respectively. The expression of ID2, another transcription factor implicated in $CD8^+$ DCs as well as Langerhans cell development and which was reported to be up-regulated by TGF-β (Felker et al., 2010; Hacker et al., 2003b), was not affected by DC-specific Smad7 deletion.

Previously, it was shown that the stimulation of murine DC progenitor cells with TGF-β1, led to increased development of conventional DCs at the expense of pDCs (Felker et al., 2010). However, the resulting conventional DC subsets and their function were not further analysed in this study. Development of $CD8^+$ and $CD103^+$ DCs is dependent on the transcription factors IRF8 and Batf3 (Hildner et al., 2008; Tailor et al., 2008). To date, the mediators that induce these transcription factors during DC differentiation remain poorly defined. As $S7^{\Delta DC}$ mice displayed increased frequencies of splenic $CD8^+$ $CD103^+$ DCs associated with elevated expression of IRF8 and Batf3, this work suggests that Smad7 can inhibit the expression of $CD8^+CD103^+$ lineage-defining transcription factors. However, the expression of Batf3 or IRF8 in un-stimulated splenic DCs derived from $S7^{\Delta DC}$ mice was not elevated and increased only upon stimulation. Moreover, it remains elusive whether IRF8 and Batf3 expression in $CD8^+$ $CD103^+$ DCs is constitutive high or transient.

The conclusion that Smad7 controls expression of transcription factors is supported by a previous publication in which blockade of the TGF-β1 pathway by ectopic expression of Smad7 abolished the up-regulation of IRF8, which indicates a direct role for Smad7 in IRF8 repression (Ju et al., 2007). Smad7 is able to bind DNA through its MH2 domain (Shi et al., 2008; Zhang et al., 2007) and associate with the histone deacetylases HDAC1 and SIRT1, thus regulating transcription by repressing promoter activity (Gronroos et al., 2002b; Kume et al., 2007a; Simonsson et al., 2005). However, whether Smad7 affects $CD8^+CD103^+$ DC differentiation by direct

repression of IRF8 and Batf3 promoter activity or regulates another unknown factor(s) controlling Batf3 and IRF8 expression remains elusive.

The increase of $CD8^+$ $CD103^+$ DCs was only detected in the spleen, suggesting that this microenvironment might be different during steady state from that found for example in the LN and might affect the composition of DC subsets.

Although pDC development is likewise dependent on IRF8, the percentages and absolute numbers of pDCs in $S7^{\Delta DC}$ mice remained unchanged. One possible explanation would be that although CD11c-Cre was reported to effectively target all DC subsets including pDCs (Caton et al., 2007), accessibility of the Smad7 target gene in pDCs might be reduced leading to inefficient Cre-mediated recombination in in these cells. In fact, in another study pDCs were actually not targeted by the same CD11c-Cre (Yogev et al., 2012). Alternatively, it is conceivable that other molecules besides Smad7 control IRF8 expression in pDCs.

Further experiments using common DC progenitor cells derived from $S7^{\Delta DC}$ mice and controls stimulated with Flt3L, which instructs conventional DC lineage development, in presence or absence of Smad7 inducing signals as TGF-β or IFN-γ might clarify under which specific conditions loss of Smad7 affects the $CD8^+$ $CD103^+$ DC development. Such experiments could reveal why during steady the loss of Smad7 affects DC lineage commitment solely in the spleen whereas during autoimmune inflammation the main effect is seen in the draining LN.

4.2.4 Macrophages, neutrophils and granulocytes remain unaffected by Smad7 deletion in $CD11c^+$ cells during steady state

CD11c-Cre-mediated loss of Smad7 did not affect macrophages, neutrophils or granulocytes homeostasis in $S7^{\Delta DC}$ mice during steady state. Several macrophages subsets are known to express CD11c, as injection of diphtheria toxin to CD11c-DTR/GFP mice completely depleted marginal zone and metallophilic macrophages from the spleen and their sinusoidal counterparts from the lymph nodes (Probst et al., 2005). In contrast, another study tested CD11c-Cre efficiency as based on EYFP reporter expression of CD11c-Cre *R26*-EYFP mice (Caton et al., 2007). Deletion efficiency was less than 1% in myeloid cells such as granulocytes and only partial recombination was observed in $CD11c^{low}$ monocytes (Caton et al., 2007).

Macrophages stimulated with TGF-β display elevated chemotaxis, reduced effector function and antigen presentation while anti-inflammatory cytokine secretion and M2 polarization increases (Akhurst and Hata, 2012). Neutrophils respond to TGF-β with reduction of effector function and increased anti-inflammatory cytokine secretion as well as N2 polarization (Akhurst and Hata, 2012).

4.2.5 Smad7 deficiency in DCs does not affect thymic T cell development

Thymocytes and in particular thymic nTreg generation in $S7^{\Delta DC}$ mice was not affected by DC-specific Smad7 deletion. These results are in line with unaltered composition of thymic DC substes and unaffected expression of co-stimulatory molecules upon DC-specific Smad7 ablation. In the thymus mTecs cooperate with $CD8^+$ DCs to shape T cell repertoire and to generate Tregs (Perry et al., 2014), yet Smad7 did not affect thymic- but rather splenic $CD8^+$ $CD103^+$ DCs. Analysis of mice with a DC-specific ablation of the TGF-βR had two-fold increased frequencies of CD4 single positive (SP) cells in the thymus, although the total numbers were not significantly different (Ramalingam et al., 2012). However, as these mice developed autoimmunity, the increase in $CD4^+$ SP cells might presumably be due to peripheral CD4 T cell recirculation into the thymus.

4.2.6 Peripheral T cells remain unaffected by DC specific Smad7 deletion during steady state

The peripheral T cell compartment is unaltered in $S7^{\Delta DC}$ mice. Likewise, the activation status of T cells in the peripheral lymphoid organs such as spleen and LN was not affected. In addition, during steady state Tregs in peripheral lymphoid organs were comparable to controls. These data were rather unexpected, as steady state $S7^{\Delta DC}$ mice had increased splenic $CD8^+$ $CD103^+$ DC frequencies, a subset that has been implicated in Treg induction and associated with a tolerogenic rather than inflammatory phenotype (Belladonna et al., 2008; Matteoli et al., 2010; Pallotta et al., 2011; Pettersson et al., 2004; Yamazaki et al., 2008). Yet, it is possible that without additional presumably pro-inflammatory stimulus, these DCs do not act tolerogenic. In addition, these subsets might be involved in the generation of iTregs rather than nTreg induction.

Mice with DC-specific TGF-βR deletion display increased amounts of activated $CD4^+$ T cells together with Treg phenotype. In addition Laouar et al. have reported that DC specific dominant negative TGF-βR does induce spontaneous autoimmunity (Laouar et al., 2008).

This data suggests, that an inflammatory stimulus is necessary to induce tolerogenic potential of $CD8^+$ $CD103^+$ DCs. Moreover, though TGF-β signalling during steady state is essential for immune homeostasis, exacerbated TGF-β signalling as a result of Smad7 deletion would maintain immune homeostasis but will not tip the balance towards an even more tolerogenic environment.

4.3 The impact of dendritic cell specific deletion on the outcome of murine experimental encephalomyelitis (EAE)

4.3.1 Mice deficient of Smad7 specifically in DCs are resistant to EAE

Steady state expression of MHC-II and co-stimulatory molecules was not affected by the deletion of Smad7. Hence, T cell homeostasis and activation were unchanged in $S7^{\Delta DC}$ mice, including similar numbers of Tregs despite the increased frequency of splenic $CD8^+CD103^+$ DCs. In contrast, when subjected to EAE $S7^{\Delta DC}$ mice displayed significantly milder disease progression, accompanied by elevated numbers of CNS infiltrating Tregs and reduced numbers of MOG reactive effector T cells as based on transient CD40L expression upon MOG restimulation of CNS infiltrating lymphocytes.

Since lack of Smad7 also did not affect DC maturation, i.e. antigen presentation or co-stimulation, these data strongly suggest that upon EAE induction absent Smad7 in DCs augmented the numbers of Tregs, which in turn suppress the differentiation of encephalitogenic effector T cells. In agreement, abrogated TGF-β receptor signalling in DCs resulted in severe EAE (Laouar et al., 2008) and in spontaneous multi-organ autoimmune disease with increasing age (Ramalingam et al., 2012), indicating that TGF-β signalling is critical for the suppressive function of the DCs. However, these studies did not detect differences in the development of DC sub-populations, nor in IDO expression. It was recently demonstrated, that absent TGF-β signalling in mature $CD4^+$ T cells does not lead to breakdown of peripheral tolerance (Sledzinska et al.,

2013), suggesting that TGF-β signalling in DCs and not in T cells may be mandatory for peripheral tolerance. On the other hand, mice with a T cell-specific deletion of Smad7 are resistant to EAE induction (Kleiter et al., 2010).

$S7^{\Delta DC}$ mice subjected to EAE, displayed significantly reduced ROS levels in their blood circulation. In the pathogenesis of multiple sclerosis, inflammation-associated oxidative burst in macrophages and activated microglia contributes to demyelination and free radical-mediated tissue injury (Fischer et al., 2012). TGF-β was reported to induce expression of the NAD(P)H oxidase homologs NOX2 and NOX4, which are involved in the generation of ROS (Bondi et al., 2010). DC-antigen processing is affected following NOX2 recruitment to the early phagosome (Rybicka et al., 2012; Savina et al., 2006). Yet, antigen presentation and T cell proliferation was not affected by DC-specific Smad7 deletion, suggesting that Smad7 does not impair antigen processing in the early phagosome of DCs. Reduced ROS levels observed in $S7^{\Delta DC}$ mice are presumably a consequence of reduced inflammation and contribution of DCs to the oxidative burst is minimal.

4.3.1.1 Smad7 deletion does not affect dendritic cell migration and antigen presentation during EAE

$S7^{\Delta DC}$ mice displayed normal DC antigen-uptake and migration to the draining LN when subjected to EAE. In addition, the expression of co-stimulatory molecules in response to inflammatory stimuli was not affected when Smad7 was deleted. In line with this data, mice lacking TGF-βR specifically in DCs displayed unaltered expression of co-stimulatory molecules *in vivo* (Ramalingam et al., 2012). This is contradictory to a previous study, which suggested that TGF-β1 was important for the induction of the chemokine receptor CCR7 expression, which mediates the emigration of DCs from peripheral tissues to the draining LNs towards its ligand ELC (Ju et al., 2007). Moreover, analysis of IRF-8 knockout mice revealed a reduction in CCR7 expression by DCs, leading to reduced migratory activity (Ju et al., 2007).

$S7^{\Delta DC}$ mice manifested comparable frequencies of DCs in the CNS. CNS infiltrating DCs and monocytes expresses CCR2, which during early effector phase binds to

MCP-1 (CCL2) and guides their migration from the blood stream across the vascular endothelium into the cerebrospinal fluid and brain (Mahad and Ransohoff, 2003). It was recently shown that during EAE, DC accumulation in the CNS is dependent on CCR2 and that these DCs are essential for re-stimulation of effector T cells and consequently promote disease progression (Clarkson et al., 2015; Mahad and Ransohoff, 2003). However, frequencies of DCs in the CNS of $S7^{\Delta DC}$ mice during EAE as well as their expression of PD-L1, a co-inhibitory molecule involved in the generation of iTregs, remained unaffected by DC-specific Smad7 deletion, thus DC infiltration to the CNS is independent of Smad7 expression in DCs. In addition, these data suggest that the tolerance observed in $S7^{\Delta DC}$ mice is induced in the periphery and does not include improper licensing of effector T cells in the CNS.

Splenic $CD8^+$ $CD103^+$ DC frequencies do not increase any further upon inflammation, yet in response to MOG_{35-55} immunization this DC subset increases in the LN. One possible explanation for this discrepancy could come from the different effects TGF-β and IFN-γ exert on DCs. While TGF-β is necessary for $CD8^+$ $CD103^+$ DC development and homeostasis, IFN-γ might be required for their suppressive function (via IDO production). As these mice are kept in regular SPF housing conditions and not in a germ-free facility, it is conceivable that already during steady state, certain organs (e.g. the spleen) would be exposed to low levels of chronic stimuli / inflammation. This in turn would lead to the accumulation/expansion of $CD8^+$ $CD103^+$ DCs in the spleen but not in other peripheral lymphoid organs (i.e. skin-draining LN), where such low-grade inflammation does not persist. Following MOG/CFA immunization however, inflammatory mediators in the draining LN such as IFN-γ might drive the accumulation and/or expansion of $CD8^+$ $CD103^+$ DCs.

DCs of $S7^{\Delta DC}$ mice exhibit similar potential in differentiating effector Th1 and Th17 cells, both *in vivo* and *in vitro*. Yet, loss of Smad7 increases Treg frequencies in these mice during EAE. It is therefore likely that although peripheral Th1 and Th17 levels were similar, increased Treg amounts mediated suppression of these cells and prevented them from entry into the CNS and/or exerting their pathogenic function.
The expression of pro- and anti-inflammatory cytokines IL-6, TNF-α, IL-10 and TGF-β by DCs devoid of Smad7 was not affected under all conditions tested. This is

in contrast to a previously published study, in which it was suggested that TGF-β signaling induces TGF-β production, forming an autocrine loop, which further drives an anti-inflammatory environment (Kim et al., 1989a; Kim et al., 1989b; Kim et al., 1989c). Importantly however, the latter study was performed using human and mouse fibroblast cell lines rather than the primary DCs examined in this thesis.

$S7^{\Delta DC}$ mice subjected to EAE developed comparable ear swelling response upon MOG_{35-55} re-challenge as wild type controls. This delayed type hypersensitivity (DTH) response is in contrast to the reduced CNS-infiltration during EAE. It is well characterized that T cell homing to the spinal cord and brain is regulated by different chemokine receptors such as CCR6, VLA-4 and LFA-1, respectively (Glatigny et al., 2011; Reboldi et al., 2009; Rothhammer et al., 2011b). Monocytes and DCs recruitment to the skin and the CNS is likewise regulated by different chemokine receptors (i.e. CCR2 and CX3CR1) (Nedoszytko et al., 2014; Prinz and Priller, 2010). Thus, it is possible that the different outcome of T-cell homing to the CNS during EAE and to the ears following DTH, results from altered chemokine ligands expression by the different tissues, controlling DC migration and thereafter T cell activation.

4.3.1.2 Smad7 deletion increases IDO mediated Treg induction which provides protection from EAE

This work supports a critical role of Smad7 as an inhibitor of tolerogenic DC phenotype. In particular, $CD8^{+}CD103^{+}$ DCs have been previously linked with tolerance induction in part due to increased IDO expression mediating enhanced Treg differentiation upon challenge (Belladonna et al., 2008; Matteoli et al., 2010; Pallotta et al., 2011; Pettersson et al., 2004; Yamazaki et al., 2008). In agreement with the requirement of a pro-inflammatory stimulus, all conventional DC subsets devoid of Smad7 exhibited elevated IDO expression following IFN-γ stimulation *in vitro* and during EAE. Indeed, IDO plays a prominent role in multiple sclerosis and during EAE increased IDO protein levels can be detected in wild type mice in peripheral lymphoid organs as well as in the CNS (Kwidzinski et al., 2005; Kwidzinski et al., 2003; Orsini et al., 2014; Sakurai et al., 2002). Using $IDO^{-/-}$ mice, it was shown that IDO augments

Tregs via tryptophan metabolites and suppresses encephalitogenic T cell responses in EAE (Yan et al., 2010). IDO expression is induced upon both TGF-β as well as IFN-γ signalling (Belladonna et al., 2008; Pallotta et al., 2011) and likewise IFNγR$^{-/-}$ mice lack IDO activity (O'Connor et al., 2009). Hence, during EAE IDO might be produced in response to IFNγ and contribute to terminate inflammation in a negative feedback loop (Kwidzinski et al., 2005; Kwidzinski et al., 2003; Orsini et al., 2014; Sakurai et al., 2002). However, most studies addressing the tolerogenic function of IDO used models of global overexpression or inhibition of IDO. This work provides for the first time direct evidence that upon inflammation DC-specific IDO expression supports Treg mediated tolerance, and that Smad7 controls this tolerogenic DC phenotype in response to IFN-γ.

While DC-specific Smad7 deletion resulted in complete EAE resistance, DC-specific ablation of both IFN-γR2 together with Smad7 resulted in normal disease development, with slightly delayed onset and milder disease clinical scores, as compared to wild type controls. In contrast, DC-specific IFN-γR2 deletion on its own did not affect EAE progression, as DC-specific IFN-γR2 knockout mice developed similar clinical EAE signs as wild type controls.
These data suggest that the EAE resistance observed in the S7$^{\Delta DC}$ mice is critically dependent on IFN-γ signaling, and that the contribution of TGF-β signaling to EAE resistance in the S7$^{\Delta DC}$ mice is rather minor. Albeit IFN-γ was originally described as a pro-inflammatory cytokine, as its expression was associated to pathogenic Th1 cells, it became evident that IFN-γ actually ameliorates EAE disease progression (Chu et al., 2000; Pettersson et al., 2004; Tran et al., 2000; Weishaupt et al., 2000; Willenborg et al., 1999). Moreover, the tolerogenic function of IFN-γ is not limited to EAE, but similarly applies to other autoimmune diseases such as autoimmune myocarditis (Eriksson et al., 2001) and collagen-induced arthritis (Vermeire et al., 2000). During inflammation Smad7 expression in response to IFN-γ would not only inhibit TGF-β signaling, but would also suppress the expression of the transcription factor IRF8 important for IDO induction. Abrogated IDO expression would consequently result in reduced iTreg induction and increased susceptibility to EAE. In DC-specific IFN-γR2 knockout mice, Smad7 expression could still be induced in response to TGF-β

signaling and thus Smad7 could inhibit IDO and consequently Treg induction, resulting in a full-blown EAE.
Further experiments will determine whether the disease susceptibility of double deficient (IFN-γR2$^{\Delta DC}$S7$^{\Delta DC}$) mice can be attributed to diminished IDO levels and in consequence to lower amounts of Tregs than present in S7$^{\Delta DC}$ animals. In addition, analysis of DC subsets in double deficient mice will unravel whether the increased CD8^{+} CD103^{+} DC development observed in S7$^{\Delta DC}$ mice is dependent on IFN-γ or TGF-β.

Given that Smad7 in DCs represents a key molecular switch that regulates IDO expression during on-going inflammation, DC-specific Smad7 inhibition may provide a promising therapeutic approach for the treatment of chronic inflammatory diseases. Indeed, Smad7 antisense oligonucleotide therapy in mice suppressed both EAE (Kleiter et al., 2007) and experimental colitis (Monteleone et al., 2001), and is currently tested in a phase I clinical trial with promising prospects in Crohn's disease patients (Monteleone et al., 2012). In addition, simvastatin efficiently abrogates Smad7, resulting in a higher frequency of FoxP3^{+} Tregs in mice (Kim et al., 2010). Notably, both Smad7 antisense oligonucleotide and simvastatin do not target cell type-specific. Based on the results obtained during this work, a Smad7 inhibitor that targets specifically DCs would offer an attractive approach to treat autoimmune patients, while minimizing possible deleterious side effects.

In conclusion, this thesis identified a crucial, yet previously unappreciated role for Smad7 in DC differentiation and function. Smad7 regulates the expression of the transcription factors Batf3 and IRF8 that promote the development of CD8^{+} CD103^{+} DCs. During inflammation, Smad7 governs the tolerogenic function of conventional DCs by regulating IDO mediated Treg induction in response to IFN-γ. Hence, DC-specific Smad7 deletion alleviates EAE, which may be exploited for improved immunotherapy of autoimmune disease.

5 Summary

Smad7 negatively controls the anti-inflammatory cytokine transforming growth factor-β (TGF-β) signalling. Previous work suggested a role for Smad7 in the generation of auto-reactive T cells. However, the role of Smad7 in dendritic cells (DCs) remains elusive and was addressed in this thesis by using a conditional DC-specific Smad7 knockout mouse model ($S7^{\Delta DC}$ mice). In response to both TGF-β or IFN-γ, Smad7-deficiency in DCs resulted in elevated expression of the transcription factors Batf3 and IRF8, which are important for $CD8^+$ $CD103^+$ DC development. During steady state loss of Smad7 increased $CD8^+$ $CD103^+$ DC frequencies in the spleen, yet did not affect T cell development and function. Moreover, Smad7-deficient DCs expressed higher levels of indoleamine 2,3-dioxygenase (IDO), an enzyme involved in tryptophan catabolism and associated with tolerance induction. Mice devoid of Smad7 specifically in DCs developed attenuated experimental autoimmune encephalomyelitis (EAE), a mouse model of multiple sclerosis. Analysis of central nervous system (CNS) infiltrating lymphocytes at the peak of disease revealed a significant increase of protective regulatory T cells (Tregs) and reduction of encephalitogenic effector T cells. Inhibition of IDO activity using 1-Methyl-D-Tryptophan (1-MT) restored susceptibility to EAE. Similarly, antibody-mediated depletion of Tregs (PC61) aggravated disease progression in $S7^{\Delta DC}$ mice. Intriguingly, mice harbouring a DC-specific loss of IFN-γR2 and Smad7 were susceptible to EAE, suggesting that reduced susceptibility of $S7^{\Delta DC}$ mice is predominantly mediated by an IFN-γ dependant mechanism.

In conclusion, the data presented in this thesis indicates a previously unappreciated effect of Smad7 on DC subset differentiation. Absence of Smad7 promotes a tolerogenic DC phenotype *in vivo*, which can be further exploited for therapeutic intervention during autoimmune disorders.

6 Zusammenfassung

Smad7 inhibiert den Signalweg des anti-inflammatorischen Zytokins transforming growth factor-β (TGF-β). Bisherige Studien haben eine Rolle von Smad7 in der Entstehung von selbst-reaktiven T Zellen nahegelegt. Die Rolle, die Smad7 in Dendritischen Zellen (DC) spielt, bleibt jedoch unklar und wurde in dieser Dissertation anhand eines konditionellen DC-spezifischen Smad7 Knockout- Maus Modells ($S7^{\Delta DC}$ Maus) untersucht. In Reaktion auf TGF-β oder IFN-γ führte die DC-spezifische Smad7 Defizienz zur erhöhten Expression der für die Entwicklung von $CD8^+$ $CD103^+$ DCs wichtigen Transkriptionsfaktoren Batf3 und IRF8. Im stationären Zustand erhöhte der Verlust von Smad7 das Vorkommen von $CD8^+$ $CD103^+$ DCs in der Milz welches jedoch keinen Effekt auf die T Zell Entwicklung und Funktion hatte. Des Weiteren exprimierten Smad7 defiziente DCs mehr indoleamine 2,3-dioxygenase (IDO), ein Enzym welches im Tryptohan Stoffwechsel beteiligt und mit der Induktion von Toleranz verknüpft ist. Mäuse mit einer DC spezifischen Smad7 Deletion entwickelten verminderte autoimmune experimentelle Enzephalomyelitis (EAE) welches als ein Mausmodell für Multiple Sklerose dient. Die Analyse der am Höhepunkt der Krankheit in das Zentrale Nervensystem (ZNS) einwandernden Lymphozyten zeigte eine signifkante Zunahme regulatorischer T Zellen und eine Abnahme enzephalitogener Effektor- T Zellen auf. Die Inhibition der IDO Aktivität mittels 1-Methyl-D-Tryptophan (1-MT) stellte die Empfänglichkeit für die Krankheit EAE wieder her. Ebenso führte die Antikörper-vermittelte (PC61) Entfernung von regulatorischen T Zellen zu einem schweren Krankheitsverlauf in $S7^{\Delta DC}$ Mäusen. Interessanterweise waren Mäuse die einen DC-spezifischen Verlust des IFN-γR2 als auch von Smad7 hatten, empfänglich für die Krankheit EAE, was darauf hinweist, dass die verminderte Krankheitsanfälligkeit von $S7^{\Delta DC}$ Mäusen vorwiegend über einen dem IFN-γ Signalweg abhängigen Mechanismus vermittelt wird.

Zusammenfassend weisen die in dieser Doktorarbeit beschriebenen Daten, auf einen bisher unbeachteten Einfluss von Smad7 auf die Differenzierung von DC Subpopulationen hin. Die Abwesenheit von Smad7 *in vivo* fördert einen tolerogenen DC Phänotyp, welcher weiterhin für therapeutische Zwecke in der Behandung von Autoimmunerkrankungen ausgenutzt werden kann.

7 References

Akhurst, R.J., and A. Hata. 2012. Targeting the TGFbeta signalling pathway in disease. *Nature reviews. Drug discovery* 11:790-811.

Allan, R.S., C.M. Smith, G.T. Belz, A.L. van Lint, L.M. Wakim, W.R. Heath, and F.R. Carbone. 2003. Epidermal viral immunity induced by CD8alpha+ dendritic cells but not by Langerhans cells. *Science* 301:1925-1928.

Allenspach, E.J., M.P. Lemos, P.M. Porrett, L.A. Turka, and T.M. Laufer. 2008. Migratory and lymphoid-resident dendritic cells cooperate to efficiently prime naive CD4 T cells. *Immunity* 29:795-806.

Bedoui, S., P.G. Whitney, J. Waithman, L. Eidsmo, L. Wakim, I. Caminschi, R.S. Allan, M. Wojtasiak, K. Shortman, F.R. Carbone, A.G. Brooks, and W.R. Heath. 2009. Cross-presentation of viral and self antigens by skin-derived CD103+ dendritic cells. *Nature immunology* 10:488-495.

Belladonna, M.L., C. Volpi, R. Bianchi, C. Vacca, C. Orabona, M.T. Pallotta, L. Boon, S. Gizzi, M.C. Fioretti, U. Grohmann, and P. Puccetti. 2008. Cutting edge: Autocrine TGF-beta sustains default tolerogenesis by IDO-competent dendritic cells. *Journal of immunology* 181:5194-5198.

Belz, G.T., W.R. Heath, and F.R. Carbone. 2002. The role of dendritic cell subsets in selection between tolerance and immunity. *Immunology and cell biology* 80:463-468.

Belz, G.T., and S.L. Nutt. 2012. Transcriptional programming of the dendritic cell network. *Nature reviews. Immunology* 12:101-113.

Belz, G.T., C.M. Smith, D. Eichner, K. Shortman, G. Karupiah, F.R. Carbone, and W.R. Heath. 2004a. Cutting edge: conventional CD8 alpha+ dendritic cells are generally involved in priming CTL immunity to viruses. *Journal of immunology* 172:1996-2000.

Belz, G.T., C.M. Smith, L. Kleinert, P. Reading, A. Brooks, K. Shortman, F.R. Carbone, and W.R. Heath. 2004b. Distinct migrating and nonmigrating dendritic cell populations are involved in MHC class I-restricted antigen presentation after lung infection with virus. *Proceedings of the National Academy of Sciences of the United States of America* 101:8670-8675.

Bennett, S.R., F.R. Carbone, F. Karamalis, R.A. Flavell, J.F. Miller, and W.R. Heath. 1998. Help for cytotoxic-T-cell responses is mediated by CD40 signalling. *Nature* 393:478-480.

Bettelli, E., Y. Carrier, W. Gao, T. Korn, T.B. Strom, M. Oukka, H.L. Weiner, and V.K. Kuchroo. 2006. Reciprocal developmental pathways for the generation of pathogenic effector TH17 and regulatory T cells. *Nature* 441:235-238.

Bettelli, E., M. Pagany, H.L. Weiner, C. Linington, R.A. Sobel, and V.K. Kuchroo. 2003. Myelin oligodendrocyte glycoprotein-specific T cell receptor transgenic mice develop spontaneous autoimmune optic neuritis. *The Journal of experimental medicine* 197:1073-1081.

Beyer, M., H. Wang, N. Peters, S. Doths, C. Koerner-Rettberg, P.J. Openshaw, and J. Schwarze. 2005. The beta2 integrin CD11c distinguishes a subset of cytotoxic pulmonary T cells with potent antiviral effects in vitro and in vivo. *Respir Res* 6:70.

Biddison, W.E., P.E. Rao, M.A. Talle, G. Goldstein, and S. Shaw. 1982. Possible involvement of the OKT4 molecule in T cell recognition of class II HLA antigens. Evidence from studies of cytotoxic T lymphocytes specific for SB antigens. *The Journal of experimental medicine* 156:1065-1076.

Billiau, A., and P. Matthys. 2001. Modes of action of Freund's adjuvants in experimental models of autoimmune diseases. *Journal of leukocyte biology* 70:849-860.

Bitzer, M., G. von Gersdorff, D. Liang, A. Dominguez-Rosales, A.A. Beg, M. Rojkind, and E.P. Bottinger. 2000. A mechanism of suppression of TGF-beta/SMAD signaling by NF-kappa B/RelA. *Genes & development* 14:187-197.

Bonasio, R., M.L. Scimone, P. Schaerli, N. Grabie, A.H. Lichtman, and U.H. von Andrian. 2006. Clonal deletion of thymocytes by circulating dendritic cells homing to the thymus. *Nature immunology* 7:1092-1100.

Bondi, C.D., N. Manickam, D.Y. Lee, K. Block, Y. Gorin, H.E. Abboud, and J.L. Barnes. 2010. NAD(P)H oxidase mediates TGF-beta1-induced activation of kidney myofibroblasts. *Journal of the American Society of Nephrology : JASN* 21:93-102.

Borkowski, T.A., J.J. Letterio, A.G. Farr, and M.C. Udey. 1996. A role for endogenous transforming growth factor beta 1 in Langerhans cell biology: the skin of transforming growth factor beta 1 null mice is devoid of epidermal Langerhans cells. *The Journal of experimental medicine* 184:2417-2422.

Brocker, T., M. Riedinger, and K. Karjalainen. 1997. Targeted expression of major histocompatibility complex (MHC) class II molecules demonstrates that dendritic cells can induce negative but not positive selection of thymocytes in vivo. *The Journal of experimental medicine* 185:541-550.

Brodin, G., A. Ahgren, P. ten Dijke, C.H. Heldin, and R. Heuchel. 2000. Efficient TGF-beta induction of the Smad7 gene requires cooperation between AP-1, Sp1, and Smad proteins on the mouse Smad7 promoter. *J Biol Chem* 275:29023-29030.

Cady, S.G., and M. Sono. 1991. 1-Methyl-DL-tryptophan, beta-(3-benzofuranyl)-DL-alanine (the oxygen analog of tryptophan), and beta-[3-benzo(b)thienyl]-DL-alanine (the sulfur analog of tryptophan) are competitive inhibitors for indoleamine 2,3-dioxygenase. *Archives of biochemistry and biophysics* 291:326-333.

Caton, M.L., M.R. Smith-Raska, and B. Reizis. 2007. Notch-RBP-J signaling controls the homeostasis of CD8- dendritic cells in the spleen. *The Journal of experimental medicine* 204:1653-1664.

Chen, C.H., C. Seguin-Devaux, N.A. Burke, T.B. Oriss, S.C. Watkins, N. Clipstone, and A. Ray. 2003. Transforming growth factor beta blocks Tec kinase phosphorylation, Ca2+ influx, and NFATc translocation causing inhibition of T cell differentiation. *J Exp Med* 197:1689-1699.

Chen, Q., H. Chen, D. Zheng, C. Kuang, H. Fang, B. Zou, W. Zhu, G. Bu, T. Jin, Z. Wang, X. Zhang, J. Chen, L.J. Field, M. Rubart, W. Shou, and Y. Chen. 2009. Smad7 is required for the development and function of the heart. *The Journal of biological chemistry* 284:292-300.

Cheong, C., I. Matos, J.H. Choi, D.B. Dandamudi, E. Shrestha, M.P. Longhi, K.L. Jeffrey, R.M. Anthony, C. Kluger, G. Nchinda, H. Koh, A. Rodriguez, J. Idoyaga, M. Pack, K. Velinzon, C.G. Park, and R.M. Steinman. 2010.

Microbial stimulation fully differentiates monocytes to DC-SIGN/CD209(+) dendritic cells for immune T cell areas. *Cell* 143:416-429.

Chorro, L., A. Sarde, M. Li, K.J. Woollard, P. Chambon, B. Malissen, A. Kissenpfennig, J.B. Barbaroux, R. Groves, and F. Geissmann. 2009. Langerhans cell (LC) proliferation mediates neonatal development, homeostasis, and inflammation-associated expansion of the epidermal LC network. *The Journal of experimental medicine* 206:3089-3100.

Chu, C.Q., S. Wittmer, and D.K. Dalton. 2000. Failure to suppress the expansion of the activated CD4 T cell population in interferon gamma-deficient mice leads to exacerbation of experimental autoimmune encephalomyelitis. *The Journal of experimental medicine* 192:123-128.

Chung, A.C., X.R. Huang, L. Zhou, R. Heuchel, K.N. Lai, and H.Y. Lan. 2009. Disruption of the Smad7 gene promotes renal fibrosis and inflammation in unilateral ureteral obstruction (UUO) in mice. *Nephrol Dial Transplant* 24:1443-1454.

Clarkson, B.D., A. Walker, M.G. Harris, A. Rayasam, M. Sandor, and Z. Fabry. 2015. CCR2-dependent dendritic cell accumulation in the central nervous system during early effector experimental autoimmune encephalomyelitis is essential for effector T cell restimulation in situ and disease progression. *Journal of immunology* 194:531-541.

Corbi, A.L., and C. Lopez-Rodriguez. 1997. CD11c integrin gene promoter activity during myeloid differentiation. *Leukemia & lymphoma* 25:415-425.

Cua, D.J., J. Sherlock, Y. Chen, C.A. Murphy, B. Joyce, B. Seymour, L. Lucian, W. To, S. Kwan, T. Churakova, S. Zurawski, M. Wiekowski, S.A. Lira, D. Gorman, R.A. Kastelein, and J.D. Sedgwick. 2003. Interleukin-23 rather than interleukin-12 is the critical cytokine for autoimmune inflammation of the brain. *Nature* 421:744-748.

Cumberbatch, M., R.J. Dearman, and I. Kimber. 2002. Influence of ageing on Langerhans cell migration in mice: identification of a putative deficiency of epidermal interleukin-1beta. *Immunology* 105:466-477.

Curotto de Lafaille, M.A., and J.J. Lafaille. 2009. Natural and adaptive foxp3+ regulatory T cells: more of the same or a division of labor? *Immunity* 30:626-635.

Daiber, A., M. August, S. Baldus, M. Wendt, M. Oelze, K. Sydow, A.L. Kleschyov, and T. Munzel. 2004. Measurement of NAD(P)H oxidase-derived superoxide with the luminol analogue L-012. *Free radical biology & medicine* 36:101-111.

Dang, H., A.G. Geiser, J.J. Letterio, T. Nakabayashi, L. Kong, G. Fernandes, and N. Talal. 1995. SLE-like autoantibodies and Sjogren's syndrome-like lymphoproliferation in TGF-beta knockout mice. *Journal of immunology* 155:3205-3212.

den Haan, J.M., and M.J. Bevan. 2002. Constitutive versus activation-dependent cross-presentation of immune complexes by CD8(+) and CD8(-) dendritic cells in vivo. *The Journal of experimental medicine* 196:817-827.

Denissova, N.G., C. Pouponnot, J. Long, D. He, and F. Liu. 2000. Transforming growth factor beta -inducible independent binding of SMAD to the Smad7 promoter. *Proc Natl Acad Sci U S A* 97:6397-6402.

Derynck, R., and Y.E. Zhang. 2003. Smad-dependent and Smad-independent pathways in TGF-beta family signalling. *Nature* 425:577-584.

Dittel, B.N., I. Visintin, R.M. Merchant, and C.A. Janeway, Jr. 1999. Presentation of the self antigen myelin basic protein by dendritic cells leads to experimental autoimmune encephalomyelitis. *Journal of immunology* 163:32-39.

Dominitzki, S., M.C. Fantini, C. Neufert, A. Nikolaev, P.R. Galle, J. Scheller, G. Monteleone, S. Rose-John, M.F. Neurath, and C. Becker. 2007. Cutting edge: trans-signaling via the soluble IL-6R abrogates the induction of FoxP3 in naive CD4+CD25 T cells. *J Immunol* 179:2041-2045.

Dong, C. 2008. TH17 cells in development: an updated view of their molecular identity and genetic programming. *Nature reviews. Immunology* 8:337-348.

Dooley, S., J. Hamzavi, K. Breitkopf, E. Wiercinska, H.M. Said, J. Lorenzen, P. Ten Dijke, and A.M. Gressner. 2003. Smad7 prevents activation of hepatic stellate cells and liver fibrosis in rats. *Gastroenterology* 125:178-191.

Dubois, C.M., M.H. Laprise, F. Blanchette, L.E. Gentry, and R. Leduc. 1995. Processing of transforming growth factor beta 1 precursor by human furin convertase. *J Biol Chem* 270:10618-10624.

Ebisawa, T., M. Fukuchi, G. Murakami, T. Chiba, K. Tanaka, T. Imamura, and K. Miyazono. 2001. Smurf1 interacts with transforming growth factor-beta type I receptor through Smad7 and induces receptor degradation. *J Biol Chem* 276:12477-12480.

Edelson, B.T., W. Kc, R. Juang, M. Kohyama, L.A. Benoit, P.A. Klekotka, C. Moon, J.C. Albring, W. Ise, D.G. Michael, D. Bhattacharya, T.S. Stappenbeck, M.J. Holtzman, S.S. Sung, T.L. Murphy, K. Hildner, and K.M. Murphy. 2010. Peripheral CD103+ dendritic cells form a unified subset developmentally related to CD8alpha+ conventional dendritic cells. *The Journal of experimental medicine* 207:823-836.

Eriksson, U., M.O. Kurrer, R. Bingisser, H.P. Eugster, P. Saremaslani, F. Follath, S. Marsch, and U. Widmer. 2001. Lethal autoimmune myocarditis in interferon-gamma receptor-deficient mice: enhanced disease severity by impaired inducible nitric oxide synthase induction. *Circulation* 103:18-21.

Fantini, M.C., C. Becker, G. Monteleone, F. Pallone, P.R. Galle, and M.F. Neurath. 2004. Cutting edge: TGF-beta induces a regulatory phenotype in CD4+CD25- T cells through Foxp3 induction and down-regulation of Smad7. *Journal of immunology* 172:5149-5153.

Felker, P., K. Sere, Q. Lin, C. Becker, M. Hristov, T. Hieronymus, and M. Zenke. 2010. TGF-beta1 accelerates dendritic cell differentiation from common dendritic cell progenitors and directs subset specification toward conventional dendritic cells. *Journal of immunology* 185:5326-5335.

Ferber, I.A., S. Brocke, C. Taylor-Edwards, W. Ridgway, C. Dinisco, L. Steinman, D. Dalton, and C.G. Fathman. 1996. Mice with a disrupted IFN-gamma gene are susceptible to the induction of experimental autoimmune encephalomyelitis (EAE). *Journal of immunology* 156:5-7.

Fischer, M.T., R. Sharma, J.L. Lim, L. Haider, J.M. Frischer, J. Drexhage, D. Mahad, M. Bradl, J. van Horssen, and H. Lassmann. 2012. NADPH oxidase expression in active multiple sclerosis lesions in relation to oxidative tissue damage and mitochondrial injury. *Brain : a journal of neurology* 135:886-899.

Freeman, M. 2000. Feedback control of intercellular signalling in development. *Nature* 408:313-319.

Fu, S., N. Zhang, A.C. Yopp, D. Chen, M. Mao, H. Zhang, Y. Ding, and J.S. Bromberg. 2004. TGF-beta induces Foxp3 + T-regulatory cells from CD4 + CD25 - precursors. *American journal of transplantation : official journal of*

the American Society of Transplantation and the American Society of Transplant Surgeons 4:1614-1627.

Gallegos, A.M., and M.J. Bevan. 2004. Central tolerance to tissue-specific antigens mediated by direct and indirect antigen presentation. *The Journal of experimental medicine* 200:1039-1049.

Gao, E.K., D. Lo, and J. Sprent. 1990. Strong T cell tolerance in parent----F1 bone marrow chimeras prepared with supralethal irradiation. Evidence for clonal deletion and anergy. *The Journal of experimental medicine* 171:1101-1121.

Garbi, N., and T. Kreutzberg. 2012. Dendritic cells enhance the antigen sensitivity of T cells. *Frontiers in immunology* 3:389.

Gartner, D., H. Hoff, U. Gimsa, G.R. Burmester, and M.C. Brunner-Weinzierl. 2006. CD25 regulatory T cells determine secondary but not primary remission in EAE: impact on long-term disease progression. *Journal of neuroimmunology* 172:73-84.

Geissmann, F., M.G. Manz, S. Jung, M.H. Sieweke, M. Merad, and K. Ley. 2010. Development of monocytes, macrophages, and dendritic cells. *Science* 327:656-661.

Geissmann, F., C. Prost, J.P. Monnet, M. Dy, N. Brousse, and O. Hermine. 1998. Transforming growth factor beta1, in the presence of granulocyte/macrophage colony-stimulating factor and interleukin 4, induces differentiation of human peripheral blood monocytes into dendritic Langerhans cells. *The Journal of experimental medicine* 187:961-966.

Geissmann, F., P. Revy, A. Regnault, Y. Lepelletier, M. Dy, N. Brousse, S. Amigorena, O. Hermine, and A. Durandy. 1999. TGF-beta 1 prevents the noncognate maturation of human dendritic Langerhans cells. *Journal of immunology* 162:4567-4575.

Germain, R.N. 1994. MHC-dependent antigen processing and peptide presentation: providing ligands for T lymphocyte activation. *Cell* 76:287-299.

GeurtsvanKessel, C.H., M.A. Willart, L.S. van Rijt, F. Muskens, M. Kool, C. Baas, K. Thielemans, C. Bennett, B.E. Clausen, H.C. Hoogsteden, A.D. Osterhaus, G.F. Rimmelzwaan, and B.N. Lambrecht. 2008. Clearance of influenza virus from the lung depends on migratory langerin+CD11b- but not plasmacytoid dendritic cells. *The Journal of experimental medicine* 205:1621-1634.

Ginhoux, F., and S. Jung. 2014. Monocytes and macrophages: developmental pathways and tissue homeostasis. *Nat Rev Immunol* 14:392-404.

Glatigny, S., R. Duhen, M. Oukka, and E. Bettelli. 2011. Cutting edge: loss of alpha4 integrin expression differentially affects the homing of Th1 and Th17 cells. *Journal of immunology* 187:6176-6179.

Gleizes, P.E., J.S. Munger, I. Nunes, J.G. Harpel, R. Mazzieri, I. Noguera, and D.B. Rifkin. 1997. TGF-beta latency: biological significance and mechanisms of activation. *Stem Cells* 15:190-197.

Godfrey, D.I., J. Kennedy, T. Suda, and A. Zlotnik. 1993. A developmental pathway involving four phenotypically and functionally distinct subsets of CD3-CD4-CD8- triple-negative adult mouse thymocytes defined by CD44 and CD25 expression. *Journal of immunology* 150:4244-4252.

Gohla, G., K. Krieglstein, and B. Spittau. 2008. Tieg3/Klf11 induces apoptosis in OLI-neu cells and enhances the TGF-beta signaling pathway by transcriptional repression of Smad7. *J Cell Biochem* 104:850-861.

Gold, R., C. Linington, and H. Lassmann. 2006. Understanding pathogenesis and therapy of multiple sclerosis via animal models: 70 years of merits and

culprits in experimental autoimmune encephalomyelitis research. *Brain : a journal of neurology* 129:1953-1971.

Gorelik, L., S. Constant, and R.A. Flavell. 2002. Mechanism of transforming growth factor beta-induced inhibition of T helper type 1 differentiation. *The Journal of experimental medicine* 195:1499-1505.

Greter, M., F.L. Heppner, M.P. Lemos, B.M. Odermatt, N. Goebels, T. Laufer, R.J. Noelle, and B. Becher. 2005. Dendritic cells permit immune invasion of the CNS in an animal model of multiple sclerosis. *Nature medicine* 11:328-334.

Gronroos, E., U. Hellman, C.H. Heldin, and J. Ericsson. 2002a. Control of Smad7 stability by competition between acetylation and ubiquitination. *Mol Cell* 10:483-493.

Gronroos, E., U. Hellman, C.H. Heldin, and J. Ericsson. 2002b. Control of Smad7 stability by competition between acetylation and ubiquitination. *Mol Cell* 10:483-493.

Guermonprez, P., J. Valladeau, L. Zitvogel, C. Thery, and S. Amigorena. 2002. Antigen presentation and T cell stimulation by dendritic cells. *Annual review of immunology* 20:621-667.

Haak, S., A.L. Croxford, K. Kreymborg, F.L. Heppner, S. Pouly, B. Becher, and A. Waisman. 2009. IL-17A and IL-17F do not contribute vitally to autoimmune neuro-inflammation in mice. *The Journal of clinical investigation* 119:61-69.

Hacker, C., R.D. Kirsch, X.S. Ju, T. Hieronymus, T.C. Gust, C. Kuhl, T. Jorgas, S.M. Kurz, S. Rose-John, Y. Yokota, and M. Zenke. 2003a. Transcriptional profiling identifies Id2 function in dendritic cell development. *Nat Immunol* 4:380-386.

Hacker, C., R.D. Kirsch, X.S. Ju, T. Hieronymus, T.C. Gust, C. Kuhl, T. Jorgas, S.M. Kurz, S. Rose-John, Y. Yokota, and M. Zenke. 2003b. Transcriptional profiling identifies Id2 function in dendritic cell development. *Nature immunology* 4:380-386.

Hayashi, H., S. Abdollah, Y. Qiu, J. Cai, Y.Y. Xu, B.W. Grinnell, M.A. Richardson, J.N. Topper, M.A. Gimbrone, Jr., J.L. Wrana, and D. Falb. 1997. The MAD-related protein Smad7 associates with the TGFbeta receptor and functions as an antagonist of TGFbeta signaling. *Cell* 89:1165-1173.

He, J., X. Sun, K.Q. Qian, X. Liu, Z. Wang, and Y. Chen. 2009. Protection of cerulein-induced pancreatic fibrosis by pancreas-specific expression of Smad7. *Biochim Biophys Acta* 1792:56-60.

Hildner, K., B.T. Edelson, W.E. Purtha, M. Diamond, H. Matsushita, M. Kohyama, B. Calderon, B.U. Schraml, E.R. Unanue, M.S. Diamond, R.D. Schreiber, T.L. Murphy, and K.M. Murphy. 2008. Batf3 deficiency reveals a critical role for CD8alpha+ dendritic cells in cytotoxic T cell immunity. *Science* 322:1097-1100.

Hirota, K., J.H. Duarte, M. Veldhoen, E. Hornsby, Y. Li, D.J. Cua, H. Ahlfors, C. Wilhelm, M. Tolaini, U. Menzel, A. Garefalaki, A.J. Potocnik, and B. Stockinger. 2011. Fate mapping of IL-17-producing T cells in inflammatory responses. *Nat Immunol* 12:255-263.

Hohl, T.M., H.L. Van Epps, A. Rivera, L.A. Morgan, P.L. Chen, M. Feldmesser, and E.G. Pamer. 2005. Aspergillus fumigatus triggers inflammatory responses by stage-specific beta-glucan display. *PLoS pathogens* 1:e30.

Hori, S., M. Haury, A. Coutinho, and J. Demengeot. 2002. Specificity requirements for selection and effector functions of CD25+4+ regulatory T cells in anti-

myelin basic protein T cell receptor transgenic mice. *Proceedings of the National Academy of Sciences of the United States of America* 99:8213-8218.

Hou, D.Y., A.J. Muller, M.D. Sharma, J. DuHadaway, T. Banerjee, M. Johnson, A.L. Mellor, G.C. Prendergast, and D.H. Munn. 2007. Inhibition of indoleamine 2,3-dioxygenase in dendritic cells by stereoisomers of 1-methyl-tryptophan correlates with antitumor responses. *Cancer research* 67:792-801.

Hua, X., Z.A. Miller, H. Benchabane, J.L. Wrana, and H.F. Lodish. 2000. Synergism between transcription factors TFE3 and Smad3 in transforming growth factor-beta-induced transcription of the Smad7 gene. *J Biol Chem* 275:33205-33208.

Huber, S., C. Schramm, H.A. Lehr, A. Mann, S. Schmitt, C. Becker, M. Protschka, P.R. Galle, M.F. Neurath, and M. Blessing. 2004. Cutting edge: TGF-beta signaling is required for the in vivo expansion and immunosuppressive capacity of regulatory CD4+CD25+ T cells. *Journal of immunology* 173:6526-6531.

Huleatt, J.W., and L. Lefrancois. 1995. Antigen-driven induction of CD11c on intestinal intraepithelial lymphocytes and CD8+ T cells in vivo. *J Immunol* 154:5684-5693.

Janeway, C.A., Jr., and R. Medzhitov. 1998. Introduction: the role of innate immunity in the adaptive immune response. *Semin Immunol* 10:349-350.

Jang, C.W., C.H. Chen, C.C. Chen, J.Y. Chen, Y.H. Su, and R.H. Chen. 2002. TGF-beta induces apoptosis through Smad-mediated expression of DAP-kinase. *Nature cell biology* 4:51-58.

Ju, X.S., D. Ruau, P. Jantti, K. Sere, C. Becker, E. Wiercinska, C. Bartz, B. Erdmann, S. Dooley, and M. Zenke. 2007. Transforming growth factor beta1 up-regulates interferon regulatory factor 8 during dendritic cell development. *European journal of immunology* 37:1174-1183.

Jungert, K., A. Buck, M. Buchholz, M. Wagner, G. Adler, T.M. Gress, and V. Ellenrieder. 2006. Smad-Sp1 complexes mediate TGFbeta-induced early transcription of oncogenic Smad7 in pancreatic cancer cells. *Carcinogenesis* 27:2392-2401.

Kaiko, G.E., J.C. Horvat, K.W. Beagley, and P.M. Hansbro. 2008. Immunological decision-making: how does the immune system decide to mount a helper T-cell response? *Immunology* 123:326-338.

Kaisho, T., and S. Akira. 2001. Dendritic-cell function in Toll-like receptor- and MyD88-knockout mice. *Trends in immunology* 22:78-83.

Kamiya, Y., K. Miyazono, and K. Miyazawa. 2010. Smad7 inhibits transforming growth factor-beta family type i receptors through two distinct modes of interaction. *J Biol Chem* 285:30804-30813.

Kavsak, P., R.K. Rasmussen, C.G. Causing, S. Bonni, H. Zhu, G.H. Thomsen, and J.L. Wrana. 2000. Smad7 binds to Smurf2 to form an E3 ubiquitin ligase that targets the TGF beta receptor for degradation. *Mol Cell* 6:1365-1375.

Kehrl, J.H., A.B. Roberts, L.M. Wakefield, S. Jakowlew, M.B. Sporn, and A.S. Fauci. 1986a. Transforming growth factor beta is an important immunomodulatory protein for human B lymphocytes. *J Immunol* 137:3855-3860.

Kehrl, J.H., L.M. Wakefield, A.B. Roberts, S. Jakowlew, M. Alvarez-Mon, R. Derynck, M.B. Sporn, and A.S. Fauci. 1986b. Production of transforming growth factor beta by human T lymphocytes and its potential role in the regulation of T cell growth. *The Journal of experimental medicine* 163:1037-1050.

Kellersch, B., and T. Brocker. 2013. Langerhans cell homeostasis in mice is dependent on mTORC1 but not mTORC2 function. *Blood* 121:298-307.

Kidd, P. 2003. Th1/Th2 balance: the hypothesis, its limitations, and implications for health and disease. *Alternative medicine review : a journal of clinical therapeutic* 8:223-246.

Kim, S.J., F. Denhez, K.Y. Kim, J.T. Holt, M.B. Sporn, and A.B. Roberts. 1989a. Activation of the second promoter of the transforming growth factor-beta 1 gene by transforming growth factor-beta 1 and phorbol ester occurs through the same target sequences. *The Journal of biological chemistry* 264:19373-19378.

Kim, S.J., A. Glick, M.B. Sporn, and A.B. Roberts. 1989b. Characterization of the promoter region of the human transforming growth factor-beta 1 gene. *The Journal of biological chemistry* 264:402-408.

Kim, S.J., K.T. Jeang, A.B. Glick, M.B. Sporn, and A.B. Roberts. 1989c. Promoter sequences of the human transforming growth factor-beta 1 gene responsive to transforming growth factor-beta 1 autoinduction. *The Journal of biological chemistry* 264:7041-7045.

Kim, T.S., and T.J. Braciale. 2009. Respiratory dendritic cell subsets differ in their capacity to support the induction of virus-specific cytotoxic CD8+ T cell responses. *PloS one* 4:e4204.

Kim, Y.C., K.K. Kim, and E.M. Shevach. 2010. Simvastatin induces Foxp3+ T regulatory cells by modulation of transforming growth factor-beta signal transduction. *Immunology* 130:484-493.

Klein, L., B. Kyewski, P.M. Allen, and K.A. Hogquist. 2014. Positive and negative selection of the T cell repertoire: what thymocytes see (and don't see). *Nature reviews. Immunology* 14:377-391.

Kleiter, I., X. Pedre, A.M. Mueller, P. Poeschl, S. Couillard-Despres, T. Spruss, U. Bogdahn, G. Giegerich, and A. Steinbrecher. 2007. Inhibition of Smad7, a negative regulator of TGF-beta signaling, suppresses autoimmune encephalomyelitis. *Journal of neuroimmunology* 187:61-73.

Kleiter, I., J. Song, D. Lukas, M. Hasan, B. Neumann, A.L. Croxford, X. Pedre, N. Hovelmeyer, N. Yogev, A. Mildner, M. Prinz, E. Wiese, K. Reifenberg, S. Bittner, H. Wiendl, L. Steinman, C. Becker, U. Bogdahn, M.F. Neurath, A. Steinbrecher, and A. Waisman. 2010. Smad7 in T cells drives T helper 1 responses in multiple sclerosis and experimental autoimmune encephalomyelitis. *Brain : a journal of neurology* 133:1067-1081.

Kohm, A.P., P.A. Carpentier, H.A. Anger, and S.D. Miller. 2002. Cutting edge: CD4+CD25+ regulatory T cells suppress antigen-specific autoreactive immune responses and central nervous system inflammation during active experimental autoimmune encephalomyelitis. *Journal of immunology* 169:4712-4716.

Kool, M., T. Soullie, M. van Nimwegen, M.A. Willart, F. Muskens, S. Jung, H.C. Hoogsteden, H. Hammad, and B.N. Lambrecht. 2008. Alum adjuvant boosts adaptive immunity by inducing uric acid and activating inflammatory dendritic cells. *The Journal of experimental medicine* 205:869-882.

Korn, T., A.C. Anderson, E. Bettelli, and M. Oukka. 2007a. The dynamics of effector T cells and Foxp3+ regulatory T cells in the promotion and regulation of autoimmune encephalomyelitis. *Journal of neuroimmunology* 191:51-60.

Korn, T., J. Reddy, W. Gao, E. Bettelli, A. Awasthi, T.R. Petersen, B.T. Backstrom, R.A. Sobel, K.W. Wucherpfennig, T.B. Strom, M. Oukka, and V.K. Kuchroo.

2007b. Myelin-specific regulatory T cells accumulate in the CNS but fail to control autoimmune inflammation. *Nature medicine* 13:423-431.

Koutrolos, M., K. Berer, N. Kawakami, H. Wekerle, and G. Krishnamoorthy. 2014. Treg cells mediate recovery from EAE by controlling effector T cell proliferation and motility in the CNS. *Acta neuropathologica communications* 2:163.

Kulkarni, A.B., C.G. Huh, D. Becker, A. Geiser, M. Lyght, K.C. Flanders, A.B. Roberts, M.B. Sporn, J.M. Ward, and S. Karlsson. 1993a. Transforming growth factor beta 1 null mutation in mice causes excessive inflammatory response and early death. *Proceedings of the National Academy of Sciences of the United States of America* 90:770-774.

Kulkarni, A.B., C.G. Huh, D. Becker, A. Geiser, M. Lyght, K.C. Flanders, A.B. Roberts, M.B. Sporn, J.M. Ward, and S. Karlsson. 1993b. Transforming growth factor beta 1 null mutation in mice causes excessive inflammatory response and early death. *Proc Natl Acad Sci U S A* 90:770-774.

Kume, S., M. Haneda, K. Kanasaki, T. Sugimoto, S. Araki, K. Isshiki, M. Isono, T. Uzu, L. Guarente, A. Kashiwagi, and D. Koya. 2007a. SIRT1 inhibits transforming growth factor beta-induced apoptosis in glomerular mesangial cells via Smad7 deacetylation. *The Journal of biological chemistry* 282:151-158.

Kume, S., M. Haneda, K. Kanasaki, T. Sugimoto, S. Araki, K. Isshiki, M. Isono, T. Uzu, L. Guarente, A. Kashiwagi, and D. Koya. 2007b. SIRT1 inhibits transforming growth factor beta-induced apoptosis in glomerular mesangial cells via Smad7 deacetylation. *J Biol Chem* 282:151-158.

Kurschus, F.C. 2015. T cell mediated pathogenesis in EAE: Molecular mechanisms. *Biomed J* 38:183-193.

Kurschus, F.C., A.L. Croxford, A.P. Heinen, S. Wortge, D. Ielo, and A. Waisman. 2010. Genetic proof for the transient nature of the Th17 phenotype. *European journal of immunology* 40:3336-3346.

Kushwah, R., and J. Hu. 2011. Role of dendritic cells in the induction of regulatory T cells. *Cell & bioscience* 1:20.

Kwidzinski, E., J. Bunse, O. Aktas, D. Richter, L. Mutlu, F. Zipp, R. Nitsch, and I. Bechmann. 2005. Indolamine 2,3-dioxygenase is expressed in the CNS and down-regulates autoimmune inflammation. *FASEB journal : official publication of the Federation of American Societies for Experimental Biology* 19:1347-1349.

Kwidzinski, E., J. Bunse, A.D. Kovac, O. Ullrich, F. Zipp, R. Nitsch, and I. Bechmann. 2003. IDO (indolamine 2,3-dioxygenase) expression and function in the CNS. *Advances in experimental medicine and biology* 527:113-118.

Lahoud, M.H., A.I. Proietto, K.H. Gartlan, S. Kitsoulis, J. Curtis, J. Wettenhall, M. Sofi, C. Daunt, M. O'Keeffe, I. Caminschi, K. Satterley, A. Rizzitelli, P. Schnorrer, A. Hinohara, Y. Yamaguchi, L. Wu, G. Smyth, E. Handman, K. Shortman, and M.D. Wright. 2006. Signal regulatory protein molecules are differentially expressed by CD8- dendritic cells. *Journal of immunology* 177:372-382.

Langrish, C.L., Y. Chen, W.M. Blumenschein, J. Mattson, B. Basham, J.D. Sedgwick, T. McClanahan, R.A. Kastelein, and D.J. Cua. 2005. IL-23 drives a pathogenic T cell population that induces autoimmune inflammation. *J Exp Med* 201:233-240.

Laouar, Y., T. Town, D. Jeng, E. Tran, Y. Wan, V.K. Kuchroo, and R.A. Flavell. 2008. TGF-beta signaling in dendritic cells is a prerequisite for the control of autoimmune encephalomyelitis. *Proceedings of the National Academy of Sciences of the United States of America* 105:10865-10870.

Lassmann, H. 1983. Comparative neuropathology of chronic experimental allergic encephalomyelitis and multiple sclerosis. *Schriftenreihe Neurologie* 25:1-135.

Lee, Y., A. Awasthi, N. Yosef, F.J. Quintana, S. Xiao, A. Peters, C. Wu, M. Kleinewietfeld, S. Kunder, D.A. Hafler, R.A. Sobel, A. Regev, and V.K. Kuchroo. 2012. Induction and molecular signature of pathogenic TH17 cells. *Nature immunology* 13:991-999.

Leon, B., M. Lopez-Bravo, and C. Ardavin. 2007. Monocyte-derived dendritic cells formed at the infection site control the induction of protective T helper 1 responses against Leishmania. *Immunity* 26:519-531.

Letterio, J.J., and E.P. Bottinger. 1998. TGF-beta knockout and dominant-negative receptor transgenic mice. *Mineral and electrolyte metabolism* 24:161-167.

Li, M.O., S. Sanjabi, and R.A. Flavell. 2006a. Transforming growth factor-beta controls development, homeostasis, and tolerance of T cells by regulatory T cell-dependent and -independent mechanisms. *Immunity* 25:455-471.

Li, M.O., Y.Y. Wan, S. Sanjabi, A.K. Robertson, and R.A. Flavell. 2006b. Transforming growth factor-beta regulation of immune responses. *Annu Rev Immunol* 24:99-146.

Li, M.O., Y.Y. Wan, S. Sanjabi, A.K. Robertson, and R.A. Flavell. 2006c. Transforming growth factor-beta regulation of immune responses. *Annual review of immunology* 24:99-146.

Li, R., A. Rosendahl, G. Brodin, A.M. Cheng, A. Ahgren, C. Sundquist, S. Kulkarni, T. Pawson, C.H. Heldin, and R.L. Heuchel. 2006d. Deletion of exon I of SMAD7 in mice results in altered B cell responses. *Journal of immunology* 176:6777-6784.

Li, R., A. Rosendahl, G. Brodin, A.M. Cheng, A. Ahgren, C. Sundquist, S. Kulkarni, T. Pawson, C.H. Heldin, and R.L. Heuchel. 2006e. Deletion of exon I of SMAD7 in mice results in altered B cell responses. *J Immunol* 176:6777-6784.

Lievens, D., K.L. Habets, A.K. Robertson, Y. Laouar, H. Winkels, T. Rademakers, L. Beckers, E. Wijnands, L. Boon, M. Mosaheb, H. Ait-Oufella, Z. Mallat, R.A. Flavell, M. Rudling, C.J. Binder, N. Gerdes, E.A. Biessen, C. Weber, M.J. Daemen, J. Kuiper, and E. Lutgens. 2012. Abrogated transforming growth factor beta receptor II (TGFbetaRII) signalling in dendritic cells promotes immune reactivity of T cells resulting in enhanced atherosclerosis. *European heart journal*

Liu, K., and M.C. Nussenzweig. 2010. Origin and development of dendritic cells. *Immunological reviews* 234:45-54.

Lowther, D.E., D.L. Chong, S. Ascough, A. Ettorre, R.J. Ingram, R.J. Boyton, and D.M. Altmann. 2013. Th1 not Th17 cells drive spontaneous MS-like disease despite a functional regulatory T cell response. *Acta neuropathologica* 126:501-515.

Lukens, M.V., D. Kruijsen, F.E. Coenjaerts, J.L. Kimpen, and G.M. van Bleek. 2009. Respiratory syncytial virus-induced activation and migration of respiratory dendritic cells and subsequent antigen presentation in the lung-draining lymph node. *Journal of virology* 83:7235-7243.

Lundie, R.J., T.F. de Koning-Ward, G.M. Davey, C.Q. Nie, D.S. Hansen, L.S. Lau, J.D. Mintern, G.T. Belz, L. Schofield, F.R. Carbone, J.A. Villadangos, B.S.

Crabb, and W.R. Heath. 2008. Blood-stage Plasmodium infection induces CD8+ T lymphocytes to parasite-expressed antigens, largely regulated by CD8alpha+ dendritic cells. *Proceedings of the National Academy of Sciences of the United States of America* 105:14509-14514.

Lyons, A.B., and C.R. Parish. 1994. Determination of lymphocyte division by flow cytometry. *Journal of immunological methods* 171:131-137.

Mahad, D.J., and R.M. Ransohoff. 2003. The role of MCP-1 (CCL2) and CCR2 in multiple sclerosis and experimental autoimmune encephalomyelitis (EAE). *Seminars in immunology* 15:23-32.

Mangan, P.R., L.E. Harrington, D.B. O'Quinn, W.S. Helms, D.C. Bullard, C.O. Elson, R.D. Hatton, S.M. Wahl, T.R. Schoeb, and C.T. Weaver. 2006. Transforming growth factor-beta induces development of the T(H)17 lineage. *Nature* 441:231-234.

Martin-Gayo, E., E. Sierra-Filardi, A.L. Corbi, and M.L. Toribio. 2010. Plasmacytoid dendritic cells resident in human thymus drive natural Treg cell development. *Blood* 115:5366-5375.

Massague, J. 2008. TGF beta in cancer. *Cell* 134:215-230.

Massague, J. 2012. TGFbeta signalling in context. *Nat Rev Mol Cell Biol* 13:616-630.

Massague, J., and D. Wotton. 2000. Transcriptional control by the TGF-beta/Smad signaling system. *Embo J* 19:1745-1754.

Matteoli, G., E. Mazzini, I.D. Iliev, E. Mileti, F. Fallarino, P. Puccetti, M. Chieppa, and M. Rescigno. 2010. Gut CD103+ dendritic cells express indoleamine 2,3-dioxygenase which influences T regulatory/T effector cell balance and oral tolerance induction. *Gut* 59:595-604.

McDonnell, A.M., A.C. Prosser, I. van Bruggen, B.W. Robinson, and A.J. Currie. 2010. CD8alpha+ DC are not the sole subset cross-presenting cell-associated tumor antigens from a solid tumor. *European journal of immunology* 40:1617-1627.

McGeachy, M.J., and D.J. Cua. 2008. Th17 cell differentiation: the long and winding road. *Immunity* 28:445-453.

McGeachy, M.J., L.A. Stephens, and S.M. Anderton. 2005. Natural recovery and protection from autoimmune encephalomyelitis: contribution of CD4+CD25+ regulatory cells within the central nervous system. *Journal of immunology* 175:3025-3032.

McMahon, E.J., S.L. Bailey, C.V. Castenada, H. Waldner, and S.D. Miller. 2005. Epitope spreading initiates in the CNS in two mouse models of multiple sclerosis. *Nature medicine* 11:335-339.

Medzhitov, R., and C.A. Janeway, Jr. 1997. Innate immunity: the virtues of a nonclonal system of recognition. *Cell* 91:295-298.

Medzhitov, R., and C.A. Janeway, Jr. 1998. Innate immune recognition and control of adaptive immune responses. *Semin Immunol* 10:351-353.

Mellor, A.L., and D.H. Munn. 2004. IDO expression by dendritic cells: tolerance and tryptophan catabolism. *Nature reviews. Immunology* 4:762-774.

Melton, A.C., S.L. Bailey-Bucktrout, M.A. Travis, B.T. Fife, J.A. Bluestone, and D. Sheppard. 2010. Expression of alphavbeta8 integrin on dendritic cells regulates Th17 cell development and experimental autoimmune encephalomyelitis in mice. *J Clin Invest* 120:4436-4444.

Mendel, I., N. Kerlero de Rosbo, and A. Ben-Nun. 1995. A myelin oligodendrocyte glycoprotein peptide induces typical chronic experimental autoimmune encephalomyelitis in H-2b mice: fine specificity and T cell receptor V beta

expression of encephalitogenic T cells. *European journal of immunology* 25:1951-1959.

Merad, M., F. Ginhoux, and M. Collin. 2008. Origin, homeostasis and function of Langerhans cells and other langerin-expressing dendritic cells. *Nature reviews. Immunology* 8:935-947.

Merad, M., P. Sathe, J. Helft, J. Miller, and A. Mortha. 2013. The dendritic cell lineage: ontogeny and function of dendritic cells and their subsets in the steady state and the inflamed setting. *Annual review of immunology* 31:563-604.

Miltenyi, S., W. Muller, W. Weichel, and A. Radbruch. 1990. High gradient magnetic cell separation with MACS. *Cytometry* 11:231-238.

Mochizuki, T., H. Miyazaki, T. Hara, T. Furuya, T. Imamura, T. Watabe, and K. Miyazono. 2004. Roles for the MH2 domain of Smad7 in the specific inhibition of transforming growth factor-beta superfamily signaling. *J Biol Chem* 279:31568-31574.

Mogensen, T.H. 2009. Pathogen recognition and inflammatory signaling in innate immune defenses. *Clin Microbiol Rev* 22:240-273, Table of Contents.

Mokrani, M., J. Klibi, D. Bluteau, G. Bismuth, and F. Mami-Chouaib. 2014. Smad and NFAT pathways cooperate to induce CD103 expression in human CD8 T lymphocytes. *Journal of immunology* 192:2471-2479.

Monteleone, G., M. Boirivant, F. Pallone, and T.T. MacDonald. 2008. TGF-beta1 and Smad7 in the regulation of IBD. *Mucosal immunology* 1 Suppl 1:S50-53.

Monteleone, G., M.C. Fantini, S. Onali, F. Zorzi, G. Sancesario, S. Bernardini, E. Calabrese, F. Viti, I. Monteleone, L. Biancone, and F. Pallone. 2012. Phase I clinical trial of Smad7 knockdown using antisense oligonucleotide in patients with active Crohn's disease. *Molecular therapy : the journal of the American Society of Gene Therapy* 20:870-876.

Monteleone, G., A. Kumberova, N.M. Croft, C. McKenzie, H.W. Steer, and T.T. MacDonald. 2001. Blocking Smad7 restores TGF-beta1 signaling in chronic inflammatory bowel disease. *The Journal of clinical investigation* 108:601-609.

Montero, E., G. Nussbaum, J.F. Kaye, R. Perez, A. Lage, A. Ben-Nun, and I.R. Cohen. 2004. Regulation of experimental autoimmune encephalomyelitis by CD4+, CD25+ and CD8+ T cells: analysis using depleting antibodies. *Journal of autoimmunity* 23:1-7.

Mount, A.M., C.M. Smith, F. Kupresanin, K. Stoermer, W.R. Heath, and G.T. Belz. 2008. Multiple dendritic cell populations activate CD4+ T cells after viral stimulation. *PloS one* 3:e1691.

Mu, Y., S.K. Gudey, and M. Landstrom. 2012. Non-Smad signaling pathways. *Cell Tissue Res* 347:11-20.

Mullis, K., F. Faloona, S. Scharf, R. Saiki, G. Horn, and H. Erlich. 1986. Specific enzymatic amplification of DNA in vitro: the polymerase chain reaction. *Cold Spring Harbor symposia on quantitative biology* 51 Pt 1:263-273.

Mullis, K.B. 1990. The unusual origin of the polymerase chain reaction. *Scientific American* 262:56-61, 64-55.

Munger, J.S., J.G. Harpel, P.E. Gleizes, R. Mazzieri, I. Nunes, and D.B. Rifkin. 1997. Latent transforming growth factor-beta: structural features and mechanisms of activation. *Kidney Int* 51:1376-1382.

Munn, D.H. 2006. Indoleamine 2,3-dioxygenase, tumor-induced tolerance and counter-regulation. *Current opinion in immunology* 18:220-225.

Murphy, K.M., and S.L. Reiner. 2002. The lineage decisions of helper T cells. *Nature reviews. Immunology* 2:933-944.

Nagao, K., F. Ginhoux, W.W. Leitner, S. Motegi, C.L. Bennett, B.E. Clausen, M. Merad, and M.C. Udey. 2009. Murine epidermal Langerhans cells and langerin-expressing dermal dendritic cells are unrelated and exhibit distinct functions. *Proc Natl Acad Sci U S A* 106:3312-3317.

Naik, S.H., D. Metcalf, A. van Nieuwenhuijze, I. Wicks, L. Wu, M. O'Keeffe, and K. Shortman. 2006. Intrasplenic steady-state dendritic cell precursors that are distinct from monocytes. *Nature immunology* 7:663-671.

Nakao, A., M. Afrakhte, A. Moren, T. Nakayama, J.L. Christian, R. Heuchel, S. Itoh, M. Kawabata, N.E. Heldin, C.H. Heldin, and P. ten Dijke. 1997. Identification of Smad7, a TGFbeta-inducible antagonist of TGF-beta signalling. *Nature* 389:631-635.

Nakao, A., M. Fujii, R. Matsumura, K. Kumano, Y. Saito, K. Miyazono, and I. Iwamoto. 1999. Transient gene transfer and expression of Smad7 prevents bleomycin-induced lung fibrosis in mice. *J Clin Invest* 104:5-11.

Nedoszytko, B., M. Sokolowska-Wojdylo, K. Ruckemann-Dziurdzinska, J. Roszkiewicz, and R.J. Nowicki. 2014. Chemokines and cytokines network in the pathogenesis of the inflammatory skin diseases: atopic dermatitis, psoriasis and skin mastocytosis. *Postepy dermatologii i alergologii* 31:84-91.

O'Connor, J.C., C. Andre, Y. Wang, M.A. Lawson, S.S. Szegedi, J. Lestage, N. Castanon, K.W. Kelley, and R. Dantzer. 2009. Interferon-gamma and tumor necrosis factor-alpha mediate the upregulation of indoleamine 2,3-dioxygenase and the induction of depressive-like behavior in mice in response to bacillus Calmette-Guerin. *The Journal of neuroscience : the official journal of the Society for Neuroscience* 29:4200-4209.

O'Connor, R.A., K.H. Malpass, and S.M. Anderton. 2007. The inflamed central nervous system drives the activation and rapid proliferation of Foxp3+ regulatory T cells. *Journal of immunology* 179:958-966.

Oelze, M., A. Daiber, R.P. Brandes, M. Hortmann, P. Wenzel, U. Hink, E. Schulz, H. Mollnau, A. von Sandersleben, A.L. Kleschyov, A. Mulsch, H. Li, U. Forstermann, and T. Munzel. 2006. Nebivolol inhibits superoxide formation by NADPH oxidase and endothelial dysfunction in angiotensin II-treated rats. *Hypertension* 48:677-684.

Olivares-Villagomez, D., Y. Wang, and J.J. Lafaille. 1998. Regulatory CD4(+) T cells expressing endogenous T cell receptor chains protect myelin basic protein-specific transgenic mice from spontaneous autoimmune encephalomyelitis. *The Journal of experimental medicine* 188:1883-1894.

Orsini, H., L.P. Araujo, J.T. Maricato, M.G. Guereschi, M. Mariano, B.A. Castilho, and A.S. Basso. 2014. GCN2 kinase plays an important role triggering the remission phase of experimental autoimmune encephalomyelitis (EAE) in mice. *Brain, behavior, and immunity* 37:177-186.

Pallotta, M.T., C. Orabona, C. Volpi, C. Vacca, M.L. Belladonna, R. Bianchi, G. Servillo, C. Brunacci, M. Calvitti, S. Bicciato, E.M. Mazza, L. Boon, F. Grassi, M.C. Fioretti, F. Fallarino, P. Puccetti, and U. Grohmann. 2011. Indoleamine 2,3-dioxygenase is a signaling protein in long-term tolerance by dendritic cells. *Nature immunology* 12:870-878.

Perry, J.S., C.W. Lio, A.L. Kau, K. Nutsch, Z. Yang, J.I. Gordon, K.M. Murphy, and C.S. Hsieh. 2014. Distinct contributions of Aire and antigen-presenting-cell

subsets to the generation of self-tolerance in the thymus. *Immunity* 41:414-426.

Perussia, B., V. Fanning, and G. Trinchieri. 1985. A leukocyte subset bearing HLA-DR antigens is responsible for in vitro alpha interferon production in response to viruses. *Natural immunity and cell growth regulation* 4:120-137.

Pettersson, A., X.C. Wu, C. Ciumas, H. Lian, V. Chirsky, Y.M. Huang, B. Bjelke, H. Link, and B.G. Xiao. 2004. CD8alpha dendritic cells and immune protection from experimental allergic encephalomyelitis. *Clinical and experimental immunology* 137:486-495.

Pooley, J.L., W.R. Heath, and K. Shortman. 2001. Cutting edge: intravenous soluble antigen is presented to CD4 T cells by CD8- dendritic cells, but cross-presented to CD8 T cells by CD8+ dendritic cells. *Journal of immunology* 166:5327-5330.

Prinz, M., and J. Priller. 2010. Tickets to the brain: role of CCR2 and CX3CR1 in myeloid cell entry in the CNS. *Journal of neuroimmunology* 224:80-84.

Prinz, M., H. Schmidt, A. Mildner, K.P. Knobeloch, U.K. Hanisch, J. Raasch, D. Merkler, C. Detje, I. Gutcher, J. Mages, R. Lang, R. Martin, R. Gold, B. Becher, W. Bruck, and U. Kalinke. 2008. Distinct and nonredundant in vivo functions of IFNAR on myeloid cells limit autoimmunity in the central nervous system. *Immunity* 28:675-686.

Probst, H.C., K. Tschannen, B. Odermatt, R. Schwendener, R.M. Zinkernagel, and M. Van Den Broek. 2005. Histological analysis of CD11c-DTR/GFP mice after in vivo depletion of dendritic cells. *Clinical and experimental immunology* 141:398-404.

Proietto, A.I., M.H. Lahoud, and L. Wu. 2008. Distinct functional capacities of mouse thymic and splenic dendritic cell populations. *Immunology and cell biology* 86:700-708.

Ramalingam, R., C.B. Larmonier, R.D. Thurston, M.T. Midura-Kiela, S.G. Zheng, F.K. Ghishan, and P.R. Kiela. 2012. Dendritic Cell-Specific Disruption of TGF-beta Receptor II Leads to Altered Regulatory T Cell Phenotype and Spontaneous Multiorgan Autoimmunity. *Journal of immunology* 189:3878-3893.

Reboldi, A., C. Coisne, D. Baumjohann, F. Benvenuto, D. Bottinelli, S. Lira, A. Uccelli, A. Lanzavecchia, B. Engelhardt, and F. Sallusto. 2009. C-C chemokine receptor 6-regulated entry of TH-17 cells into the CNS through the choroid plexus is required for the initiation of EAE. *Nature immunology* 10:514-523.

Reizis, B., A. Bunin, H.S. Ghosh, K.L. Lewis, and V. Sisirak. 2011a. Plasmacytoid dendritic cells: recent progress and open questions. *Annual review of immunology* 29:163-183.

Reizis, B., M. Colonna, G. Trinchieri, F. Barrat, and M. Gilliet. 2011b. Plasmacytoid dendritic cells: one-trick ponies or workhorses of the immune system? *Nature reviews. Immunology* 11:558-565.

Rittman, B.R., M.W. Hill, G.A. Rittman, and I.C. Mackenzie. 1987. Age-associated changes in Langerhans cells of murine oral epithelium and epidermis. *Archives of oral biology* 32:885-889.

Robey, E., and B.J. Fowlkes. 1994. Selective events in T cell development. *Annual review of immunology* 12:675-705.

Rodewald, H.R. 2008. Thymus organogenesis. *Annual review of immunology* 26:355-388.

Rothhammer, V., S. Heink, F. Petermann, R. Srivastava, M.C. Claussen, B. Hemmer, and T. Korn. 2011a. Th17 lymphocytes traffic to the central nervous system independently of alpha4 integrin expression during EAE. *J Exp Med* 208:2465-2476.

Rothhammer, V., S. Heink, F. Petermann, R. Srivastava, M.C. Claussen, B. Hemmer, and T. Korn. 2011b. Th17 lymphocytes traffic to the central nervous system independently of alpha4 integrin expression during EAE. *The Journal of experimental medicine* 208:2465-2476.

Rubtsov, Y.P., and A.Y. Rudensky. 2007. TGFbeta signalling in control of T-cell-mediated self-reactivity. *Nature reviews. Immunology* 7:443-453.

Rybicka, J.M., D.R. Balce, S. Chaudhuri, E.R. Allan, and R.M. Yates. 2012. Phagosomal proteolysis in dendritic cells is modulated by NADPH oxidase in a pH-independent manner. *The EMBO journal* 31:932-944.

Saharinen, J., and J. Keski-Oja. 2000. Specific sequence motif of 8-Cys repeats of TGF-beta binding proteins, LTBPs, creates a hydrophobic interaction surface for binding of small latent TGF-beta. *Mol Biol Cell* 11:2691-2704.

Saiki, R.K., D.H. Gelfand, S. Stoffel, S.J. Scharf, R. Higuchi, G.T. Horn, K.B. Mullis, and H.A. Erlich. 1988. Primer-directed enzymatic amplification of DNA with a thermostable DNA polymerase. *Science* 239:487-491.

Sakurai, K., J.P. Zou, J.R. Tschetter, J.M. Ward, and G.M. Shearer. 2002. Effect of indoleamine 2,3-dioxygenase on induction of experimental autoimmune encephalomyelitis. *Journal of neuroimmunology* 129:186-196.

Savina, A., C. Jancic, S. Hugues, P. Guermonprez, P. Vargas, I.C. Moura, A.M. Lennon-Dumenil, M.C. Seabra, G. Raposo, and S. Amigorena. 2006. NOX2 controls phagosomal pH to regulate antigen processing during crosspresentation by dendritic cells. *Cell* 126:205-218.

Schmierer, B., and C.S. Hill. 2007a. TGFbeta-SMAD signal transduction: molecular specificity and functional flexibility. *Nat Rev Mol Cell Biol* 8:970-982.

Schmierer, B., and C.S. Hill. 2007b. TGFbeta-SMAD signal transduction: molecular specificity and functional flexibility. *Nature reviews. Molecular cell biology* 8:970-982.

Schoenberger, S.P., R.E. Toes, E.I. van der Voort, R. Offringa, and C.J. Melief. 1998. T-cell help for cytotoxic T lymphocytes is mediated by CD40-CD40L interactions. *Nature* 393:480-483.

Schwartz, J.L., R. Weichselbaum, and S.R. Frim. 1983. The effect of aging on the density and distribution of oral mucosal Langerhans cells. *Experimental gerontology* 18:65-71.

Serbina, N.V., T.P. Salazar-Mather, C.A. Biron, W.A. Kuziel, and E.G. Pamer. 2003. TNF/iNOS-producing dendritic cells mediate innate immune defense against bacterial infection. *Immunity* 19:59-70.

Shi, X., F. Chen, J. Yu, Y. Xu, S. Zhang, Y.G. Chen, and X. Fang. 2008. Study of interaction between Smad7 and DNA by single-molecule force spectroscopy. *Biochemical and biophysical research communications* 377:1284-1287.

Shi, Y., and J. Massague. 2003. Mechanisms of TGF-beta signaling from cell membrane to the nucleus. *Cell* 113:685-700.

Shull, M.M., I. Ormsby, A.B. Kier, S. Pawlowski, R.J. Diebold, M. Yin, R. Allen, C. Sidman, G. Proetzel, D. Calvin, and et al. 1992. Targeted disruption of the mouse transforming growth factor-beta 1 gene results in multifocal inflammatory disease. *Nature* 359:693-699.

Simonsson, M., C.H. Heldin, J. Ericsson, and E. Gronroos. 2005. The balance between acetylation and deacetylation controls Smad7 stability. *The Journal of biological chemistry* 280:21797-21803.

Sledzinska, A., S. Hemmers, F. Mair, O. Gorka, J. Ruland, L. Fairbairn, A. Nissler, W. Muller, A. Waisman, B. Becher, and T. Buch. 2013. TGF-beta signalling is required for CD4(+) T cell homeostasis but dispensable for regulatory T cell function. *PLoS biology* 11:e1001674.

Smith, C.M., G.T. Belz, N.S. Wilson, J.A. Villadangos, K. Shortman, F.R. Carbone, and W.R. Heath. 2003. Cutting edge: conventional CD8 alpha+ dendritic cells are preferentially involved in CTL priming after footpad infection with herpes simplex virus-1. *Journal of immunology* 170:4437-4440.

Snider, P., S. Tang, G. Lin, J. Wang, and S.J. Conway. 2009. Generation of Smad7(-Cre) recombinase mice: A useful tool for the study of epithelial-mesenchymal transformation within the embryonic heart. *Genesis* 47:469-475.

Sponaas, A.M., E.T. Cadman, C. Voisine, V. Harrison, A. Boonstra, A. O'Garra, and J. Langhorne. 2006. Malaria infection changes the ability of splenic dendritic cell populations to stimulate antigen-specific T cells. *The Journal of experimental medicine* 203:1427-1433.

Sprecher, E., Y. Becker, G. Kraal, E. Hall, D. Harrison, and L.D. Shultz. 1990. Effect of aging on epidermal dendritic cell populations in C57BL/6J mice. *The Journal of investigative dermatology* 94:247-253.

Steinman, L., and S.S. Zamvil. 2006. How to successfully apply animal studies in experimental allergic encephalomyelitis to research on multiple sclerosis. *Annals of neurology* 60:12-21.

Steinman, R.M., D. Hawiger, and M.C. Nussenzweig. 2003. Tolerogenic dendritic cells. *Annual review of immunology* 21:685-711.

Stephens, L.A., K.H. Malpass, and S.M. Anderton. 2009. Curing CNS autoimmune disease with myelin-reactive Foxp3+ Treg. *European journal of immunology* 39:1108-1117.

Stopa, M., D. Anhuf, L. Terstegen, P. Gatsios, A.M. Gressner, and S. Dooley. 2000. Participation of Smad2, Smad3, and Smad4 in transforming growth factor beta (TGF-beta)-induced activation of Smad7. THE TGF-beta response element of the promoter requires functional Smad binding element and E-box sequences for transcriptional regulation. *J Biol Chem* 275:29308-29317.

Strobl, H., C. Bello-Fernandez, E. Riedl, W.F. Pickl, O. Majdic, S.D. Lyman, and W. Knapp. 1997. flt3 ligand in cooperation with transforming growth factor-beta1 potentiates in vitro development of Langerhans-type dendritic cells and allows single-cell dendritic cell cluster formation under serum-free conditions. *Blood* 90:1425-1434.

Suter, T., G. Biollaz, D. Gatto, L. Bernasconi, T. Herren, W. Reith, and A. Fontana. 2003. The brain as an immune privileged site: dendritic cells of the central nervous system inhibit T cell activation. *European journal of immunology* 33:2998-3006.

Suzuki, C., G. Murakami, M. Fukuchi, T. Shimanuki, Y. Shikauchi, T. Imamura, and K. Miyazono. 2002. Smurf1 regulates the inhibitory activity of Smad7 by targeting Smad7 to the plasma membrane. *The Journal of biological chemistry* 277:39919-39925.

Tailor, P., T. Tamura, H.C. Morse, 3rd, and K. Ozato. 2008. The BXH2 mutation in IRF8 differentially impairs dendritic cell subset development in the mouse. *Blood* 111:1942-1945.

Thornton, A.M., P.E. Korty, D.Q. Tran, E.A. Wohlfert, P.E. Murray, Y. Belkaid, and E.M. Shevach. 2010. Expression of Helios, an Ikaros transcription factor family member, differentiates thymic-derived from peripherally induced Foxp3+ T regulatory cells. *Journal of immunology* 184:3433-3441.

Tran, E.H., E.N. Prince, and T. Owens. 2000. IFN-gamma shapes immune invasion of the central nervous system via regulation of chemokines. *Journal of immunology* 164:2759-2768.

Travis, M.A., B. Reizis, A.C. Melton, E. Masteller, Q. Tang, J.M. Proctor, Y. Wang, X. Bernstein, X. Huang, L.F. Reichardt, J.A. Bluestone, and D. Sheppard. 2007. Loss of integrin alpha(v)beta8 on dendritic cells causes autoimmunity and colitis in mice. *Nature* 449:361-365.

Travis, M.A., and D. Sheppard. 2014. TGF-beta activation and function in immunity. *Annu Rev Immunol* 32:51-82.

Trinchieri, G., D. Santoli, R.R. Dee, and B.B. Knowles. 1978. Anti-viral activity induced by culturing lymphocytes with tumor-derived or virus-transformed cells. Identification of the anti-viral activity as interferon and characterization of the human effector lymphocyte subpopulation. *The Journal of experimental medicine* 147:1299-1313.

Uchida, K., H. Suzuki, T. Ohashi, K. Nitta, W. Yumura, and H. Nihei. 2001. Involvement of MAP kinase cascades in Smad7 transcriptional regulation. *Biochem Biophys Res Commun* 289:376-381.

Ulloa, L., J. Doody, and J. Massague. 1999. Inhibition of transforming growth factor-beta/SMAD signalling by the interferon-gamma/STAT pathway. *Nature* 397:710-713.

Valladeau, J., V. Duvert-Frances, J.J. Pin, C. Dezutter-Dambuyant, C. Vincent, C. Massacrier, J. Vincent, K. Yoneda, J. Banchereau, C. Caux, J. Davoust, and S. Saeland. 1999. The monoclonal antibody DCGM4 recognizes Langerin, a protein specific of Langerhans cells, and is rapidly internalized from the cell surface. *European journal of immunology* 29:2695-2704.

Valladeau, J., O. Ravel, C. Dezutter-Dambuyant, K. Moore, M. Kleijmeer, Y. Liu, V. Duvert-Frances, C. Vincent, D. Schmitt, J. Davoust, C. Caux, S. Lebecque, and S. Saeland. 2000. Langerin, a novel C-type lectin specific to Langerhans cells, is an endocytic receptor that induces the formation of Birbeck granules. *Immunity* 12:71-81.

van Rijt, L.S., S. Jung, A. Kleinjan, N. Vos, M. Willart, C. Duez, H.C. Hoogsteden, and B.N. Lambrecht. 2005. In vivo depletion of lung CD11c+ dendritic cells during allergen challenge abrogates the characteristic features of asthma. *J Exp Med* 201:981-991.

Veldhoen, M., R.J. Hocking, C.J. Atkins, R.M. Locksley, and B. Stockinger. 2006. TGFbeta in the context of an inflammatory cytokine milieu supports de novo differentiation of IL-17-producing T cells. *Immunity* 24:179-189.

Vermeire, K., L. Thielemans, P. Matthys, and A. Billiau. 2000. The effects of NO synthase inhibitors on murine collagen-induced arthritis do not support a role of NO in the protective effect of IFN-gamma. *Journal of leukocyte biology* 68:119-124.

Vignali, D.A., L.W. Collison, and C.J. Workman. 2008. How regulatory T cells work. *Nature reviews. Immunology* 8:523-532.

von Boehmer, H., H.S. Teh, and P. Kisielow. 1989. The thymus selects the useful, neglects the useless and destroys the harmful. *Immunology today* 10:57-61.

von Gersdorff, G., K. Susztak, F. Rezvani, M. Bitzer, D. Liang, and E.P. Bottinger. 2000. Smad3 and Smad4 mediate transcriptional activation of the human Smad7 promoter by transforming growth factor beta. *J Biol Chem* 275:11320-11326.

Vremec, D., J. Pooley, H. Hochrein, L. Wu, and K. Shortman. 2000. CD4 and CD8 expression by dendritic cell subtypes in mouse thymus and spleen. *Journal of immunology* 164:2978-2986.

Wang, W., V. Koka, and H.Y. Lan. 2005. Transforming growth factor-beta and Smad signalling in kidney diseases. *Nephrology (Carlton)* 10:48-56.

Weishaupt, A., S. Jander, W. Bruck, T. Kuhlmann, M. Stienekemeier, T. Hartung, K.V. Toyka, G. Stoll, and R. Gold. 2000. Molecular mechanisms of high-dose antigen therapy in experimental autoimmune encephalomyelitis: rapid induction of Th1-type cytokines and inducible nitric oxide synthase. *Journal of immunology* 165:7157-7163.

Willenborg, D.O., S.A. Fordham, M.A. Staykova, I.A. Ramshaw, and W.B. Cowden. 1999. IFN-gamma is critical to the control of murine autoimmune encephalomyelitis and regulates both in the periphery and in the target tissue: a possible role for nitric oxide. *Journal of immunology* 163:5278-5286.

Wing, K., and S. Sakaguchi. 2010. Regulatory T cells exert checks and balances on self tolerance and autoimmunity. *Nature immunology* 11:7-13.

Worthington, J.J., B.I. Czajkowska, A.C. Melton, and M.A. Travis. 2011. Intestinal dendritic cells specialize to activate transforming growth factor-beta and induce Foxp3+ regulatory T cells via integrin alphavbeta8. *Gastroenterology* 141:1802-1812.

Xu, Y.P., Y. Shi, Z.Z. Cui, H.H. Jiang, L. Li, X.F. Wang, L. Zhou, and Q.S. Mi. 2012. TGFbeta/Smad3 signal pathway is not required for epidermal Langerhans cell development. *The Journal of investigative dermatology* 132:2106-2109.

Yamagiwa, S., J.D. Gray, S. Hashimoto, and D.A. Horwitz. 2001. A role for TGF-beta in the generation and expansion of CD4+CD25+ regulatory T cells from human peripheral blood. *Journal of immunology* 166:7282-7289.

Yamazaki, S., D. Dudziak, G.F. Heidkamp, C. Fiorese, A.J. Bonito, K. Inaba, M.C. Nussenzweig, and R.M. Steinman. 2008. CD8+ CD205+ splenic dendritic cells are specialized to induce Foxp3+ regulatory T cells. *Journal of immunology* 181:6923-6933.

Yan, X., and Y.G. Chen. 2011. Smad7: not only a regulator, but also a cross-talk mediator of TGF-beta signalling. *The Biochemical journal* 434:1-10.

Yan, Y., G.X. Zhang, B. Gran, F. Fallarino, S. Yu, H. Li, M.L. Cullimore, A. Rostami, and H. Xu. 2010. IDO upregulates regulatory T cells via tryptophan catabolite and suppresses encephalitogenic T cell responses in experimental autoimmune encephalomyelitis. *Journal of immunology* 185:5953-5961.

Yaswen, L., A.B. Kulkarni, T. Fredrickson, B. Mittleman, R. Schiffman, S. Payne, G. Longenecker, E. Mozes, and S. Karlsson. 1996. Autoimmune manifestations in the transforming growth factor-beta 1 knockout mouse. *Blood* 87:1439-1445.

Yi, J.Y., I. Shin, and C.L. Arteaga. 2005. Type I transforming growth factor beta receptor binds to and activates phosphatidylinositol 3-kinase. *The Journal of biological chemistry* 280:10870-10876.

Yogev, N., F. Frommer, D. Lukas, K. Kautz-Neu, K. Karram, D. Ielo, E. von Stebut, H.C. Probst, M. van den Broek, D. Riethmacher, T. Birnberg, T. Blank, B. Reizis, T. Korn, H. Wiendl, S. Jung, M. Prinz, F.C. Kurschus, and A.

Waisman. 2012. Dendritic Cells Ameliorate Autoimmunity in the CNS by Controlling the Homeostasis of PD-1 Receptor(+) Regulatory T Cells. *Immunity* 37:264-275.

Zahner, S.P., J.M. Kel, C.A. Martina, I. Brouwers-Haspels, M.A. van Roon, and B.E. Clausen. 2011. Conditional deletion of TGF-betaR1 using Langerin-Cre mice results in Langerhans cell deficiency and reduced contact hypersensitivity. *Journal of immunology* 187:5069-5076.

Zhang, S., T. Fei, L. Zhang, R. Zhang, F. Chen, Y. Ning, Y. Han, X.H. Feng, A. Meng, and Y.G. Chen. 2007. Smad7 antagonizes transforming growth factor beta signaling in the nucleus by interfering with functional Smad-DNA complex formation. *Molecular and cellular biology* 27:4488-4499.

Zhang, X., D.N. Koldzic, L. Izikson, J. Reddy, R.F. Nazareno, S. Sakaguchi, V.K. Kuchroo, and H.L. Weiner. 2004. IL-10 is involved in the suppression of experimental autoimmune encephalomyelitis by CD25+CD4+ regulatory T cells. *International immunology* 16:249-256.

Zhang, Y.E. 2009. Non-Smad pathways in TGF-beta signaling. *Cell research* 19:128-139.

Zheng, Y., and A.Y. Rudensky. 2007. Foxp3 in control of the regulatory T cell lineage. *Nature immunology* 8:457-462.

Zhu, L., S. Chen, and Y. Chen. 2011. Unraveling the biological functions of Smad7 with mouse models. *Cell Biosci* 1:44.

8 Acknowledgements

9 Versicherung

10 Curriculum vitae

11 Publikationen

1.

Dendritic cells ameliorate autoimmunity in the CNS by controlling the homeostasis of PD-1 receptor(+) regulatory T cells.

Yogev N, Frommer F, Lukas D, Kautz-Neu K, Karram K, Ielo D, von Stebut E, Probst HC, van den Broek M, Riethmacher D, Birnberg T, Blank T, Reizis B, Korn T, Wiendl H, Jung S, Prinz M, Kurschus FC, Waisman A.

Immunity. 2012 Aug 24;37(2):264-75. doi: 10.1016/j.immuni.2012.05.025. Epub 2012 Aug 16.

2.

A20 deficiency in B cells enhances B-cell proliferation and results in the development of autoantibodies.

Hövelmeyer N, Reissig S, Xuan NT, Adams-Quack P, Lukas D, Nikolaev A, Schlüter D, Waisman A.

Eur J Immunol. 2011 Mar;41(3):595-601. doi: 10.1002/eji.201041313. Epub 2011 Feb 10.

3.

Smad7 in T cells drives T helper 1 responses in multiple sclerosis and experimental autoimmune encephalomyelitis.

Kleiter I, Song J, Lukas D, Hasan M, Neumann B, Croxford AL, Pedré X, Hövelmeyer N, Yogev N, Mildner A, Prinz M, Wiese E, Reifenberg K, Bittner S, Wiendl H, Steinman L, Becker C, Bogdahn U, Neurath MF, Steinbrecher A, Waisman A.

Brain. 2010 Apr;133(Pt 4):1067-81. Epub 2010 Mar 30.